Maternal and Fetal Genetic Contributions to Preterm Birth

by

Sarah Jean Cunningham

University Program in Genetic and Genomics
Duke University

Date:_____

Approved:

_____
Timothy Reddy, Supervisor

_____
Elizabeth Hauser

_____
Simon Gregory

_____
Charles Gersbach

Dissertation submitted in partial fulfillment of
the requirements for the degree of Doctor
of Philosophy in the University Program in Genetic and Genomics in the Graduate School
of Duke University

2022

ABSTRACT

Maternal and Fetal Genetic Contributions to Preterm Birth

by

Sarah Jean Cunningham

University Program in Genetic and Genomics
Duke University

Date:_____

Approved:

_____
Timothy Reddy, Supervisor

_____
Elizabeth Hauser

_____
Simon Gregory

_____
Charles Gersbach

An abstract of a dissertation submitted in partial
fulfillment of the requirements for the degree
of Doctor of Philosophy in University Program in Genetics and Genomics in the
Graduate School of
Duke University

2022

Abstract

Preterm birth is a major public health issue, affecting approximately 10% of pregnancies in the United States. The causes of preterm birth include the genetics of the mother, the genetics of the fetus, the environment, and the interplay of any combination of these factors. Maternal genetics is a significant contributor to preterm birth but few genome wide association studies (GWAS) have identified associated genetic variants. Recently, the largest GWAS on preterm birth to date found several loci associated with preterm birth that suggest impaired decidualization of the endometrium may play a role. To investigate regulatory activity in genomic regions identified via GWAS, we used the massively parallel reporter assay STARR-seq. Motifs enriched in peaks of significant activity include many transcription factors known to have critical roles in decidualization of the endometrium. An additional factor leading to preterm birth is maternal psychological stress. Maternal psychological stress is particularly linked to PPROM, the leading identifiable cause of preterm birth. PPROM is a pregnancy complication in which the chorion and amnion weaken and rupture prior to 37 weeks of pregnancy and before contractions have begun. PPROM is responsible for 30-40% of preterm birth cases. PPROM is closely linked to maternal psychological stress, leading us to hypothesize that glucocorticoid signaling may contribute to PPROM. As a step towards testing that hypothesis, we investigated the gene expression effects of

glucocorticoids in primary amnion cells using RNA-seq. KCNA5 emerged as a potential GR regulated gene. KCNA5 has previously been reported to be a cell stress sensor that regulates proliferation and apoptosis. KCNA5 knockdown significantly increased cell proliferation without appearing to impact apoptosis and CRISPR-mediated over expression of endogenous KCNA5 decreased in cell proliferation. Taken together, these results suggest that glucocorticoid-mediated activation of KCNA5 contributes to decreased cell proliferation in the amnion epithelium. Decreases in amnion epithelial proliferation could impair the ability of these cells to repair microfractures in the membrane and lead to overall membrane weakening. We were able to study endocrine responses in pregnancy relevant cells to understand more broadly how these interactions affect preterm birth. Greater understanding of the interaction between preterm birth risk factors will move our understanding of the field forward.

Dedication

This work is dedicated to my family, both in New Jersey and North Carolina. My parents who continuously fed my love of science from an early age and encouraged me to explore whatever path I was interested in at the time. My mom providing an example of a successful career woman and taking me to women in business networking events shaped me to become the woman I am today. My dad's love for the technical details of his work and fascination with transformer stations spurred my need to understand how things work. My brother and extended family have always provided support and encouragement.

Additionally, this is dedicated to my family in North Carolina, my fiancé Zack. Although we may have only known each other in the last year and a half of the PhD, this has been some of the most challenging times. His continuous love and support have helped me get over the finish line. He's sleeping on the couch as I write this late at night so he can be there for the exact moment I finish.

Contents

List of Tables

List of Figures

Acknowledgements

This work would not have been possible without the guidance from my mentor Dr. Timothy Reddy. Dr. Reddy allowed me to explore my project and follow it whichever way it might go. His guidance and the opportunities he provided for me have trained me to be the scientist I am today, and I would not have been able to grow as much without him. I would also like to thank the guidance of my thesis committee, Dr. Beth Hauser, Dr. Simon Gregory, Dr. Charlie Gersbach, and Dr. Liping Feng, for their helpful counseling throughout my project's development.

I would not have been able to get this far in my PhD without the guidance of Dr. Graham Johnson. Graham trained me when I first started in the lab and became my go to for all questions big and small in the lab to this day. I'm extremely fortunate to have been able to bounce ideas off him and discuss any technical issues I was dealing with to figure it out as soon as I could.

My lab mates Laavanya Sankaranarayanan, Kari Strouse, Alex Barrera, Apoorva Iyengar, and Young-Sook Kim have made my lab experience much more enjoyable.

I would not have been able to learn all the background in pregnancy and fetal membranes needed without my collaborators Dr. Terrence Allen and Dr. Liping Feng. Through them, I learned so much more about pregnancy and fetal membranes that allowed my project to develop.

This work would not have been possible without the guidance from my early mentors Dr. George Pangalos who introduced me to research and Dr. Jonathan Arnold who introduced me to bioinformatics.

1. Introduction

1.1 The public health consequences of preterm birth.

Preterm birth is defined as birth before 37 weeks of pregnancy and the fetus is fully developed (World Health Organization, 2016). Preterm birth remains a major public health problem. Ten percent of children are born prematurely in the US (World Health Organization, 2016). Preterm birth and related complications lead to over one million deaths per year and are the leading cause of death for children under five years of age (World Heath Organization, 2016). Approximately 75% of perinatal mortality and over half of long term morbidity is caused by preterm birth (McCormick, 1985). Approximately half of children born preterm have neurodevelopmental deficits that require special education and, generally, children who are born premature have higher incidences of cardiac problems, metabolic syndrome and pulmonary issues (Luu, Rehman Mian and Nuyt, 2017). Preterm birth remains a large problem in the US, which has the third highest preterm birth rate of the 39 most economically developed countries (McCabe *et al.*, 2014). The overall costs of preterm birth in United States is estimated to be $26.2 billion annually or $51,500 per preterm infant in medical costs, special education, and indirect costs of labor loss (Alexander, 2007).

Preterm birth remains a difficult problem to understand biologically. The factors influencing preterm birth include the maternal genetics, the fetal genetics, the

environment and the interaction of any of those factors (Goldenberg *et al.*, 2008). Preventative treatment options are currently very limited (da Fonseca, Damião and Moreira, 2020). Understanding the mechanism of preterm birth in even a subset of women, potentially leading to novel therapeutic targets would have large improvements in neonatal health.

In this chapter, I will first review progress the progress that has been made towards understanding the genetics of preterm birth and the challenges of interpreting genetic associations through the lens of gene regulation. I will then review the role of fetal membranes in the maintenance of pregnancy. Finally, I will discuss the role of psychological stress in pregnancy and the interaction with fetal membranes.

1.2 The maternal genetics of preterm birth

While preterm birth remains multifactorial, family and twin studies suggest approximately 23% of the risk for preterm birth can be explained by maternal genetics (Zhang *et al.*, 2017). Women who have had a sister give birth preterm have an 80% higher risk of giving birth early themselves (Winkvist, Mogren and Högberg, 1998). If a woman gives birth preterm, her grandparents are more likely to have also been born preterm (Porter *et al.*, 1997). Women who have given birth preterm are over seven times as likely to give birth preterm in a subsequent pregnancy (Sondike, Pisetsky and Luzier, 2016).

Targeted have found significant loci within immune related genes (Crider, Whitehead and Buus, 2005; Engel *et al.*, 2005; Menon *et al.*, 2006). The first genome wide association studies of maternal genetics contributing to preterm birth, however, did not find any significant variants (Myking *et al.*, 2013; Zhang *et al.*, 2015), likely due to small sample size. More recently, a very large genome wide association study (Zhang *et al.*, 2017) has been able to identify several causal variants at a genome wide scale. . To date, very few of these variants have causal mechanisms explaining their effect.

Additionally, several variants have been identified that interact with environmental factors but do not lead to increased risk of preterm birth on their own. A maternal allele of TNFα has been identified that interacts with bacterial vaginosis to lead to increased risk of preterm birth, although neither factor increases risk on its own (Macones *et al.*, 2004). Similarly, an allele of IL-6 was identified that did not lead to increased risk of preterm birth in black or white women, except when black women had the allele and bacterial vaginosis. In that case, the risk of preterm doubled for those women (Engel *et al.*, 2005).

This again underlies the complexity of preterm birth. There are many possible environmental factors that could influence preterm birth (Goldenberg *et al.*, 2008). Understanding the genetics that may interact with these environmental factors is a daunting task.

1.3 Non-coding variants in common human disease

Long before the structure of DNA was identified, physicians knew that many diseases ran in families (Portal, 1809). As our understanding of genetics grew, scientists began to understand more about the inheritance of human diseases. The first gene identified to be associated with a human disease occurred with the discovery of abnormal hemoglobin in sickle cell patients (Ingram, 1958). In 1983, researchers were able to map the location of the disease causing gene for Huntington's Disease using family studies and recombinant DNA (Gusella *et al.*, 1983). The Huntington's gene was the first disease causing gene mapped on the human genome by studying affected and unaffected individuals.

The completion of the draft sequence of the human genome (Lander *et al.*, 2001; Venter *et al.*, 2001) created newfound potential to identify the causal gene of many major common diseases more quickly and more easily. While the two examples above represent Mendelian disorders that have become simple to detect (Bamshad *et al.*, 2011), mechanistic causes of common diseases remain difficult to identify (Wray *et al.*, 2018).

To identify genes associated with common diseases, researchers have deployed several approaches to identify alleles that contribute to human phenotypes and diseases. One common approach are genome wide association studies (GWAS). GWAS attempt to discover genetic associations with a trait by comparing allele frequencies between large

groups of affected and unaffected individuals. In a typical GWAS study, subjects are phenotyped as cases or controls and a DNA sample is collected for genotyping. Genotyping is commonly completed via hybridization to a microarray. The most recent and most densely tiled SNP microarrays test approximately ~4 million markers (Verlouw *et al.*, 2021), although typical modern SNP microarrays test around ~700,000 SNPs or one variant every ~5000 base pairs (Thompson, 2018). Those microarrays contain very few if any copy number variants (Verlouw *et al.*, 2021). The SNPs are then mapped back to the human genome to identify variants specifically associated with the trait phenotype and linkage blocks for the SNP are identified (Ikegawa, 2012). To estimate genotype-specific effects on the observed phenotype or trait, a linear or logistic regression model -- for continuous or binary phenotypes, respectively – is used. The regression model typically uses the observed phenotype as a dependent variable, and the genotype and measured confounding effects as independent variables. Fitting coefficients to all of the independent variables allows for simultaneous estimation of the effect of the genotype while also accounting for confounding effects (Uffelmann *et al.*, 2021).

For weak effect sizes that are typical for complex traits, very large sample sizes are needed to reach genome wide significance in GWAS. An allele that causes a 30% increase of disease in heterozygotes and 60% increase in homozygotes would need a

samples size of 1,974 cases for 80% power assuming 5% disease prevalence and 5% minor allele frequency (Hong and Park, 2012). A minority of variants identified by genome wide association studies have large odds ratios but these variants contribute disproportionately to the heritability explained (Zhang *et al.*, 2018). Extremely large sample sizes are needed to explain the remaining heritability due to smaller effect sizes. Sample sized of approximately 500,000 to 1 million are needed for most adult-onset chronic disorders and 700,000 to 1.5 million for most psychiatric disorders to explain 80% of heritability (Zhang *et al.*, 2018). Nonetheless, GWA studies have now found variants on every chromosome of the human genome, including Y as of 2020 (Figure 1).

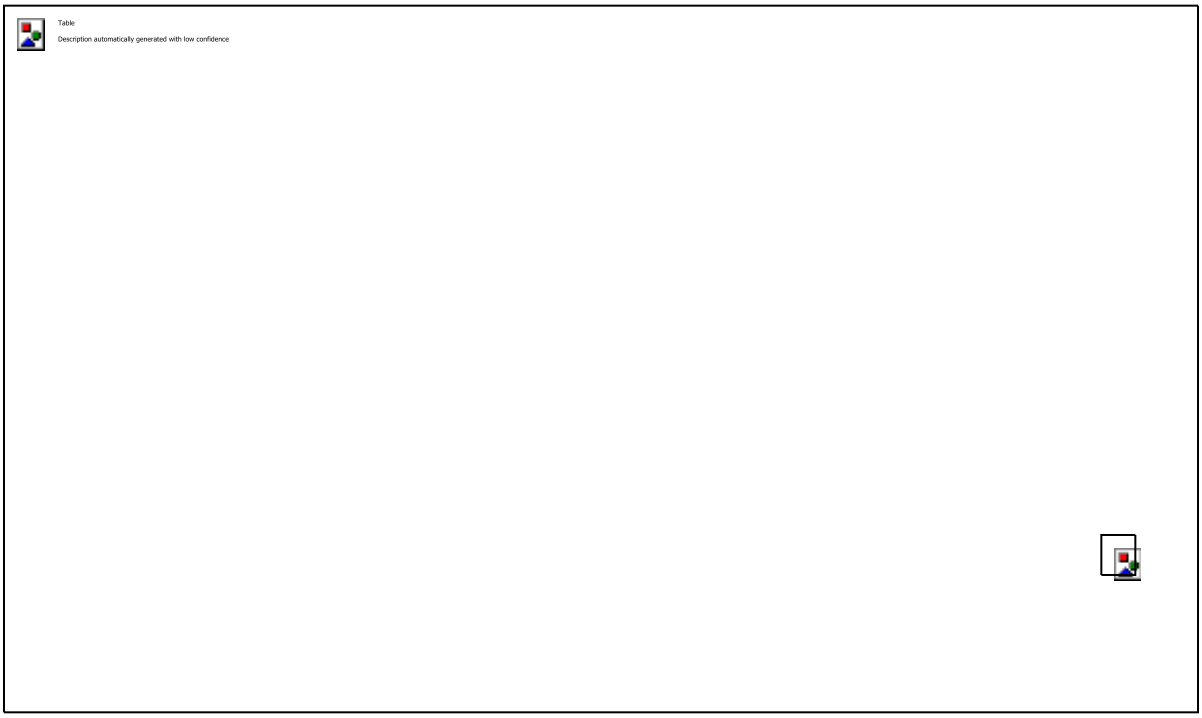

Figure 1: Catalog of variants identified in genome wide association studies.

The chromosomes show the approximate location of all variants with a p-value ≤ 5.0 x10-8 published in the genome wide association catalog (https://www.ebi.ac.uk/gwas/) prior to April 8, 2022 (Buniello et al., 2019)

Often, noncoding variants are identified in GWAS, but the casual variant and mechanism is not. GWA studies analyze common SNPs that tile the human genome (Poot, 2011) to identify a region in linkage disequilibrium with the true casual variant or variants (Schaid, Chen and Larson, 2018). The tiling of SNPs take advantage of linkage

disequilibrium in which alleles in close chromosomal proximity are more likely to be inherited together (Bush and Moore, 2012). The use of these arrays reduces the multiple testing burden by lowering the number of tests to the number of SNPs on the array while still allowing the linkage block of the variant of interest (Poot, 2011). Following GWAS, the true search space of the potential disease-causing variant is within the linkage disequilibrium block of genotyped variant. Within this linkage disequilibrium block, copy number variants, rare variants, or variants in higher frequency in non-European populations that are not always found on SNP arrays could be the disease causing variant (Lachance and Tishkoff, 2013). Casual variant are often imputed from more deeply sequenced populations, limiting identified variants to those in the reference panel (Z. Zhang *et al.*, 2021).

1.4 Eukaryotic gene regulation

The effect of noncoding variation identified in genome wide association studies is primarily understood in the context of gene regulation. The same copy of DNA is contained within every cell of the body, yet as of April 2022, 3,624 unique cell types have been identified in the body by CELLPEDIA (Hatano *et al.*, 2011, accessed April 2022). Additionally, each of these cells must respond to environmental stimuli received.

One strategy to tailor gene expression is through the compaction of DNA. In the nucleus, DNA is wrapped around histones and other proteins to form chromatin.

Chromatin is broadly organized into two categories. Compacted heterochromatin is highly organized, dense and not accessible to transcription factors of RNA polymerase (Verschure *et al.*, 1999a). Euchromatin, on the other hand, is much less compact. It is enriched for genes and allows much more RNA transcription than heterochromatin (Verschure *et al.*, 1999b). This control of compaction is achieved by modifications of the histone proteins itself. Each of the four histone proteins have post-translational modifications of N- and sometimes C- terminal tail including acetylation, methylation, or phosphorylation (Figure 2) (Dai and Wang, 2014). Together, the modifications of a histone make up the "histone code" (Jenuwein and Allis, 2001).

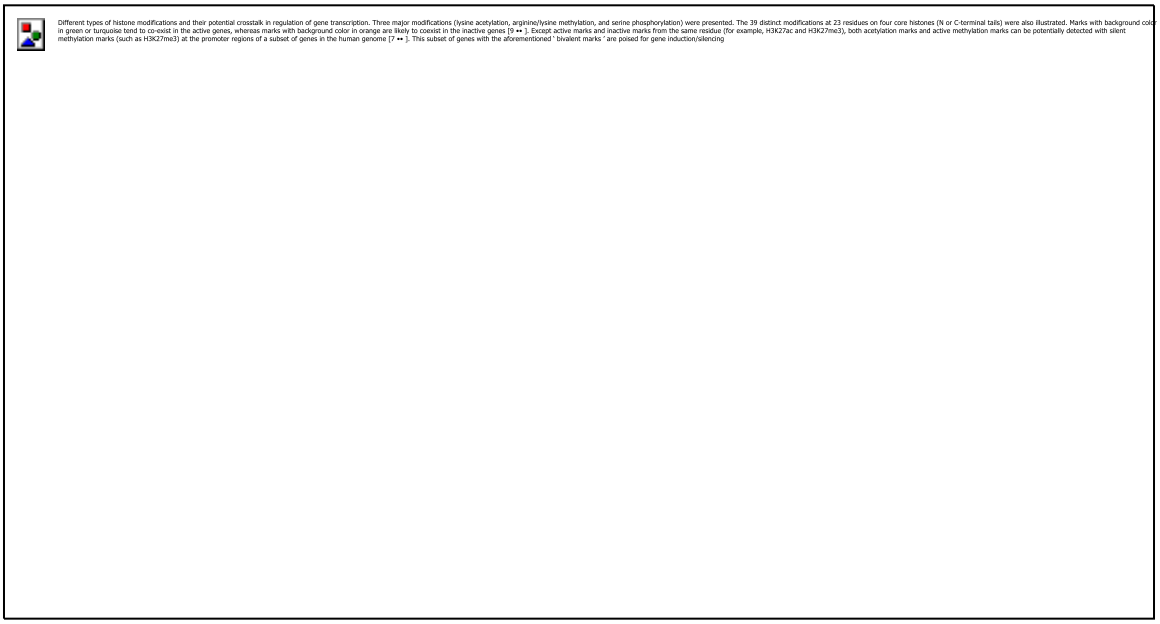

Figure 2: Histone modifications seen in eukaryotic cells.

Teal and green marks represent marks of more open DNA and active transcription while orange marks represent silencing marks that compact chromatin. Adapted from (Dai and Wang, 2014)**.**

Histone modifications include marks that are signatures of active gene regulatory regions. Promoters are found upstream of the gene itself (usually within 200 base pairs) surrounding the transcriptional start site. Promoters act as the binding site for transcription machinery to assembly and then begin the initiation of transcription (Smale and Kadonaga, 2003). Active promoters are typically marked by tri-methylation of lysine 4 of histone H3 (H3K4me3) (Heintzman *et al.*, 2007).

Enhancers increase the expression of genes, from long genetic distance to the gene itself. Human genes are typically controlled by many enhancers to regulate the timing and specificity of transcription (Blackwood and Kadonaga, 1998). Enhancers recruit transcription factors through short (5 - 20 bp) specific DNA sequences (Spitz and Furlong, 2012). Enhancers exist in both an active and poised, able to be either repressed of activated, state that can be distinguished by their histone modifications. While both active and poised enhancers are bound by transcription factors and histone acetylase P300, poised enhancers are bound to Polycomb Group protein complexes that compact DNA (Crispatzu *et al.*, 2021). While both enhancers typically contain mono-methylation on lysine 3 of histone H3 (H3K4me1), active enhancers also contain acetylation of lysine 27 on histone H3 while poised enhancers contain a tri-methyl modification on the same amino acid (H3K27me3) (Rada-Iglesias *et al.*, 2011).

Enhancers can regulate genes at long distances through chromatin looping or other indirect mechanisms. Enhancers recruit chromatin remodeling complexes that modify the histones of the promoter, altering accessibility of the promoter. They bring the chromatin remodeler and other transcription factors in proximity to the promoter by strengthening association with the gene itself (Dean, 2011). Enhancers are able to directly interact with genes as well as other enhancers from long genomic distances to activate transcription based on motifs found on the enhancer specifically (Chen *et al.*, 2020).

1.5 The challenges and possibilities of studying noncoding variation

1.5.1 Noncoding variants are implicated in common diseases

One major challenge when understanding the results of GWAS is that the majority (~90%) of variants identified are found in non-coding regions of the genome (Tam *et al.*, 2019). A large portion of these variants are presumed to affect the regulation of the genes (French and Edwards, 2020).

The effect of identified variants has not been able to fully account for the narrow sense genetic heritability estimated for complex traits. This problem is known as the "missing heritability problem" (López-Cortegano and Caballero, 2019). Explanations for the source of missing heritability include limited sample size leading to lack of power to detect small effect sizes (Yang *et al.*, 2010), inability for GWAS to detect effects for rare variants (Zuk *et al.*, 2014), genetic interactions (Zuk *et al.*, 2012), and environmental

interactions (Chen *et al.*, 2015; Ni *et al.*, 2019). Likely, all factors contribute to the missing heritability.

Because the effect of a noncoding variant is not immediately obvious, identifying a casual mechanism for disease remains challenging. While variants that do not affect splicing (~85% of noncoding variants) (French and Edwards, 2020), are likely to influence the expression of genes, this needs to be tested.

1.5.2 Novel sequencing technology to study regulatory regions

One way to estimate the regulatory activity of putative enhancers is via reporter assays (Querfurth *et al.*, 1999; Dachet *et al.*, 2000). These impact of environmental effects and the challenge of understanding noncoding variants coincide to present a challenge for understanding variants of genome wide association studies. While luciferase assays are very useful to understand regulatory regions, the throughput remains limited. The search space in linkage disequilibrium with the genotyped variant can lead to an unwieldy number of luciferase assays to test. One 2015 study identified 12 variants in linkage disequilibrium with the genotyped variant, leading to 105 haplotypes to test the individual and coordinated effects of the variants (Guo *et al.*, 2015).

To study putative enhancers at high throughput, novel sequencing technologies such as Massively Parallel Reporter Assays (MPRAs) (Melnikov *et al.*, 2012; Patwardhan *et al.*, 2012) and Self-Transcribing Active Regulatory Region Sequencing (STARR-seq)

(Arnold *et al.*, 2013) have been developed. The workflow of STARR-seq is outlined in Figure 3. Briefly, the DNA of interest is fragmented and cloned into the STARR-seq vector. This vector contains a minimal promoter and a reporter gene. The fragment to be tested is cloned into the 5′ end of the reporter gene after the stop codon but before the polyadenylation (polyA) signal. That placement allows the DNA fragments of interest to be transcribed as part of the mRNA that they are regulating. Then, during high-throughput sequencing library generation, STARR-seq specific primers amplify the STARR-seq fragments specifically during PCR. This is then sequenced and aligned to the reference genome. Regions where more reads align to the genome have greater putative enhancer activity than those with minimal reads aligning. This can be quantified by comparing sequencing read in the input library when it is sequenced compared to sequencing reads in the output library.

Figure 3: The workflow of STARR-seq.

The workflow includes fragmenting DNA of interest, cloning the resulting fragments into the STARR-seq vector to create a plasmid library, transfecting the plasmid library into cells, isolating the RNA expressed from the transfected plasmids, creating high-throughput sequencing libraries, sequencing the libraries, and aligning to the genome of interest

The advent of high-throughput methods to estimate regulatory activity creates new possibilities in the follow up to GWAS. STARR-seq and MPRAs can detect regulatory activity in the whole genome in one study (Liu *et al.*, 2017; Johnson *et al.*, 2018; van Arensbergen *et al.*, 2019). Assays like MPRAs and STARR-seq can identify regions in linkage with GWAS variants that have regulatory activity in a cell type relevant for the disease studied. Additional, variation of STARR-seq incorporating patient DNA, PopSTARR, can specifically identify variants within patient populations that alter regulatory activity (Vockley *et al.*, 2015).

1.6 The role of fetal membranes in pregnancy

The fetal membranes surround the fetus and amniotic fluid in pregnancy (Gadd, 1966). The membranes are composed of the thin inner amnion layer, the innermost layer of the uterine cavity, and the thicker chorion layer, where fetal tissue interacts with maternal tissue (Gadd, 1966; Malak *et al.*, 1993). Between the two layers is a collagen rich extracellular matrix containing the amnion mesenchymal cells (Gadd, 1966; Malak *et al.*, 1993) (Figure 4). Each layer has unique functions and roles within pregnancy.

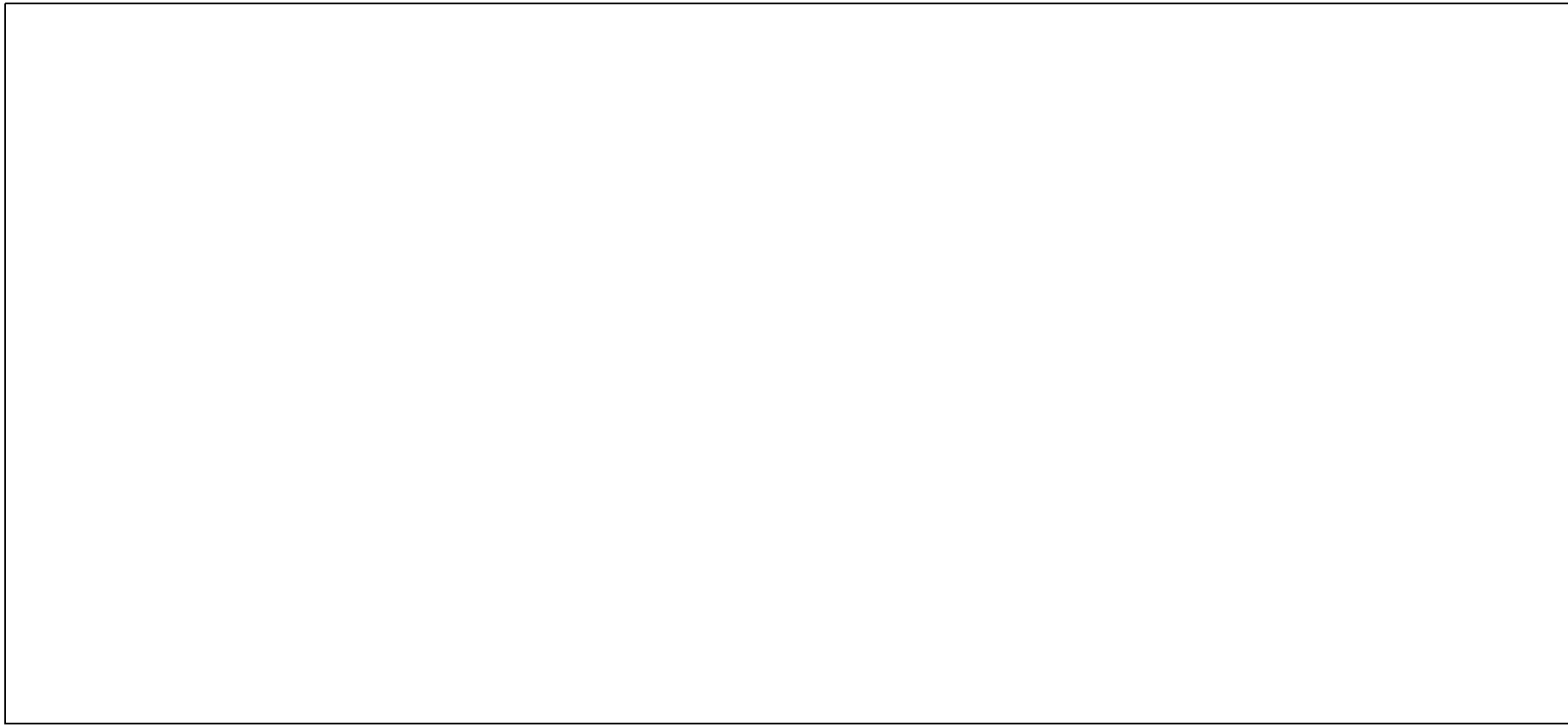

Figure 4: Diagram of fetal membranes in the uterine cavity, adapted from Martin, Richardson and Menon, 2018**.**

The innermost later consists of amnion epithelial cells (blue) attached to the basement membrane (orange strip). Next, the amnion fibroblast cells (purple) are embedded within the extracellular matrix (red), attached to another thick basement membrane. Beneath the amnion, the chorion trophoblast cells (white) interact with the maternal cells at the decidual (green).

1.6.1 The maternal fetal interface

The chorionic layer of the fetal membranes is the primary point of contact between maternal and fetal cells. Early in pregnancy, chorionic trophoblasts invade the decidua tissue of the mother to the spiral arteries where they remodel the arteries to supply nutrients (Burton *et al.*, 2009). Defective invasion is associated with early onset pre-eclampsia and fetal growth restriction (Brosens, Pijnenborg and Brosens, 2002; Pijnenborg, Vercruysse and Hanssens, 2006). At the interface, many uterine specific immune cells are responsible for attenuating the immune response to genetically foreign cells (Vento-Tormo *et al.*, 2018). As many as 32 unique cell types have been identified at the maternal fetal interface, over half of those are immune cells (Vento-Tormo *et al.*, 2018).

1.6.2 The role of the amnion

While the chorion is important for spiral artery remodeling, the amnion epithelial layer plays a crucial role in membrane integrity. The amnion has been found to be the dominant contributor to the tensile strength of the membranes. The amnion also serves as a structural barrier (Manabe, Himeno and Fukumoto, 1991). Similarly, experimental modeling of the bilayer fetal membranes have identified the amnion as the dominant structural component of the membranes and required to maintain membrane integrity (Verbruggen *et al.*, 2017). It is thought that premature rupture of membranes

occurs due to the failure of the amnion to maintain its structural integrity (McGregor *et al.*, 1987; Rajabi, Dean and Woessner, 1987).

Although much of the research on the amnion is focused on the collagen rich layer containing amnion fibroblast cells, both the extracellular matrix and the amnion epithelial cells contribute to the tensile strength of the amnion (Tanaka *et al.*, 2010). Amnion epithelial cells themselves constantly turn over and remodel (Martin, Richardson and Menon, 2018), making their control of cell cycle important to maintaining membrane identity.

The key role of the amnion in membrane integrity can been observed in the presence of microfractures in term and PPROM patient membranes. In the amnion, epithelial cell shedding and loosened collagen in the extracellular matrix in tunnels referred to as microfractures, break the continuity of the amnion surface (Richardson *et al.*, 2017). Oxidative stress can induce additional microfractures in vitro (Richardson *et al.*, 2017), strengthening findings that oxidative stress plays a key role in PPROM (Longini *et al.*, 2007; Menon, 2014; Dutta *et al.*, 2015; Martin *et al.*, 2017). Fetal membranes from term in labor patients had more microfractures than term not in labor patients from caesarean sections and PPROM patients had the most microfractures with 4.6 fold more microfractures and deeper microfractures than gestational age matched preterm birth or term labor membranes (Richardson *et al.*, 2017).

The cell cycle of amnion epithelial cells has a crucial role in microfracture and injury repair in the fetal membranes. When the amnion layer is injured, for example due to amniocentesis, the amnion epithelial layer is able to heal itself in most cases (Gratacós *et al.*, 2006; Papadopulos *et al.*, 2006). To do so, amnion epithelial cells divide. After division, a portion of the cells undergo epithelial mesenchymal transition to repopulate the collagen producing mesenchymal fibroblast layer beneath it (Richardson and Menon, 2018). While epithelial and mesenchymal cells can transition between each state (Richardson, Taylor and Menon, 2020), amnion epithelial cells maintain transitory and migratory potential that mesenchymal cells do not (Richardson *et al.*, 2019). In this way, the structural integrity of the collagen layer containing amnion fibroblast cells is dependent on the epithelial layer above it and the proliferation and migration of the epithelial layer.

1.6.3 Preterm Premature Rupture of Membranes

One complication that can emerge from the fetal membranes is preterm premature rupture of membranes (PPROM). PPROM is defined as the rupture of the fetal membranes prior to 37 weeks of pregnancy with no contractions present (Medina and Hill, 2006). PPROM has been called a "disease of the amniochorionic membranes" (Murtha and Menon, 2015). PPROM is the leading identifiable cause of preterm birth, accounting for 30-40% of cases (Mercer, 2010). In 50-75% of cases, the baby must be delivered within one week of membrane rupture (Medina and Hill, 2006). Once rupture

occurs, therapeutic measures are largely limited to progressing fetal lung maturation with glucocorticoids (Harding *et al.*, 2001), although measures to prevent birth do exist (Medina and Hill, 2006).

Although methods to detect risk of PPROM for have existed for years (Menon, 2004), reliable clinical strategies to prevent or delay PPROM do not exist. While antibiotics can be helpful to prevent PPROM in those with infections of gonorrhea, chlamydia or symptomatic bacterial vaginosis (Locksmith and Duff, 2001), others including those with asymptomatic BV are not helped by antibiotics (Brocklehurst *et al.*, 2013). More general therapeutic strategies, such as progesterone treatment, cervical cerclage and vitamin C have not been proven to be effective to date in clinical trials (Steyn *et al.*, 2003; To *et al.*, 2004; Nelson *et al.*, 2017).

1.7 Psychological stress and pregnancy

One contributing factor to all cause preterm birth and to PPROM specifically is maternal psychological stress. Maternal adversity is an independent predictor of preterm births (Olsen, 2018; Sulaiman *et al.*, 2021; Hardcastle, Ford and Bellis, 2022). In one study of PPROM specifically, women under psychological stress[1] had 100 times greater risk of PPROM compared to unstressed mothers (Lilliecreutz *et al.*, 2016).

[1] Psychological stress in this study referred to psychiatric diagnosis, previous traumatic experience with pregnancy or childbirth, lack of social support or a problematics relationship between the mother and her partner, economic or work stress or stress due to the pregnancy itself.

The interplay of psychological stress and altered cortisol levels has been shown to effect birth timing. Cortisol signaling likely plays an important role in labor initiation as evidenced by the surge in maternal, fetal and amniotic fluid levels of glucocorticoids close to term (Goldkrand, Schulte and Messer, 1976; Smith, 2007; Guo *et al.*, 2014). There is evidence of altered cortisol regulation in pregnant women who have experienced adverse childhood experiences (Bowers *et al.*, 2018; Thomas *et al.*, 2018). There is also association between plasma cortisol levels and the recurrence of preterm birth. Specifically, median maternal plasma cortisol levels are elevated in women who have had one isolated preterm birth, and elevated further in women who have had recurrent preterm birth (Mercer *et al.*, 2006). There link between maternal depression and preterm birth is thought to be due to a related increase in cortisol (Diego *et al.*, 2009).

1.8 Glucocorticoids and psychological stress

A potential mechanism by which maternal stress impacts gestation is via cortisol signaling. Cortisol is a cholesterol derived signaling hormone synthesized in the adrenal glands. It is released in a circadian manner as well as in response to physiologic signals (such as exercise) and psychological stress (Radosevich *et al.*, 1989; Miller and Auchus, 2011). When acute or chronic stress is perceived, the hypothalamus-pituitary-adrenal (HPA) axis stimulates the release of cortisol into the bloodstream (Nader, Chrousos and Kino, 2010; González-Cabrera *et al.*, 2014). Psychological stress increases circulating cortisol, in some cases up to five fold (Ranabir and Reetu, 2011).

The downstream effects of cortisol are primarily mediated by the nuclear glucocorticoid receptor, a member of the ligan activated nuclear receptor family of proteins (Ramamoorthy and Cidlowski, 2016). Cortisol, and glucocorticoids broadly, show tissue specific activity because the native chromatin landscape of each cell impacts the accessibility of each glucocorticoid response element (GRE) (John *et al.*, 2011; Burd and Archer, 2013) with many GREs found to be located far from gene promoter regions (Reddy *et al.*, 2009).

While glucocorticoid signaling is part of normal biological functioning, long-term elevated cortisol levels contribute to myriad physiological effects. Elevated cortisol signaling leads to immunosuppression (Venkatesh *et al.*, 2015; Ramezani *et al.*, 2020), impaired wound healing (Mattern, Büchler and Herr, 2007; Walburn *et al.*, 2009), and other detrimental effects (Björntorp, 1997; Raff *et al.*, 1999; Faresjö *et al.*, 2020). The genomic effect of elevated glucocorticoid levels long term is counter to expectations. In chronic stress conditions, gene expression changes show reduced glucocorticoid receptor activation and related gene expression (Miller *et al.*, 2009; Cohen *et al.*, 2012). Pro-inflammatory signaling was also increased in response to the same levels of cortisol (Miller, Cohen and Ritchey, 2002; Cole *et al.*, 2007; Miller *et al.*, 2008; Rohleder *et al.*, 2009).

1.9 Glucocorticoids and cell proliferation

The effect of glucocorticoids on cell proliferation is time, dose, and cell type dependent. Multiple studies (Freshney *et al.*, 1980; Kawamura, Tamaki and Kokunai, 1998; Kaup *et al.*, 2001) have found glucocorticoids to both stimulate and inhibit proliferation depending on experimental conditions. Generally, low doses of glucocorticoids stimulate proliferation while higher doses induce cell cycle arrest (Mattern, Büchler and Herr, 2007)

The causes of impaired wound healing due to elevated cortisol signaling include cortisol-dependent effects on cell proliferation such as cell cycle arrest in the skin epithelium (Mattern, Büchler and Herr, 2007; Walburn *et al.*, 2009). In other cell types, however, such as colon cancer and retinal stem cells, glucocorticoids increase both proliferation and self-renewal (Tian *et al.*, 2019; Grisé *et al.*, 2021). Glucocorticoids need to be studies in the cell type of interest to understand the role it will have on proliferation.

2. STARR-seq identified putative enhancers in GWA regions for preterm birth

2.1 Introduction

Preterm birth is a major public health problem globally and in the United States. For the purposes of this research, preterm birth is defined as live birth prior to 37 weeks of pregnancy. The global rate of preterm birth is 11% of all pregnancies. Complications arising due to preterm birth are the leading cause of death for children under 5 leading to 18% of deaths under age 5 and 35% deaths among newborns (Walani, 2020). In the US, preterm rate is approximately 9.5% with significantly higher rates among black women (Purisch and Gyamfi-Bannerman, 2017).

Although the cause of preterm birth are multifactorial (Goldenberg *et al.*, 2008), maternal genetics contribute a significant portion of risk. Current estimates suggest approximately 30-40% of the variation in gestation length can be explained by maternal genetics (Zhang *et al.*, 2017). Despite this estimate, identification of variants has historically been limited. Targeted genetic studies (Crider, Whitehead and Buus, 2005; Engel *et al.*, 2005; Menon *et al.*, 2006) assessing immune related genes have identified loci associated with preterm birth but the first genome wide association studies of maternal genetics contributing to preterm birth did not find any significant variants (Myking *et al.*, 2013; Zhang *et al.*, 2015), likely due to small sample size.

A more recent GWAS (Zhang *et al.*, 2017) identified variants associated with preterm birth using a much larger sample size. The researchers used 23andMe data to amass a sample size of 43,568 women of European ancestry and a replication cohort of 8,643 from three Nordic birth studies. The birth outcome data from 23andMe was collected as self-reported surveys. In addition to assessing preterm birth as a categorical variable (excluding women at 37-38 weeks as close the term boundary), gestation length was also measured as a continuous variable. For gestation duration, 12 loci were identified with an association of $P<1.0\times10^{-6}$, 4 of which had an association of $P<5.0\times10^{-8}$. For preterm birth, 5 loci were identified with an association of $P<1.0\times10^{-6}$, 2 of which had an association of $P<5.0\times10^{-8}$. Interestingly, this study did not identify any variants near immune related genes originally identified in previous targeted studies, suggesting the variants are either affecting immune genes from long distances or the original targeted studies did not address major sources of genetic risk of preterm birth. The locations of the loci identified is shown in Figure 5.

Figure 5: Genetic associations with gestational duration and preterm birth.

A. Eight loci were found to be associated with gestation length at "suggestive significance" ($p<<1.0\times10^{-6}$, in orange) and 4 loci were associated at "genome wide significance" ($p<5.0\times10^{-8}$, in red). B. Three loci were associated with preterm birth in "suggestive significance" (in orange) and two at "genome wide significance" (in red). The top 3 loci associated with gestation duration (EBF1, EEFSEC, AGTR2) were also identified in preterm birth. Loci that were replicated in the Nordic birth study are bolded. Adapted from (Zhang *et al.*, 2017)**.**

Zhang et al. 2017 made substantial progress towards identifying maternal genetic causes of preterm birth. The next logical step is to identify casual mechanisms underlying those genetic associations. Each variant identified in the study was noncoding and not located within splice sites. For that reason, the variants are likely to be in gene regulatory regions and impact gene expression (French and Edwards, 2020). We sought to understand the potential regulatory regions within linkage to the variant identified in this study. This information can be combined with chromosome contact information from Hi-C in relevant cells and variant specific regulatory assays to show how variants in an enhancer alter expression of a gene, increasing risk for preterm birth.

2.2 Results

2.2.1 Immortalized human endometrial stromal cells replicate decidualization in vitro

Many maternal tissues and cell types are implicated in preterm birth (Di Renzo, Tosto and Giardina, 2018). One of the most crucial tissues involved is the decidua. The uterine decidua is composed of endometrial stromal cells, vascular cells and maternal blood (Mori *et al.*, 2016). Endometrial stromal cells change their morphology and function in the latter half of the menstrual cycle, differentiating into decidual stromal cells, to support pregnancy (Ng *et al.*, 2020). In pregnancy, the endometrial stromal cells surround the blastocyst in early pregnancy (Mori *et al.*, 2016), become the maternal

component of the placenta as the pregnancy develops (Mori *et al.*, 2016), and initiate a signaling cascade that results in labor (Farine *et al.*, 2018).

Additionally, WNT4 was identified as a locus associated with preterm birth in Zhang et al. 2017 which specifically implicated with decidua as crucial to preterm birth (Sonderegger, Pollheimer and Knöfler, 2010). WNT4 is crucial to the decidualization of the endometrium (Li *et al.*, 2013). Failure to completely decidualize has been hypothesized to be a key driver in adverse pregnancy outcomes (Ng *et al.*, 2020).

We sought to replicate decidualization of the endometrium in vitro. In vivo, decidualization is triggered by rises in progesterone and estrogen later in the menstrual cycle (Wetendorf and DeMayo, 2012). For our study, we used human endometrial stromal cells immortalized with hTERT (Krikun *et al.*, 2004). In vitro, decidualization can be stimulated with a 48 hour treatment of progesterone and cyclic AMP (cAMP) (Gellersen and Brosens, 2003; Gellersen, Brosens and Brosens, 2007). To identify if our cells successfully decidualized, we used qPCR to detect markers of decidualization Prolactin (PL) and IGFBP1 (Figure 6). Both gene were undetected in untreated cells so a pseudo-CT of 40 was used to measure ΔCT. MALAT1 was used as a negative control.

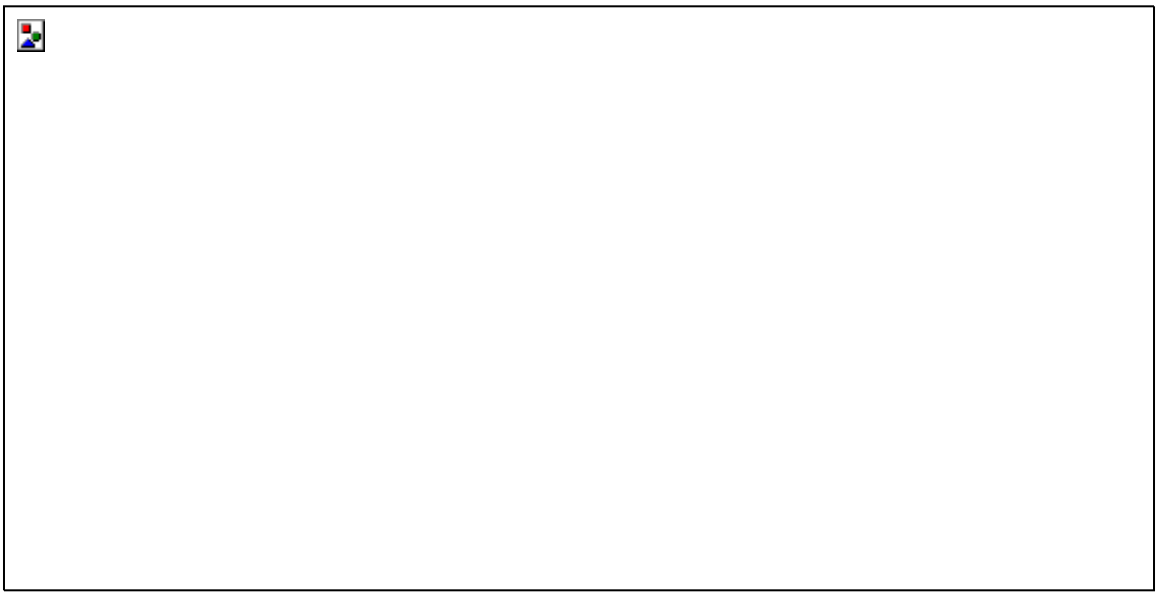

Figure 6: qPCR of decidualization marker after 48 hours of progesterone and cAMP.

Expression of decidualization markers IGFBP1 (A) and Prolactin (B) were measured after 48 hours of treatment with progesterone and cAMP compared to control Malat1. IGFBP1 and Prolactin were undetected in control cells so a pseudo-CT of 40 was used in place.

Progesterone and cAMP treatment on immortalized endometrial cells in vitro replicates key makers of decidualization. This system can be used to model the decidualization process of endometrial cells and identify putative enhancers that may be responsive to decidualization.

2.2.2 Targeted STARR-seq plasmid library covers preterm birth genome wide association loci

To identify putative enhancers in preterm birth GWA regions, we created a STARR-seq library targeting the loci identified in Zhang et al. 2017. We used bacteria

artificial chromosomes (BACs) spanning the variant of interest and the gene body of the gene identified if nearby (Table 1). If the BAC did not span the gene body, multiple BACs that overlap were used.

Table 1: Location of BACs used for STARR-seq library

BAC	Chr	Start	End	Location information
CH17-93O6	1	22,000,631	22,222,195	WNT4 locus
CH17-74K24	5	158,303,154	158,505,532	EBF1 locus
CH17-28B17	3	128,133,744	128,343,165	EEFSEC locus 1st half
CH17-149P6	3	128,221,052	128,470,703	EEFSEC locus 2nd half
RP11-147L22	X	116,030,209	116,195,712	AGTR2 locus
CH17-365H10	X	132,121,527	132,321,710	RAP2C locus

We used these BACs overlapping the GWAS region to create a STARR-seq library incorporating these preterm birth relevant regions. The BACs were fragmented using sonication and cloned into a STARR-seq plasmid (Figure 7A). The resulting STARR-seq transcripts (Figure 7B) include a short fragment with an intron spliced out, a green fluorescent protein mRNA as a reporter, the putative enhancer itself, and finally a poly A tail. When assaying STARR-seq libraries, it is critical to specifically PCR amplify the mRNA and not the transfected plasmids. The exon-exon junction in STARR-seq transcripts creates a nucleotide sequence that is unique to the STARR-seq mRNA and

priming from across that junction ensures that only STARR-seq RNA fragments will be amplified during PCR and not remaining STARR-seq plasmids. The poly A tail allows the transcript to be isolated with other mRNA fragments during sequencing library creating, removing approximately 95% of non-target transcripts.

Transcription of the STARR-seq reporter mRNA is driven by a promoter known as the "super-core promoter." The super-core promoter is thought to drive high expression in many contexts. If the fragment of interest is an active enhancer, it will act on the promoter to increase expression of STARR-seq mRNA containing the enhancer itself. The abundance of reads in a genomic location in the output library is a proxy for the activity level of the transcript.

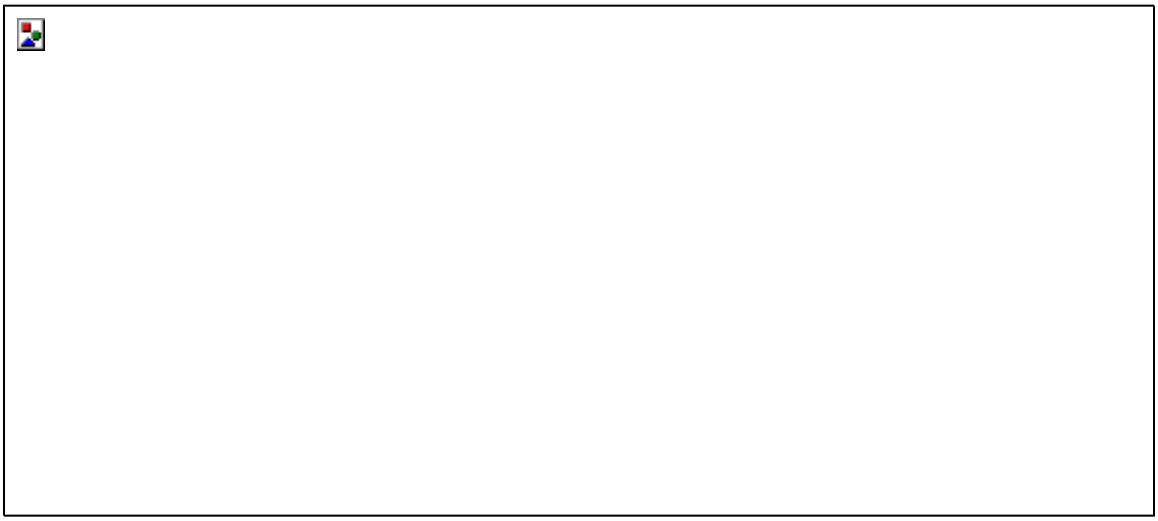

Figure 7: STARR-seq plasmid and transcript.

A. STARR-seq plasmid with an example test fragment. The plasmid contains an ampicillin resistance gene (light green) and an origin of replication (yellow) in addition to the STARR-seq transcript. The transcript expression is driven by the

fragment itself and the super core promoter (purple). B. STARR-seq transcript. The transcript contains a small fragment with, and intron spliced out (orange), the GFP reporter (lime green), the test fragment itself (red) and a poly A fragment.

The input library covers the region of interest with few dropouts (Figure 8). There is noise in the library itself but no significant patterns. Regions with overlapping BACs (Figure 7B) show roughly double the signal in the overlapping portion.

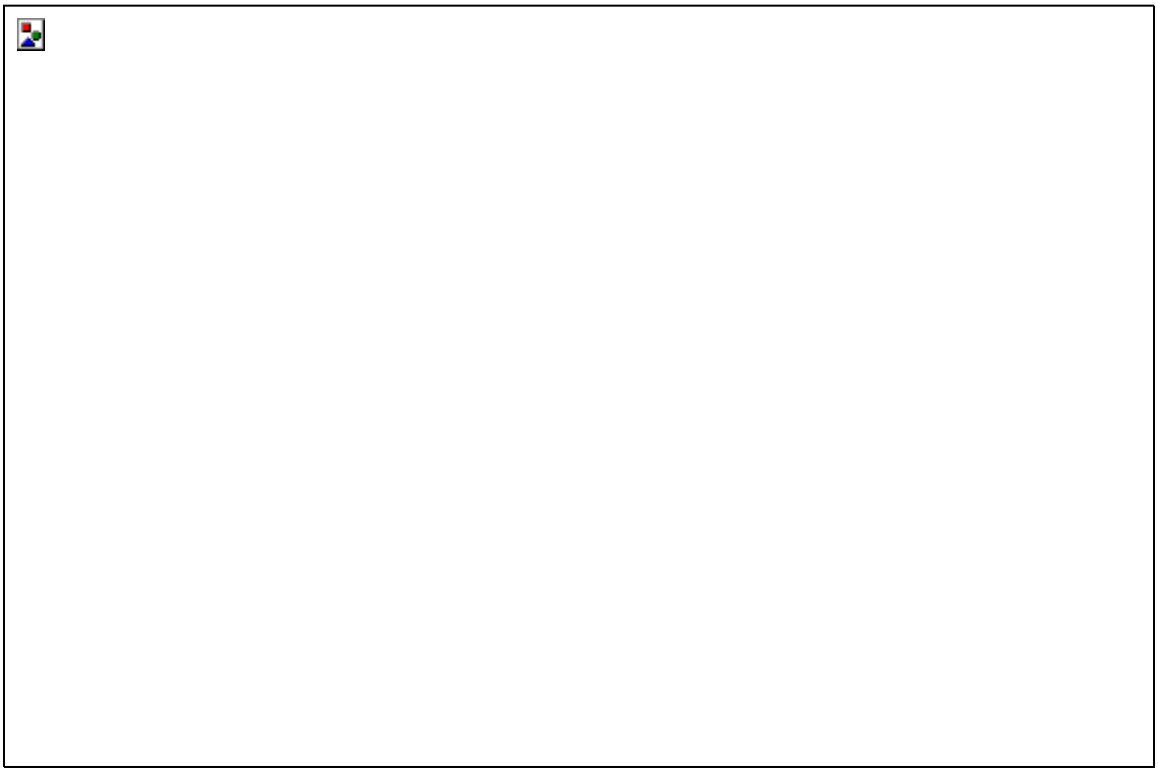

Figure 8: BAC STARR-seq input library.

A. Input library spanning WNT4 loci on chromosome 1. B. Two overlapping BACs (Black box) covering EEFSEC and related allele loci on chromosome 3.

2.2.3 Shortened transfection time improves STARR-seq transcript yield

To identify regulatory regions in preterm birth GWAS regions specific to endometrial cells, the plasmid library was transfected into immortalized endometrial stromal cell fibroblast. The cells were then exposed to a limited control media or the same media with progesterone and cAMP for 48 hours to induce decidualization (Figure 9).

Figure 9: Overview of STARR-seq experiment in endometrial cells.

In brief, the BACs overlapping preterm birth GWA regions were cloned into STARR-seq plasmids. This was transfected into endometrial cells. The cells were exposed to decidualization or control media for 48 hours.

After the 48-hour treatment, cells were collected and lysed. RNA was isolated and RNA without a poly A tail was washed out. The RNA is reverse transcribed and amplified by PCR with primers that will only amplify STARR-seq transcripts. Unique

molecular identifiers (UMIs) are added to each transcript before PCR amplification so the exact number of transcripts in a region can be identified. The number of cycles is dependent on STARR-seq RNA abundance. A set amount of RNA mass is input into the library preparation but the proportion of STARR-seq plasmids in this library varies. For this library, 36 cycles of PCR were needed to amplify the library, greatly reducing fragment diversity. This was evidence by only 1-3% of reads being identified as unique after deduplication by UMI sequence. For examples, in one untreated library, 33.4 million reads were sequenced but the estimated library size after deduplication was 844,000.

Based on data from the Reddy lab, STARR-seq transcripts are more present shortly after transfection. To increase the proportion of STARR-seq transcripts in the library, we modified the protocol (Figure 10). Decidualization of half the endometrial cells began with exposure to progesterone and cAMP in media. Forty-two hours after the addition of progesterone and cAMP, the cells were trypsinized off the plates and transfected with the STARR-seq plasmid library. Six hours after transfection, cells were collected and lysed.

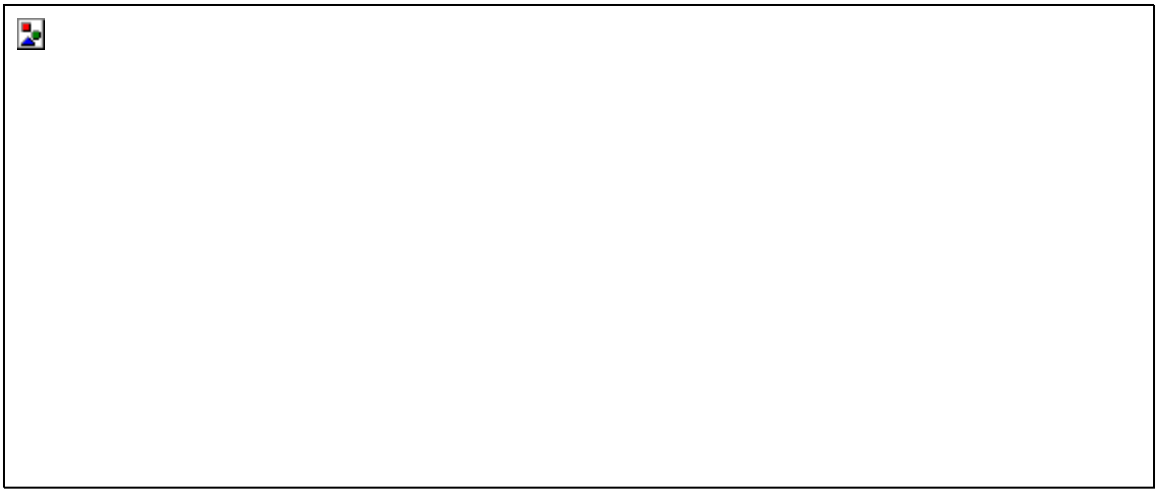

Figure 10: Modified STARR-seq transfection protocol.

Cells were now split into decidualization of control media first. Forty-two hours after the media change, cells are transfected with the STARR-seq library. Cells are then collected 6 hours after transfection.

The modified protocol introduces more noise by transfecting the decidualized and control cells separately. This is counteracted by the increase in STARR-seq transcripts. In this library prep, only 24 number of PCR cycles were needed to generate enough library to sequence. The resultant libraries were more diverse with 5-14% of transcripts identified as unique by UMI fragment.

2.2.4 Redesigned STARR-seq library and protocol improves signal to noise ratio

In addition to modifying the protocol of transfection, the plasmid library was cloned into a redesigned STARR-seq vector (Figure 11). After we began this study, new findings (Muerdter *et al.*, 2018) showed that the bacteria origin of replication served as a

promoter in mammalian STARR-seq assays. The redesigned vector took advantage of that observation and used the origin of replication as the promoter instead of the super core promoter. Additionally, the GFP reporter is shortened to less than a tenth of its original size from 722 base pairs to 63 base pairs, making for easier cloning and library recovery.

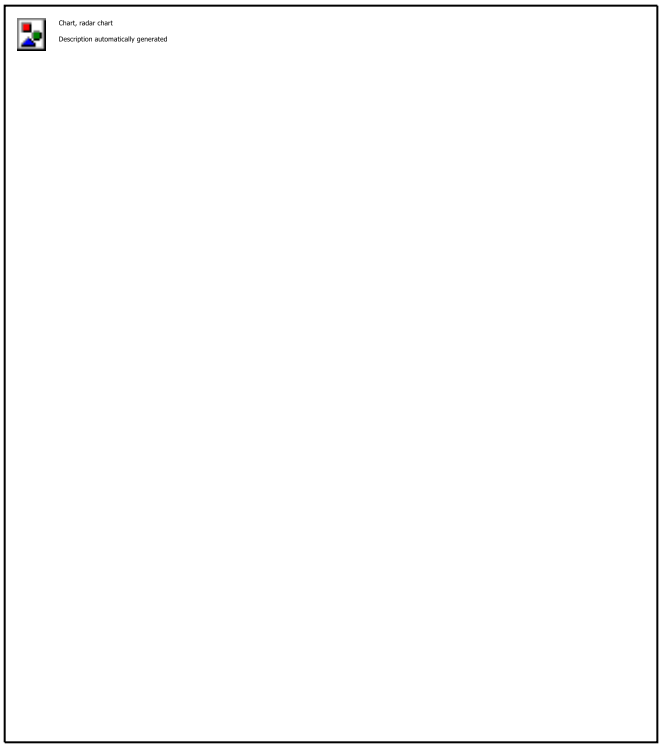

Figure 11: Redesigned STARR-seq plasmid.

The redesigned STARR-seq plasmid removes the super core promoter and uses the origin of replication (yellow) as the promoter. In addition, the GFP reporter (lime green) is greatly truncated.

There is evidence from the Reddy lab that the redesigned STARR-seq plasmid increases the signal to noise ratio on its own. In my assays, I used a plasmid library with the redesigned vector at the same time as altering the transfection protocol. It is impossible to assign contribution to either of these changes but the combination of the two changes together greatly reduced the noise of the STARR-seq output libraries. Bigwig tracks of the old protocol (Figure 12A) and the new protocol (Figure 12B) show clear differences in coverage and smoothness of bigwig files. Peaks of higher activity are easier to discern by eye.

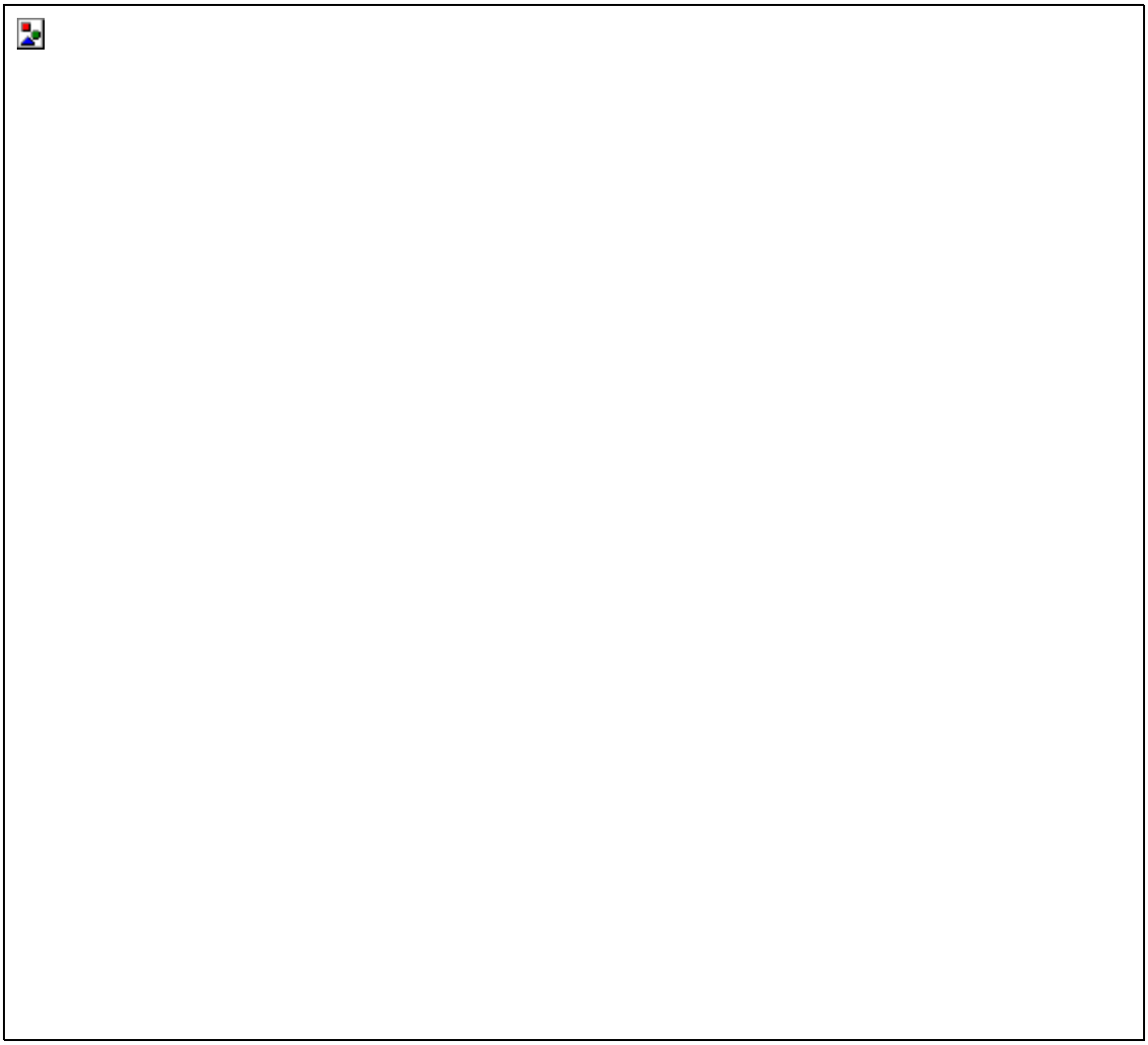

Figure 12: Old STARR-seq vector and protocol compared to redesigned vector and protocol.

A. STARR-seq output library of control (pink) and decidualized (blue) cells collected 48 hours after transfections with super core promoter driven plasmid. B. STARR-seq output library of control (green) and decidualized (purple) cells collected 6 hours after transfection with origin of replication driven plasmid. The library covering the WNT4 gene (navy) is shown in in all panels.

2.2.5 CRADLE and STARR Peaker have different peak thresholds

To analyze STARR-seq output libraries and detect peaks of regulatory activity, two published analysis tools were used, STARRPeaker (Lee *et al.*, 2020) and CRADLE (Kim *et al.*, 2021). Both tools correct biases that exist in STARR-seq library preparation and call peaks after correction. STARRPeaker uses folding energy, GC content and mappability in a negative binomial distribution model to correct biases. CRADLE, on the other hand uses DNA structure effects on fragmentation (as measured by propeller twist), Gibbs free energy, G quadraplex stability and mappability in a generalized linear regression model to correct biases.

While STARRPeaker uses sequence biases to call peaks, it does not directly correct the signal of the library. It created bigwig files of the p value and q value (FDR) along each section of the genome (Figure 13). CRADLE, on the other hand, creates a correct signal track after bias correction (Figure 13). This corrected signal also included negative values where fewer sequencing reads were found in a locus than expected by genomic predictors. CRADLE and STARRPeaker show clear differences in corrected signal (Figure 13B). While some major signals still appear in all algorithm output, minor peaks appear to be amplified by one algorithm while diminished by another.

Figure 13: Comparison of STARR-seq signal correction algorithms.

Uncorrected signal (green) compared to CRADLE corrected results (purple for positive and gold for negative) and STARRPeaker q-value (pink) for the same region overlapping the WNT4 gene (A) and the intragenic region on chromosome 5 (B). Black boxes above the tracks indicated CRADLE positive peaks.

Peak calling itself is substantially different between the two algorithms. STARRPeaker calls peaks individually in each library, ignoring replicate information. CRADLE, on the other hand, incorporated replicate information to create one set of peaks calls for all samples. The number of peaks called by each algorithm varied substantially for my dataset. The untreated library with the most peaks called for my data set had 21 peaks called. In the same dataset, CRADLE called 328 peaks for the set of all untreated libraries, 10 peaks in decidualized libraries, and 8 peaks in decidualized libraries compared to untreated libraries. Untreated libraries had significantly more coverage than decidualized libraries, likely contributing to the variation. Additionally, CRADLE identifies regions where less signal is detected than expected. Od the 329 peaks called by CRADLE, 200 (61%) were negative signals indicating repression.

CRADLE-positive peaks are found within Hi-C interactions (Sakabe *et al.*, 2020) to the promoters of genes thought to play a role in preterm birth. Multiple CRADLE positive peaks are found in an WNT4 interaction near the gene itself (Figure 14A). CRADLE positive peaks are also identified within interactions near EEFSEC and regions

distal to EEFSEC that interact with the EEFSEC promoter in decidual term in labor cells (Figure 14B).

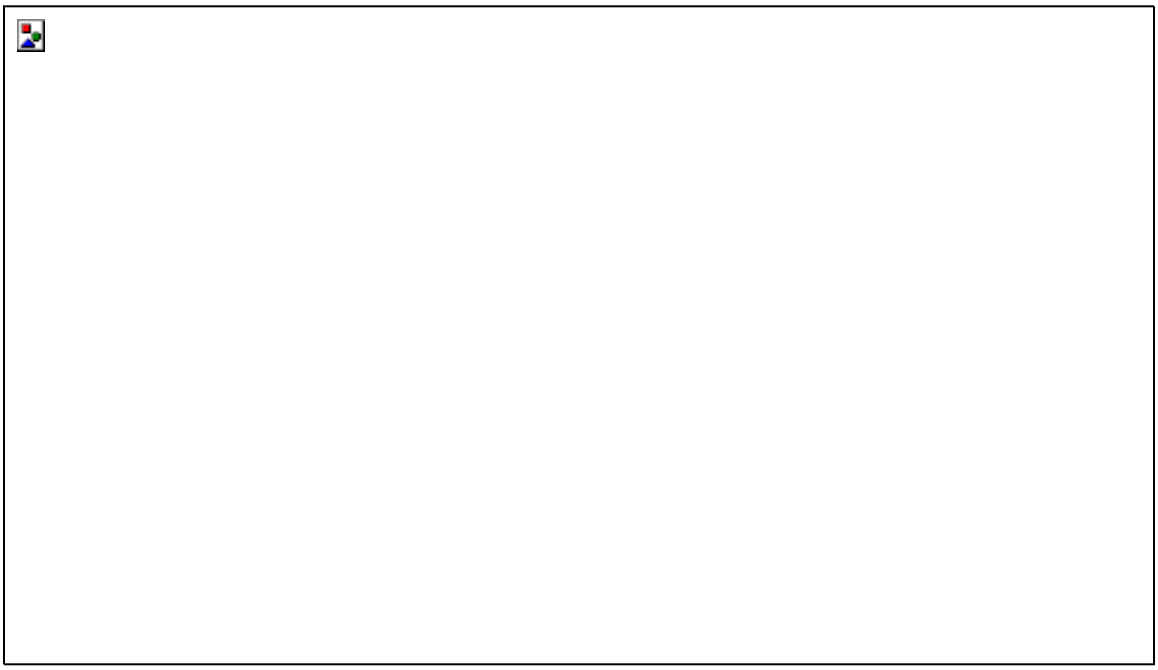

Figure 14: Hi-C Interaction in primary decidual cells from term labor.

CRADLE positive peaks (black) are found within promoter interactions near the promoter itself (green) and distal to the promoter (orange) for the WNT4 loci (A) and the EEFSEC loci (B).

2.2.6 Motif analysis

To further understand regulation at preterm birth GWA region, I analyzed transcription factor motifs enriched within called STARR-seq peaks. Identifying enriched motifs within peaks will allow us to connect regulation in the STARR-seq library with the transcription factors that impact activity. To discover enriched motifs,

positive and negative peaks sets were analyzed separately with AME (Analysis of Motif Enrichment) from the MEME suite (McLeay and Bailey, 2010). AME compared a set of motifs from a database specified (HOCOMOCO v11 Full) to the sequences it receives as input.

In the positive peaks of untreated libraries, the top motif enrichment scores are interferon response related genes (STAT2, IRF1, IRF3) as is commonly seen in STARR-seq libraries (Muerdter *et al.*, 2018) due to the cell response to foreign DNA. The motif for RBPJ was also enriched in the positive untreated peaks. Although RBPJ is known to be involved in the immune response, in the endometrium, its role in tissue repair is more important, failure of RBPJ to repair tissue injury in the endometrium has been linked to recurrent pregnancy loss (Strug *et al.*, 2018).

One of the top identified motifs outside immune response was for FOXO1. FOXO1 not only regulates about 15% is decidualization related genes directly (Adiguzel and Celik-Ozenci, 2021), but play a crucial role regulating cell processes such as polarity and proliferation to maintain homeostasis (Fan *et al.*, 2012; Kajihara, Brosens and Ishihara, 2013; Vasquez *et al.*, 2018; Adiguzel and Celik-Ozenci, 2021). The association with FOXO1 binding and CRADLE peaks can also be seen in ChIP-seq data. FOXO1 ChIP-seq from immortalized endometrial stromal fibroblasts (DeMayo Lab, unpublished) identifies peaks of binding that align with CRADLE positive peaks (Figure 15). FOXO1 also interacts with another top transcription factor identified, SOX4. SOX4

is regulated by progesterone and estrogen (Hunt and Clarke, 1999) and directly regulates FOXO1 expression and stabilizes the progesterone receptor to promote decidualization (Huang *et al.*, 2022).

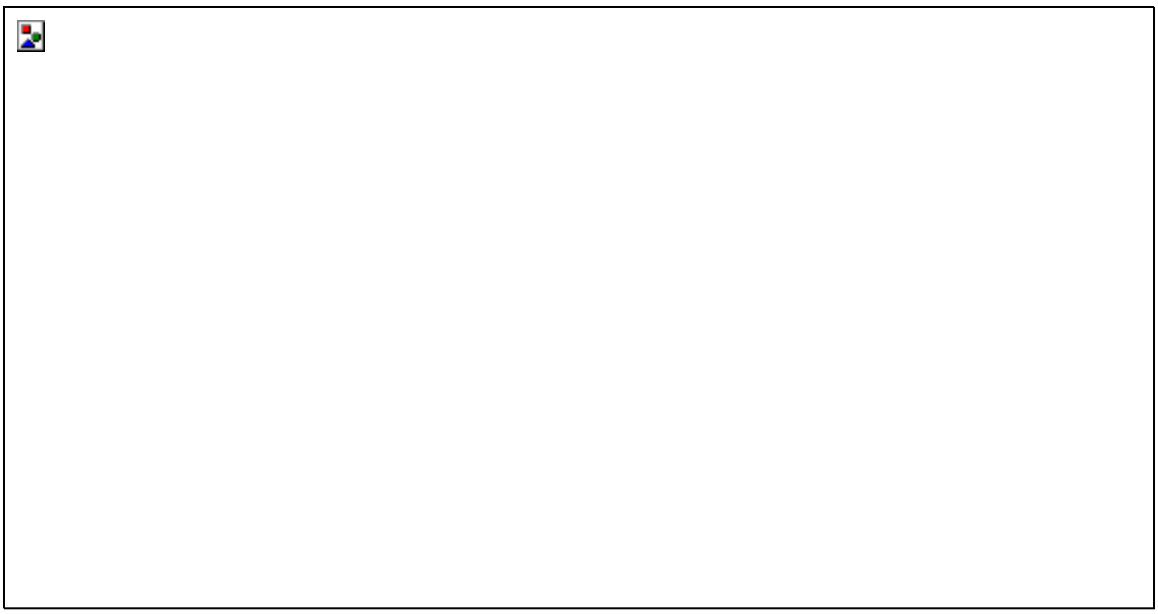

Figure 15: CRADLE positive peaks (black) align with FOXO1 ChIP binding (light blue) in the WNT4 loci.

The interpretation of motifs enriched in negative peaks is less clear unless the bound protein is a transcriptional repressor. The transcriptional repressor PRDM6 was enriched in negative peaks in the control library and the only repressor enriched in all motif sets. Although not well-studied in female reproductive tissue PRDM6's role promoting cell proliferation as a consequence of repression (Davis *et al.*, 2006) is aligned with the proliferative state of endometrial cells that have not undergone decidualization.

The SRY motif was also enriched in negative peaks, potentially due to the repression of XY specific gene expression in XX endometrial cells (Poulat, 2021).

Several motifs emerged specifically in positive peaks of decidualized cells. The motif of the steroid hormone mineralocorticoid receptor was the most enriched motif in decidualized libraries. That enrichment is consistent with evidence that decidualization is associated with the concurrent decrease of glucocorticoid receptor and increase in mineralocorticoid receptor (Kuroda *et al.*, 2013). Another decidualization related transcription factor identified in this dataset was ATF3. ATF3 is downregulated in women with recurrent implantation failure due to incomplete decidualization but overexpression of ATF3 in cells derived from theirs patients increases decidual marker genes and almost completely rescues the original phenotype (Wang *et al.*, 2021). This dataset also identified BMAL1 enriched in decidualized positive peaks. Similar to ATF3, BMAL1 downregulation has been shown to lead to impaired decidualization and recurrent implantation failure (Lv *et al.*, 2019).

2.3 Discussion

Although we have significant evidence that maternal genetics contributes to preterm birth (Crider, Whitehead and Buus, 2005; Menon *et al.*, 2006; Zhang *et al.*, 2015; Di Renzo, Tosto and Giardina, 2018), understanding biological mechanisms that lead to preterm birth risk is still complicated. Recently, the largest genome wide association study completed to date (Zhang *et al.*, 2017) took advantage of the explosion of genetic

information available to consumer genetic testing services to investigate the genetic underpinnings of risk of preterm birth.

Previous genetics studies of preterm birth limited the search space to immune related genes (Crider, Whitehead and Buus, 2005; Menon *et al.*, 2006). A genome wide approach, however, identified loci seemingly unrelated to immune function. Instead, the loci identified implicated the decidualization of the uterine endometrium with the identification of the WNT4 loci (Zhang *et al.*, 2017). Although the decidualization of the endometrium occurs in early pregnancy, it is hypothesized to affect pregnancy outcomes throughout the span of pregnancy (Gellersen, Brosens and Brosens, 2007; Mori *et al.*, 2016; Ng *et al.*, 2020). We simulated the process of decidualization in vitro by treating cells with progesterone and cAMP for 48 hours. Key decidualization marker genes, Prolactin and IGFBP1, were activated in response to this stimulus.

This system allowed us to identify putative enhancers involved in decidualization and undifferentiated endometrial cells using STARR-seq. To limit our search space, we created a plasmid library from Bacteria Artificial Chromosomes that span GWA regions from Zhang et. al 2017. This library was transfected into endometrial stromal fibroblast cells. We discovered, to best capture STARR-seq transcripts and increase the signal to noise ratio of our STARR-seq output libraries, STARR-seq vectors using the origin of replication as a promoter and limited transfection to harvest time to six hours worked best for our system.

The creation of STARR-seq libraries introduces biases that could impact results. Multiple methods to deal with this bias currently exist and the field has yet to settle on one in particular. STARRPeaker (Lee *et al.*, 2020) and CRADLE (Kim *et al.*, 2021) both correct signal in STARR-seq library by modeling information about DNA sequence information and call peaks incorporating this information. Differences in modeling parameters and peak calling lead to variation in which and how many peaks are called.

Regions of significant regulatory activity identified in STARR-seq can be used to identify enriched motifs and signaling pathways involved. Transcription factors known to play a role in baseline endometrial cell processes, such as FOXO1 and SOX4, were identified as enriched in STARR-seq putative enhancers. These putative enhancers also overlap FOXO1 binding identified in ChIP-seq. Additional transcription factors involved in the process of decidualization, such as BMAL1 and ATF3, were identified in regulatory regions activated by decidualization.

While STARR-seq peaks suggest regions of regulatory activity, interpretation often relies on integration with ChIP-seq, Hi-C, or epigenome editing information. The collection of ChIP-seq and promoter capture Hi-C information has improved our interpretation of STARR-seq peaks for endometrial stromal cells. Additional ChIP-seq datasets for factors suggested by motif analysis could add to our understanding of gene regulation within these regions at endometrial stromal fibroblasts.

While we can identify putative enhancers from STARR-seq that interact with gene promoters, we do not have direct evidence of their effects. To strengthen the evidence of association between a STARR-seq positive region and the gene itself, CRISPR epigenome editors can be targeted to STARR-seq peaks. Analyzing the effects of dCas9-P300 or dCas9-KRAB targeted to a STARR-seq peak on gene expression broadly should identify causal links between altered regulation in putative enhancers and the genes they effect.

2.4 Methods

2.4.1 Decidualization of endometrial stromal fibroblasts

Endometrial stromal fibroblasts immortalized by hTERT were obtained from ATCC (ATCC, Manassas. VA). Cells were grown in phenol-red free high glucose DMEM (Thermo Fisher Scientific, Waltham, Massachusetts) supplemented with 10% charcoal stripped FBS (Thermo Fisher Scientific, Waltham, Massachusetts) and 100x Penicillin-Streptomycin (10,000U penicillin, 10,000 μg streptomycin, Thermo Fisher Scientific, Waltham, Massachusetts) and L-glutamine to a final concentration of 2 mM (Thermo Fisher Scientific, Waltham, Massachusetts).

To begin decidualization, cells were split into control of treated groups. Cells in the control group were grown in a limited media of phenol-red free high glucose DMEM (Thermo Fisher Scientific, Waltham, Massachusetts) supplemented with 2% charcoal stripped FBS (Thermo Fisher Scientific, Waltham, Massachusetts) and pen-strep and L-

glutamine as described above. Cells exposed to the treatment media were grown in limited media of phenol-red free high glucose DMEM (Thermo Fisher Scientific, Waltham, Massachusetts) supplemented with 2% charcoal stripped FBS (Thermo Fisher Scientific, Waltham, Massachusetts) and pen-strep and L-glutamine as described above with 50 uL of 10 mM MPA stock formulation (for a final concentration of 1μM) and 100 mg of cyclic AMP (for a final concentration of 0.5 mM).

After 48 hours in control of treatment media, cells were lysed with RLT and RNA was isolated with the Qiagen RNeasy mini kit (Qiagen, Hilden, Germany) with the optional on column DNase. Complementary DNA was synthesized using Superscript 3 with and oligo dT primer (Thermo Fisher Scientific, Waltham, Massachusetts). The expression of decidualization marker genes Prolactin (Assay ID: Hs01062137_m1) and IGFBP1 (Assay ID: Hs00236877_m1) was assessed in comparison to control gene MALAT1 (Assay ID: Hs00273907_s1) by RT-qPCR using TaqMan probes.

2.4.2 Creation of plasmid library

Bacterial artificial chromosomes were streaked onto LB agar plates with 12.5 ug/mL chloramphenicol. Single colonies were selected and grown in 2 liters of LB broth with 12.5 ug/mL of chloramphenicol. BAC DNA was isolated from bacterial with the Machery-Nagel Nucleobond XtraBAC kit (Macher-Nagel, Düren, Germany). BACs were then sheared by sonication using the Covaris S2 system (Covaris, Woburn, Massachusetts) (Intensity: 3; Duty Cycle: 5%, Cycles/Burst: 200; Time: 80 s; volume level:

12). Sheared DNA was size selected to around 500 base pairs using Corning solid-phase reverse immobilization (SPRI) beads (Corning, Ithaca, New York). STARR-seq adaptors (Arnold *et al.*, 2013) were ligated to sheared BAC DNA using the NEBNext kit (New England Biolabs, Ipswich, Massachusetts) and purified by SPRI beads. Indices were added by PCR to an aliquot to be sequenced on a MiSeq for verification. STARR-seq adaptor primers (Arnold *et al.*, 2013) were added by 6 cycles of PCR using the NEB Q5 PCR Kit with GC buffer (New England Biolabs, Ipswich, Massachusetts). PCR products were purified by SPRI beads to remove primer dimers.

PCR products were cloned into linearized STARR-seq vector (Figure 7A or 11) using NEBuilder HiFi DNA Assembly Cloning Kit (New England Biolabs, Ipswich, Massachusetts). Products were purified by two successive SPRI bead cleans. Cloned plasmids were transformed into fresh ElectroMAX DH10B Cells (Thermo Fisher Scientific, Waltham, Massachusetts) by electroporation. Transformants recovered for one hour with SOC media shaking at 37°C. Transformants were then pooled and added to 3 1L flask of LB broth supplemented with 100 ug/mL carbenicillin to grow overnight. Plasmids were isolated with Machery-Nagel Endotoxin free Giga-prep kit (Machery-Nagel, Düren, Germany).

2.4.3 Transfection of STARR-seq plasmids

2.4.3.1 Forty-eight-hour transfection time

Endometrial stromal fibroblasts were grown in standard media to expand. Fifty-eight million cells were trypsinized from cell culture plates and spun down at 90xg for ten minutes. Cells were resuspended in SE media from SE Cell Line 4D-Nucelofector X Kit S (Lonza, Basel, Switzerland) and 60 ug of plasmid library was added to the cells. Immediately, 100uL of the cell and plasmid mixture was added to each of 24 cuvettes and electroporated using the CA-137 protocol on the Lonza 4D-Nucleofector (Lonza, Basel, Switzerland). Cells rested for 10 minutes in the cuvettes and then 1mL of control media was added to each. Cells were removed from each cuvette and pooled. Pooled cells were plated on 10 500 cm^2 plates. Control media was added to five plates and treatment media was added to five plates. Media formulations are described above. Twenty-four hours later, appropriate fresh media was added to all plates. Forty-eight hours after transfection, media was removed from all plates and 4 mL of RLT was added directly, moved to a 50 mL conical tube and placed in the -80°C freezer.

2.4.3.2 Six-hour transfection time

Endometrial cells were passaged and split into 12 500 cm^2 plates. Control media was added to six plates and treatment media to the other six. Forty-two hours later, 50 million cells from each condition were collected and pooled separately. Cells were spun at 90xg from 10 minutes. Cells were resuspended in SE media from SE Cell Line 4D-

Nucelofector LV Kit L (Lonza, Basel, Switzerland) and 100 ug of plasmid library was added to each cell pool. Cell plasmid solution was injected into a separate 1 mL nucleocuvette cartridge (Lonza, Basel, Switzerland) for each condition and nucleofected by program CA-137. Cells were removed from each cartridge and the cartridge was rinsed with control media. Some cells were lost from the treatment media cartridge. Control media was added to each cell pool. Control cells were plated onto five 500 cm^2 plates with control media and decidualized cells were plated onto five 500 cm^2 plated with treatment media. Six hour later, media was removed from all plated and 4 mL of RLT was added. This was removed and placed in at 50 mL conical tube where it was then placed in the -80°C freezer.

2.4.4 Creation and sequencing of STARR-seq libraries

Cell lysates were thawed, and RNA was isolated from the RNeasy Midi kit with the on-column DNase step (Qiagen, Hilden, Germany). RNA from control and treatment cells was pooled separately and three 75 ug aliquots were used for all subsequent library steps. Poly-A RNA was isolate with Dynabead Oligo-dT25 beads (Thermo Fisher Scientific, Waltham, Massachusetts) according to the manufacturer's recommended protocol. RNA was treated with Turbo DNase with 1 uL of RNase block added (Thermo Fisher Scientific, Waltham, Massachusetts) for 30 minutes. The reaction was stopped the DNase inactivation reagent provided within the Turbo DNase kit. RNA was reverse transcribed for 2 ½ hours with Superscript 3 reverse transcriptase (Thermo Fisher

Scientific, Waltham, Massachusetts) using a gene specific primer that has an eight nucleotide UMI. Following reverse transcriptase inactivation, cDNA is then incubated with 1 uL of RNase A at 37°C for one hour and then purified with SPRI beads. Products were enriched with 10 cycles of PCR using Illumina index primers following the protocol 98 °C with the Kapa HiFi Hotstart polymerase kit (Roche, Basel, Switzerland) using the optional GC Buffer. Cycling conditions were 95 °C for 3 minutes, followed by 10 cycles of 98 °C for 20 s, 67.2 °C for 15 s, 72 °C for one minute, with a final extension at 72 °C for 5 min. Five uL of sample is removed and used for a RT-qPCR reaction to assess how many cycles are needed for further enrichment. The RT-qPCR reaction uses the Kapa HiFi Hotstart kit (Roche, Basel, Switzerland) as described and 100x Sybr. The original samples then undergo additional PCR for the number of cycles needed to reach 1/3 of maximum signal in the qPCR. The samples are then cleaned up and primer dimer is removed with SPRI beads. Samples were quantified by Qubit (Invitrogen, Waltham, Massachusetts) and assed by DNA screen tape (Agilent, Santa Clara, California).

2.4.5 Sample sequencing and alignment

Samples were sequenced with a Nextseq 500 using paired end 50 base pair sequencing in high output mode. Each end of the fragment and the UMI were sequenced separately. STARR-seq libraries were aligned to human genome assembly hg38 by Bowtie2 (version 2.2.4, Langmead and Salzberg, 2012) with parameters bowtie2 -X 2000 sensitive. Successfully paired alignments with mapping quality scores (MAPQ)

greater than 30 that were not aligned to hg30 centromeres, gaps or blacklist regions were retained. UMI duplicates were marked and removed with Picard (*Picard toolkit*, 2019).

2.4.6 Reduction of signal and peak calling with CRADLES

Signals at overlapping BAC regions were normalized to signal at non-overlapping regions. CRADLE correctBias was run with the input library bigwig track as the control bigwig and the treatment or untreated bigwigs as the experimental bigwigs. Bias types of shearing, PCR, mappability, and g quadraplex structure were included. The covariate matrix for fragment length size 300 was used. ENCODE blacklist regions were removed.

To call peaks, CRADLE callPeaks was used with the input library bigwig track as the control bigwig and the treatment or untreated bigwigs as the experimental bigwigs or the intreated bigwigs as the control bigwigs and the treatment bigwigs as the experimental bigwigs. False discovery rate threshold of 0.05 was used for all peak calling.

2.4.7 Reduction of signal and peak calling with STARR-Peaker

STARRPeaker was run for all output files. ENCODE blacklist (Amemiya, Kundaje and Boyle, 2019) regions were removed. GC content in a 5 base pair window, mappability in a 100 base pair window and linear folding energy on a 100 base pair window were included as parameters. False Discovery rate of 0.05 was used for all peak calls.

2.4.8 Motif analysis within peaks

BED files of motifs were split into positive or negative peaks. Bed files were converted to FASTA files with BEDTools (version 2.25, Quinlan and Hall, 2010). Enriched motifs were identified with the Analysis of Motif Enrichment (AME) tool in the MEME suite (version 5.4.1, McLeay and Bailey, 2010). Motif enrichment was assessed compared to shuffled sequences. Motifs from the HOCOMOCO v11 full database (Kulakovskiy *et al.*, 2018) were used for comparison. Sequences were scored by the total odds score and motif enrichment was determined by Fisher's exact test. Enriched motifs had an E-value less than or equal to 10.

3. Glucocorticoid regulated KCNA5 Mediates Cell Proliferation in Human Fetal Membranes[2]

3.1 Introduction

Preterm premature rupture of membranes (PPROM) is a leading cause of preterm births. PPROM is defined be rupture of the fetal membrane rupture before 37 weeks of gestation. PPROM is the leading identifiable cause of preterm birth, accounting for 30-40% of cases (Mercer, 2010). The amnion epithelial layer plays a crucial role in membrane integrity. Amnion epithelial cells are constantly turning over and remodeling (Martin, Richardson and Menon, 2018). Amnion epithelial proliferation is crucial to wound repair and microfracture repair in the fetal membranes. The amnion epithelial layer proliferates to repopulates itself, and undergoes epithelial mesenchymal transition to repopulate the collagen producing mesenchymal layer beneath it (Richardson and Menon, 2018).

One contributing factor to all cause preterm birth and to PPROM specifically is maternal psychological stress. Maternal adversity is an independent predictor of preterm births (Olsen, 2018; Sulaiman *et al.*, 2021; Hardcastle, Ford and Bellis, 2022). In one study of PPROM specifically, women under psychological stress had 100 times

[2] This chapter is adapted from Cunningham et. al 2022, In Review. Laavanya Sankaranarayanan assited with optimization of overexpression studies. Alex Barrera assisted with ChIP-seq analysis and aligning RNA-seq. Terrence Allen and Tim Reddy helped with study design and manuscript writing.

greater risk of PPROM compared to unstressed mothers (Lilliecreutz *et al.*, 2016). Even though the risk for PPROM is high, preventative strategies are limited (Goldenberg *et al.*, 2008).

A potential mechanism by which maternal stress impacts gestation is via cortisol signaling. Psychological stress increases circulating cortisol, in some cases up to five fold (Ranabir and Reetu, 2011). The effect of elevated glucocorticoid levels long term is counter to expectations. In chronic stress conditions, gene expression changes show reduced glucocorticoid receptor activation and related gene expression and increased pro-inflammatory signaling in response to the same levels of cortisol (Cole *et al.*, 2007; Miller *et al.*, 2008, 2009; Rohleder *et al.*, 2009; Cohen *et al.*, 2012).

The interplay of psychological stress and altered cortisol levels has been shown to affect birth timing. Cortisol signaling likely plays an important role in labor initiation as evidenced by the surge in maternal, fetal and amniotic fluid levels of glucocorticoids close to term (Goldkrand, Schulte and Messer, 1976; Smith, 2007; Guo *et al.*, 2014). There is evidence of altered cortisol regulation in pregnant women who have experienced adverse childhood experiences (Bowers *et al.*, 2018; Thomas *et al.*, 2018). There is also association between plasma cortisol levels and the recurrence of preterm birth. Specifically, median maternal plasma cortisol levels are elevated in women who have had one isolated preterm birth, and elevated further in women who have had recurrent

preterm birth (Mercer *et al.*, 2006). There is a link between elevated cortisol and maternal depression that is thought to increase risk for preterm birth (Diego *et al.*, 2009).

Elevated cortisol levels contribute to myriad physiological effects including immunosuppression (Venkatesh *et al.*, 2015; Ramezani *et al.*, 2020), impaired wound healing (Mattern, Büchler and Herr, 2007; Walburn *et al.*, 2009), and other detrimental effects (Björntorp, 1997; Raff *et al.*, 1999; Faresjö *et al.*, 2020). The causes of impaired wound healing include cortisol-dependent effects on cell proliferation such as cell cycle arrest (Mattern, Büchler and Herr, 2007; Walburn *et al.*, 2009). Of particular relevance here, glucocorticoid signaling is intact in the amnion (Pringle *et al.*, 2015). Glucocorticoids have an anti-inflammatory effect in the amnion, the primary weight bearing layer in fetal membranes (Marinello, Feng and Allen, 2020). Medroxyprogesterone acetate (MPA), known to have glucocorticoid activity, has also been shown to inhibit cytokine induced matrix metalloproteinase and chemokine release in both primary amnion epithelial and mesenchymal cells via the glucocorticoid signaling pathway (Allen *et al.*, 2019; Marinello, Feng and Allen, 2020). Another study showed that in the amnion epithelial cells of fetal membranes, a local increase in glucocorticoids stimulates apoptosis via the tissue-type plasminogen system activation of caspase 3 (Wang, Liu and Sun, 2016).

At a molecular level, cortisol and related glucocorticoids act by altering gene regulation via the inducible transcription factor activity of the glucocorticoid receptor

(George, Schiltz and Hager, 2009; Meijsing *et al.*, 2009; McDowell *et al.*, 2018; Timmermans, Souffriau and Libert, 2019). In this study, we sought to determine the role of glucocorticoid signaling in maintaining fetal membrane integrity. To do so, we investigated glucocorticoid-dependent changes in gene expression in cultured primary amnion epithelial cells. That analysis revealed increased expression of the voltage gated potassium ion channel KCNA5. We further show that KCNA5 impacts proliferation in amnion epithelial cells, suggesting a molecular mechanism by which glucocorticoid signaling can contribute to PPROM.

3.2 Results

3.2.1 Glucocorticoid-mediated gene expression responses in the primary amnion epithelial cells

Previous research has shown that medroxyprogesterone acetate (MPA) attenuates the response of primary amnion cells to tumor necrosis factor alpha (TNFα) induced matrix metalloproteinase 9 (MMP9) expression and activity (Allen *et al.*, 2019). MMP9 upregulation in fetal membranes is associated with reduced tensile strength (Uchide *et al.*, 2000) and more frequent spontaneous rupture (Athayde *et al.*, 1998). Allen et al. 2019 (Allen *et al.*, 2019) demonstrated that the ability of MPA to counteract the pro-inflammatory pathways of TNFα was mediated primarily through the GR in amnion epithelial cells, demonstrating the role of GR in molecular mechanisms that lead to PPROM.

To investigate the broader consequences of MPA-dependent glucocorticoid responses on TNFα challenge in amnion epithelial cells, we measured gene expression changes in primary amnion epithelial samples from ten patients (Allen *et al.*, 2019) using RNA-seq. To identify GR-dependent effects, we compared MPA responses in cells with and without glucocorticoid receptor knock down, and with or without TNFα challenge. We sequenced the RNA-seq libraries using paired-end 25 bp reads on Illumina sequencing instruments. We sequenced between 7.5 and 215 M reads per sample, and read quality was high for all samples (Table 3-Appendix A).

Most (67%) of the variation in gene expression between samples can be attributed to the patient (Figure 16A). To account for patient variability when estimating the gene expression effects of GR knockdown and TNFα challenge, we used a linear mixed model with the patient identifier as a random effect. That model identified 1041 genes with significantly altered gene expression by GR knockdown compared to a control siRNA in the presence of MPA (Figure 16B). That result supports the ability of MPA to act through the GR. The genes significantly altered include known glucocorticoid-responsive genes including members of the interleukin and interferon family (Shimba and Ikuta, 2020), KLF9 (Chinenov *et al.*, 2014), and PER1 (Balsalobre *et al.*, 2000) (Figure 17).

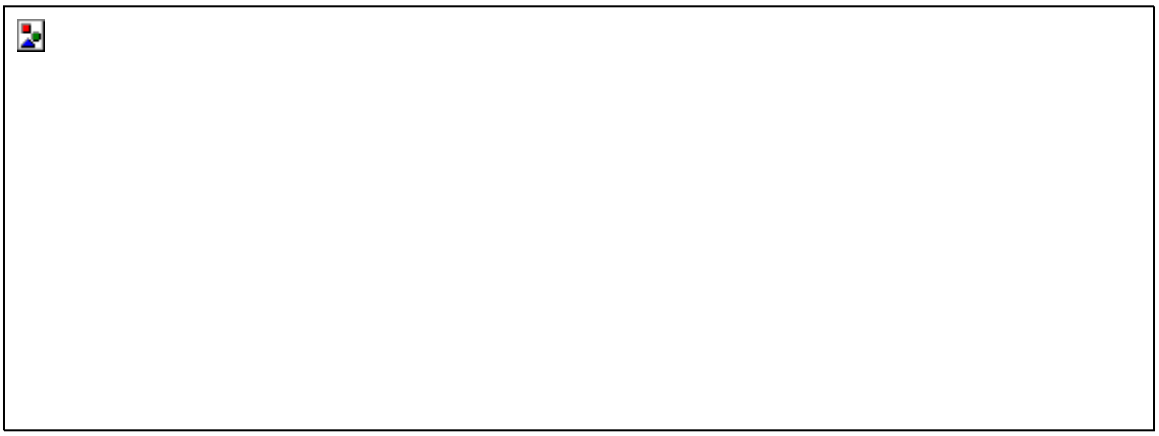

Figure 16: Clustering of libraries and differentially expressed genes.

A. Principal component analysis of RNA-seq libraries. Each patient corresponds to an individual color. Glucocorticoid receptor knockdown libraires are represented by triangle icons and control siRNA libraries are represented by open circles. B. MA plot showing differentially expressed genes. Each point on the graph represents a single gene. The x axis represents average log base 2 expression of reads after normalizing by library size and the y axis represents log base 2-fold change. Red points are significantly downregulated, blue points are significantly upregulated and black point are not significantly different between glucocorticoid receptor knockdown and control siRNA.

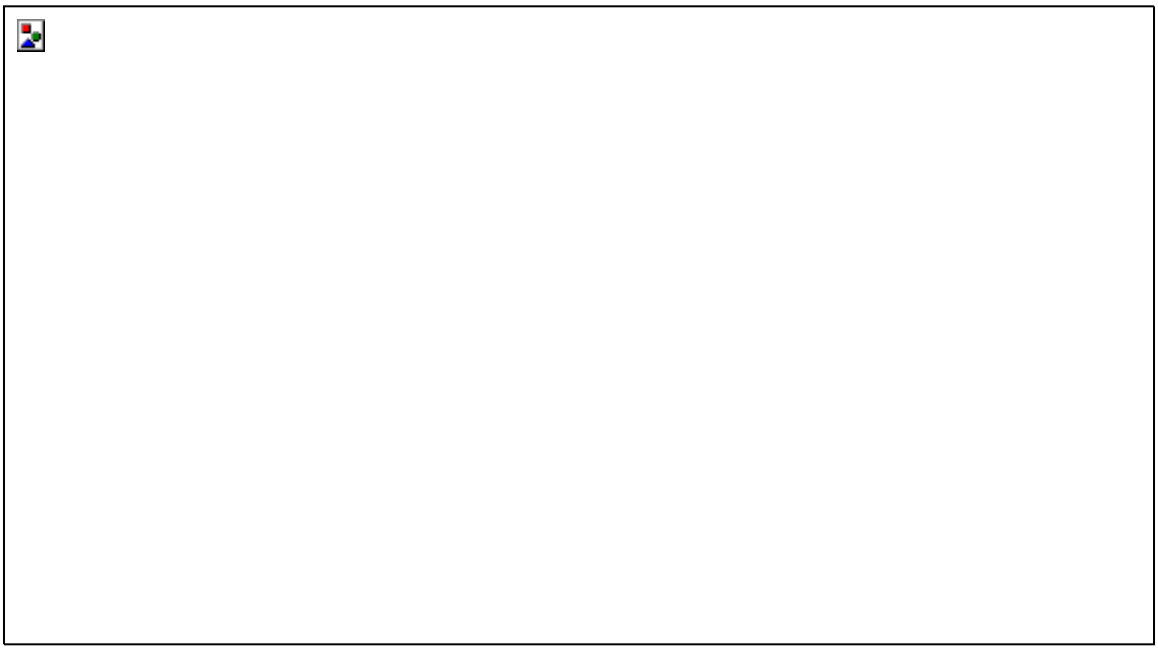

Figure 17: Known glucocorticoid regulated genes.

We found known glucocorticoid regulated genes OAS1 (A), OAS2 (B), KLF9 (C), IL-34 (D), IL-20RB (E), PER1 (F) to be differentially regulated by glucocorticoid receptor knockdown. Gene counts were first normalized by library size. The bar plots in red represent samples treated with a control siRNA and the ones in blue represent the glucocorticoid receptor knockdown.

We prioritized one gene, KCNA5, for follow up study. KCNA5 was significantly upregulated by GR knockdown ($\beta = 2.9$, false discovery rate [FDR] = 0.0002). KCNA5 is a member of the Shaker family of potassium ion channels that have been implicated in cell differentiation and proliferation. The role of KCNA5 in proliferation has been shown in several cell types. In Ewing sarcoma cells, KCNA5 acts as a cell stress sensor and reduces proliferation in response to DNA is damage. When silenced, cells proliferate

more rapidly following this damage (Ryland *et al.*, 2016). Repression of KCNA5 also decreases apoptosis in cell stress conditions is Ewing sarcoma cells (Ryland *et al.*, 2015). Reducing KCNA5 expression by siRNA in granulosa cells induces proliferation for 72 hours (Gao *et al.*, 2020). Conversely, upregulation of KCNA5 increased caspase 3 activity and apoptosis in kidney fibroblast-like cell line COS-7 (Brevnova *et al.*, 2004).

Alterations of proliferation and apoptosis could affect the barrier function of the membrane. Amnion epithelial cells increase proliferation in response to injury and microfractures of the membranes. A portion of the newly created amnion epithelial cells then undergo epithelial mesenchymal transition to repopulate the collagen producing mesenchymal layer beneath it (Richardson and Menon, 2018). Disruptions to this process could impair the ability of the amnion to remodel to repair damage and lead to rupture of membranes.

To investigate if glucocorticoid signaling regulates KCNA5 expression in other contexts, we searched for additional examples in datasets deposited in the Gene Expression Omnibus (GEO). One study (Quatrini *et al.*, 2021) measured how glucocorticoids, specifically dexamethasone, alter human hemopoietic stem cell differentiation and gene expression. In their study, they treated CD34+ hemopoietic stem cells from three healthy donors with cytokines (FLT3LG, SCF, IL-7, and IL-15) and then treated the cells with 500 nM dexamethasone or DMSO as a vehicle control for the

total time in culture, 35 days. In that study, KCNA5 was found to be downregulated by dexamethasone by more than 20-fold (FDR = 4×10^{-6}).

3.2.2 MPA does not change enhancer histone marks after 4 hours

To understand more broadly changes in regulation due to MPA, we used Chip-seq to analyze changes in histone 3 lysine 27 acetylation (H3K27ac) in primary amnion epithelial cells. Identifying changes in H3K27ac would allow us to detect enhancers that have become active (Rada-Iglesias *et al.*, 2011) in the presence of MPA. Because human amnion epithelial cells do not express a nuclear progesterone receptor (Merlino *et al.*, 2009), changes in histone modifications are likely due to the activity of the glucocorticoid receptor.

After four hours of MPA treatment in primary amnion epithelial cells from three patients, we were able to identify 11 peaks in that were differential between cells treated with MPA and those treated with EtOH as a vehicle control (Table 2). Although many of the differential binding sites are likely to be false positives due to the small number of identified peaks, a few peaks are potentially interesting. The peak on chromosome 12 is located within the intron of CRADD. CRADD is a member of the Caspase apoptosis pathway in cells (Cohen, 1997). Another interesting peak located on chromosome 6 is found in the intron of FKBP5. FKBP5 is known to be regulated by glucocorticoids and play a role in the physiological response to stress (Zannas *et al.*, 2019). The role of FKBP5

has not been studied in fetal membranes but in maternal decidual cells, it's been thought to contribute to stress-induced preterm birth (Guzeloglu-Kayisli *et al.*, 2021).

Table 2: Location of differential peaks after four hours of MPA.

Chr	Start	End	Log2FC	Adj-P	Location Information
7	47757530	47757906	1.907	0.001	Not located near gene
7	47758166	47758642	1.841	0.001	Not located near gene
7	108309258	108309729	1.675	0.0022	Intron of NRCAM
1	192907844	192908751	1.149	0.0041	Intron of ENSG00000285280
6	25006100	25008074	0.937	0.0042	Intron of RIPOR2
8	89961659	89962320	1.212	0.0120	Intron of NBN
6	35602211	35603489	0.778	0.0138	Intron of FKBP5
7	108308534	108308980	0.992	0.0207	Intron of NRCAM
6	12370226	12371604	0.397	0.0442	Not located near gene
6	30926477	30926690	0.838	0.0442	Downstream of VARS2
2	121500342	121501156	0.622	0.0482	Intron of CLASP1
12	93809351	93810079	1.462	0.004	Intron of CRADD

3.2.3 Reduced KCNA5 expression increases proliferation in primary amnion epithelial cells but does not affect apoptosis

Based on the above results, we hypothesized that KCNA5 may contribute to PPROM by impacting cell proliferation in the amnion epithelium. As a first step to test

that hypothesis, we tested whether reduced KCNA5 expression led to increased proliferation of amnion epithelial cells. To do so, we recruited 19 additional healthy term c-section patients (Figure 18) and successfully collected primary amnion epithelial cells for knockdown from 12 patients. Gestation length varied from 37 weeks to 42 weeks. Of the 19 samples collected, four did not proliferate enough for studies described below, potentially due to cell senescence in amnion close to parturition (Behnia *et al.*, 2015). Those samples were excluded from future analysis. We then knocked down KCNA5 expression using siRNA, and measured effects relative to cells from the same patients that were treated with non-targeting siRNAs. In the samples chosen to measure knockdown, we observed an 84% reduction in KCNA5 expression on average (Figure 19). These samples were chosen based on cell number after split and the number of cells needed for ELISA studies. There was substantial variability in knockdown efficiency across patients, ranging from an increase of 46% increase (half cycle difference likely to be noise) to 97% decrease. The one sample where knockdown was not seen also had no effect in subsequent ELISA studies.

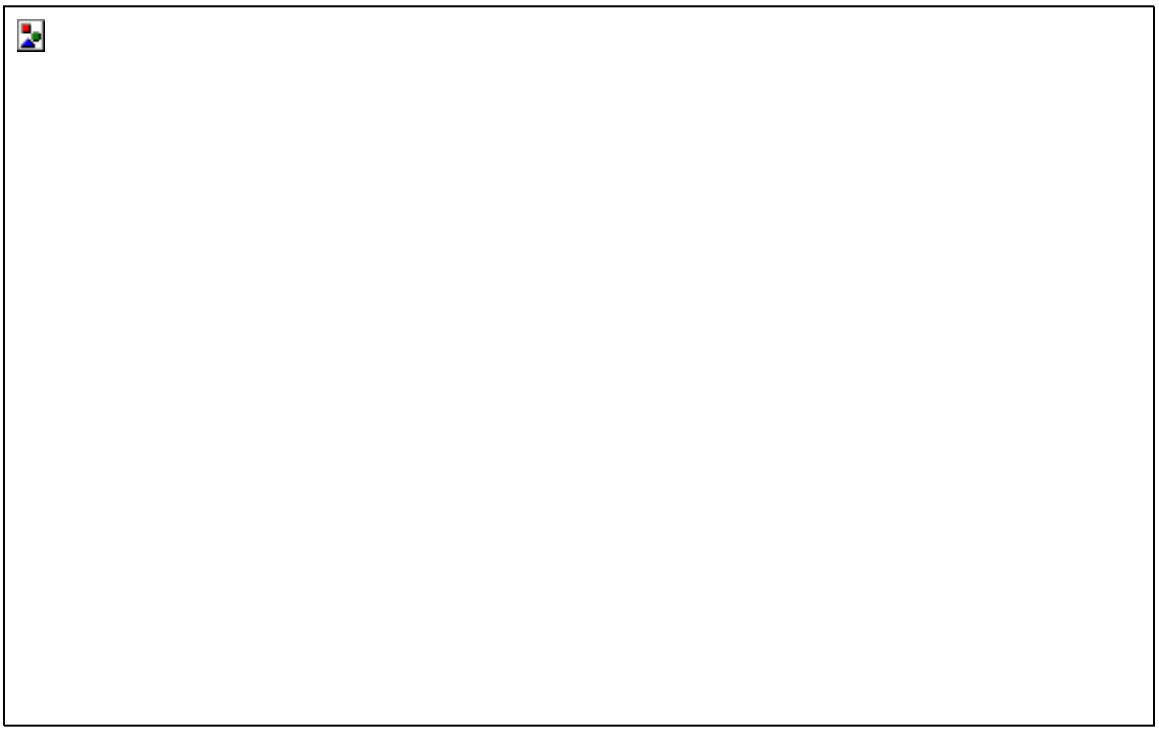

Figure 18: Diagram of tissue collection for knockdown studies.

In our study, 19 patient samples were originally collected. Of those, three samples became contaminated in culture and four samples failed to propagate. The 12 samples that were used had between 5.5 and 12 million cells at the time of split. For each patient, half of the cells were transfected with a KCNA5 siRNA and half with a control siRNA. Cells were then collected for BrdU or Caspase 3 ELISA.

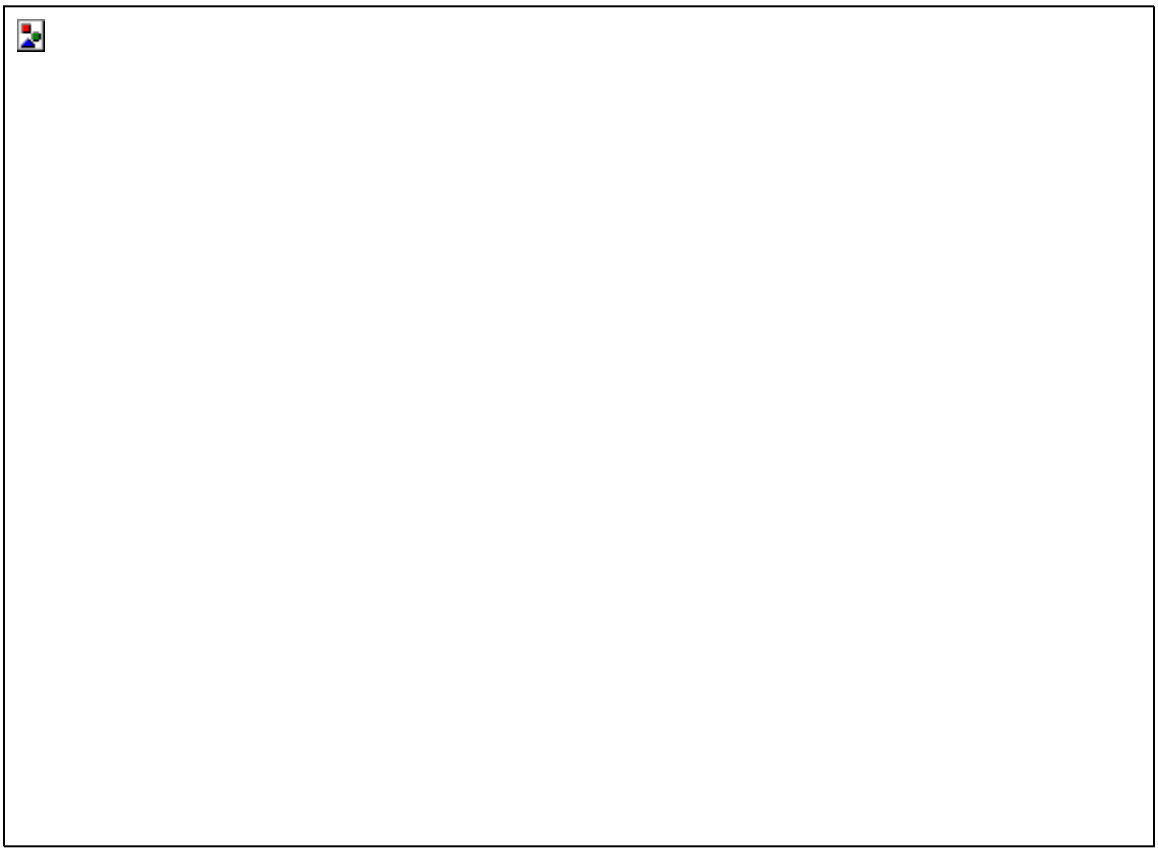

Figure 19: KCNA5 knockdown from siRNA.

qPCR was used to test knockdown efficiency by comparing KCNA5 expression to housekeeping gene ACTB. Each individual line represents a patient sample. The left are samples treated with a control siRNA and the right are samples treated with KCNA5 siRNA. Error bars represent standard error between patient samples.

To next measure the proliferative effects of changes in KCNA5 expression, we used a bromodeoxyuridine (BrdU) assay to measure changes in the amount of newly synthesized DNA when KCNA5 is knockdown. Briefly, BrdU is a synthetic nucleotide that, when included in cell culture media, integrates into newly synthesized DNA.

Changes in cell proliferation can then be estimated by measuring differences in the amount of BrdU incorporation over time.

We measured changes in BrdU incorporation with and without KCNA5 knockdown in primary amnion epithelial cells. Cells were treated with siRNA for a total of 72 hours, with BrdU included in the culture for the last 18 hours. We first completed a pilot study of three patient samples and used the preliminary results for a power calculation to determine our final population size. We estimated that 11 patient samples would give us 90% power to detect differences in proliferation due to KCNA5 knockdown. We next collected and assayed KCNA5-dependent proliferation in an additional 9 healthy term c-section patients. We observed substantial patient specific differences in proliferation. Therefore, we measured the KCNA5 knockdown proliferation relative to the control siRNA of the same patient to control for patient specific variation. By comparing knockdown effects to a value of 1 indicating no difference in siRNA samples, we estimate that KCNA5 knockdown resulted in a 19% increase in cell proliferation ($p = 0.03$, two-sided t test) (Figure 20A).

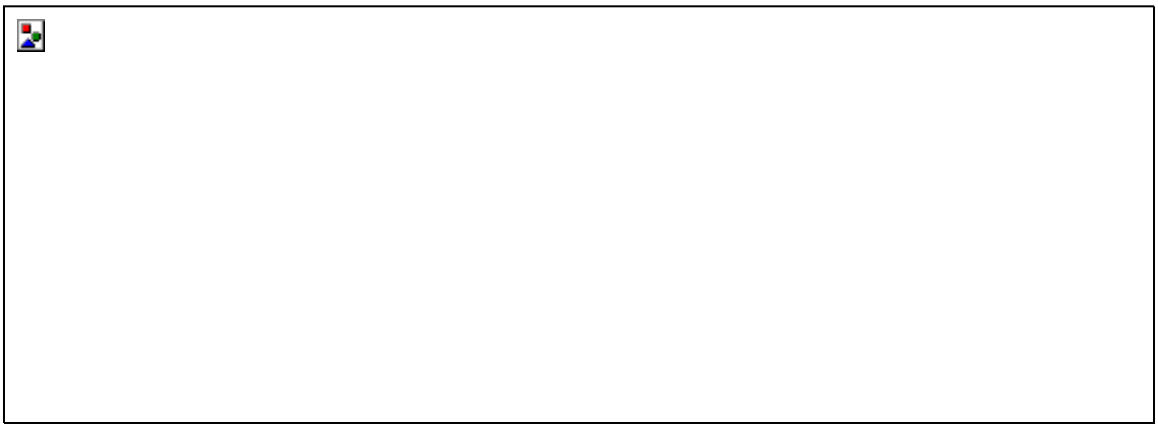

Figure 20: The effect of KCNA5 knockdown on proliferation and apoptosis.

A. Each line represents the proliferation of one patient sample relative to proliferation with the control siRNA as measured by BrdU. Eight of the 12 patients had increased cell proliferation, and the effect overall was significant (p = 0.03, t test). B. Each line represents the active caspase 3 levels in the sample. Standard error bars are shown on the knockdown side of BrdU and both sides of active Caspase 3. The solid black line at 1 shows the theoretical trace of a sample with no change between each transfected siRNA.

KCNA5 has been documented to impact both cell proliferation (Ryland *et al.*, 2015, 2016; Gao *et al.*, 2020) and apoptosis (Brevnova *et al.*, 2004). Using the same samples as above, we also tested whether KCNA5 knockdown affected apoptosis. To measure apoptosis, we measured active caspase 3 ser29 levels 72 hours after siRNA transaction, Overall, active caspase levels were low for all patients (Figure 20B), and we did not observe significant differences in active caspase levels with KCNA5 knockdown ($p = 0.547$).

3.2.4 Recruiting P300 to the KCNA5 promoter increases expression in human embryonic kidney cells

We also tested the converse hypothesis that increased KCNA5 expression reduces cell proliferation. To increase endogenous KCNA5 expression, we used a CRISPR-based epigenome editing system. In that system, catalytically inactive Cas9 (dCas9) is fused to the P300 histone acetyltransferase domain (dCas9-P300) and is recruited to target gene promoters via guide RNAs (Hilton *et al.*, 2015; Klann *et al.*, 2017). Due to a lack of cell lines to model amnion epithelial cells and challenges over expressing KCNA5 in primary amnionic cells, we used a more tractable human embryonic kidney cell line, HEK293T, that was modified to express dCas9-P300 ($HEK293T^{dCas9\text{-}P300}$). In this system, dCas9-p300 recruits histone acetyltransferase to the specified genomic loci. Targeting dCas9-P300 to gene promoters have been shown to be sufficient to increase expression of a gene in its local chromatin context (Hilton *et al.*, 2015).

We designed eight guide RNAs to the KCNA5 promoter using GuideScan (Perez *et al.*, 2017). Specifically, we targeted the genomic region immediately upstream of the transcription start site that was marked as a promoter in the ENCODE registry of candidate cis-regulatory elements (Abascal *et al.*, 2020). Sequences and targets of each individual guide can be found in Table 4 of Appendix A. We individually tested the

effects of the guide RNAs in HEK293T$^{dCas9\text{-}P300}$ cells with plasmids containing a strong promoter to express the guide RNA.

To determine the time after transfection when dCas9-P300 produced the strongest gene expression response, we tested effects at 24, 48, and 72 hours after transfection with each guide RNA (Figure 21A). The best performing guide had maximum expression of KNCA5 at 48 hours post transfection with high levels of expression remaining at 72 hours post transfection. Expression increased by almost 10-fold from the worst performing guide and timepoint (guide 3 at 72 hours) to the best performing guide and timepoint (guide 8 at 48 hours). We used those best conditions – guide 8 at 48 hours post transfection – for all subsequent experiments,

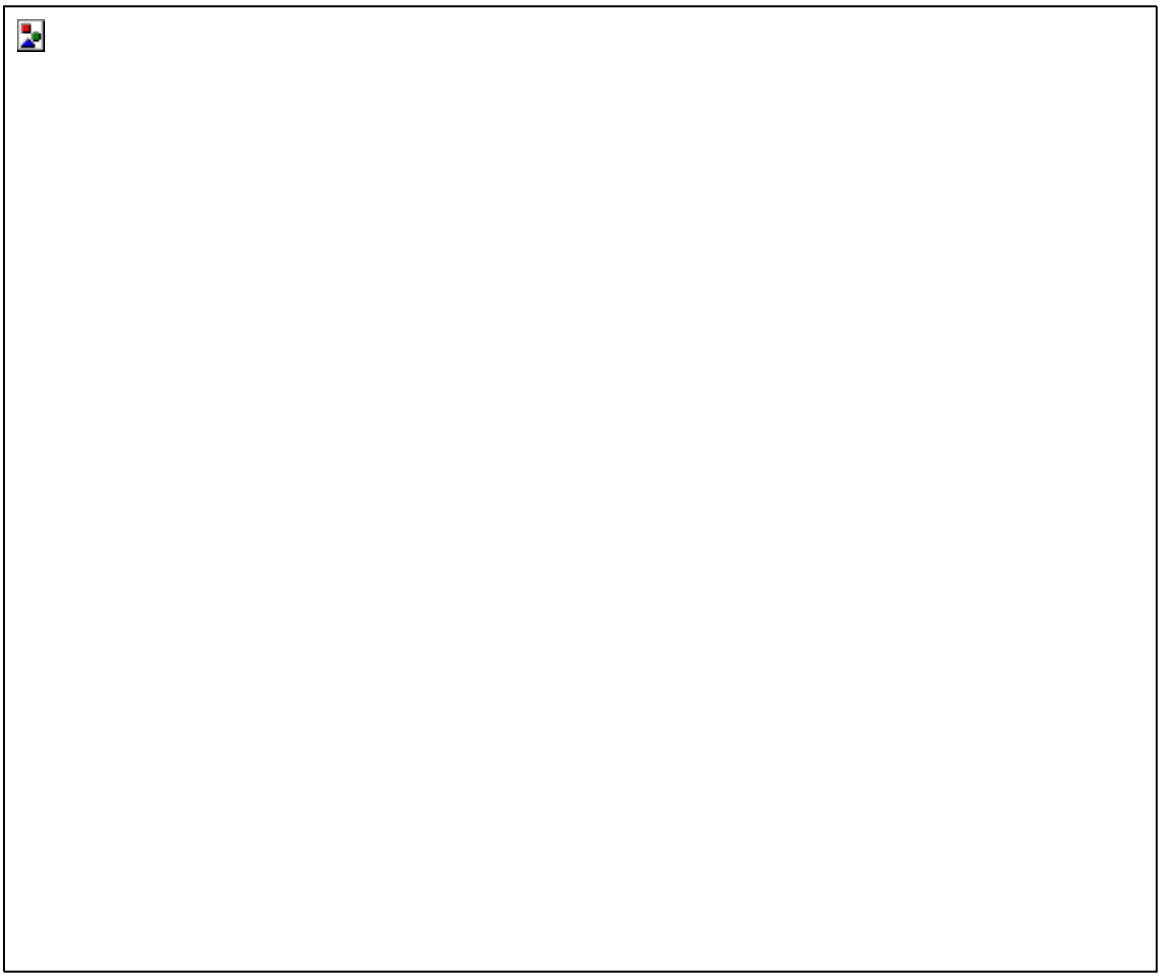

Figure 21: Evidence and effects of KCNA5 overexpression.

A. Diagram of the location of the guides tested. Blue bar represents RefSeq annotated gene and promoter. The black bars represent the promoter predicted by ENCODE registry of candidate of cis-regulatory elements. The locations of the guides are in colored lines underneath. B. Eight guides were tested in HEK293T cell lines that continuously express dCas9-P300. qPCR was used to test the induction of expression compared to housekeeping gene ACTB. Each point within a timepoint represents an independent transfection of the guide plasmid with each guide plasmid represented by its own color. C. ΔCT values of KCNA5 compared to housekeeping gene ACTB. Green bars represent cells transfected with a non-targeting guide and purple bars represent cells transfected with the top guide tested (n=3). D. BrdU values, as measured by colorimetric ELISA, of cells transfected with the nontargeting guide or the KCNA5 targeting guide (n=72).

3.2.5 Increased KCNA5 expression reduces proliferation in human embryonic kidney cells

We next measure the effect of KCNA5 overexpression on cell proliferation. Cells were transfected with the best performing guide or a non-targeting control (Table 3 – Appendix A). Forty-eight hours after transfection, RNA was isolated from cells in the 6 well plate to measure KCNA5 induction (Figure 21C). Cells transfected with the KCNA5 targeting guide had a 12-fold increase in KCNA5 expression compared to cells transfected with the nontargeting guide. At the same time point, BrdU was added to the first nine rows of the 96 well plate to mark newly synthesized DNA and actively proliferating cells. Eighteen hours after the addition of BrdU, cells were fixed to measure relative BrdU with a colorimetric ELISA. Cells with KCNA5 overexpressed showed a 35% decrease in proliferation (p-value = 0.028) (Figure 21D). The observed decrease in proliferation with increased KCNA5 expression combined with the observed increase in proliferation with reduced KCNA5 expression indicate that KCNA5 expression positively contributes to cell proliferation.

3.3 Discussion

Many signals are integrated in the cell leading to parturition; however, it is unclear how each signal may affect different tissues involved in gestation. While glucocorticoid activity is known to be altered in parturition (Goldkrand, Schulte and

Messer, 1976; Smith, 2007; Guo *et al.*, 2014), the effect of changes in its activity in fetal cells remain largely unknown. In this study, we identified an ion channel known to act as a cell stress sensor, KCNA5 (Ryland *et al.*, 2016), as a part of the glucocorticoid response in primary amnion epithelial cells. Understanding the role of this gene could lead to greater understanding of the integration of pro-inflammatory signaling and glucocorticoid signaling in a physiologically relevant context.

The relationship between voltage gated potassium channels and glucocorticoid signaling is not fully understood. Mineralocorticoid signaling upregulates protein Kv1.5 levels in atrial monocytes (Lu *et al.*, 2019). The mineralocorticoid receptor has similar affinities to mineralocorticoids and glucocorticoids and is activated by cortisol (Hellal-Levy *et al.*, 2000). Additionally, the mineralocorticoid receptor forms heterodimers with the glucocorticoid receptor (Savory *et al.*, 2001). Leukocytes, macrophages and other immune cells express voltage gated potassium channels, including KCNA5. Inflammation alters the activity of these channels, depolarizing the cells, and altering downstream cellular processes, such as proliferation (Felipe, Soler and Comes, 2010). Obesity induced inflammatory signaling through the NLRP3 inflammasome upregulates KCNA5 expression in atrial tissue (Scott *et al.*, 2021).

To isolate the effect of KCNA5 specifically and understand its role in the amnion, we used siRNA to knock down its expression in vitro using primary amnion epithelial cells. In this system, we identified a 19.2% increase in proliferation. This change in

proliferation was not accompanied by any compensatory change in apoptosis. Active Caspase 3 levels remained unchanged when KCNA5 was knocked down. One limitation of this study is that caspase independent cell death was not measured. However, the overall effect of caspase independent cell death is unlikely to substantially affect the balance between cell death and division (Danial and Korsmeyer, 2004). This one directional change in cell turnover could alter overall cell number over the course of later stages of pregnancy.

Because KCNA5 was originally identified as down regulated by glucocorticoids and via the glucocorticoid receptor, we wanted to study what the consequent effect would be on cells. Overexpression of KCNA5 would represent the cell's response without the attenuation of glucocorticoids. We used a cell line expressing dCas9-P300 and transfected guides targeting the KCNA5 promoter. This system allowed us to easily target and alter expression of our gene of interest to test its effect on proliferation. By recruiting P300 to the KCNA5 promoter, we were able to significantly increase its expression. KCNA5 overexpression significantly decreased proliferation. This is consistent with its role as a cell stress sensor halting proliferation when conditions are not optimal (Ryland *et al.*, 2016). We were unable to study overexpression specifically in primary amnion epithelial cells but the effect in those cells of KCNA5 knockdown suggests KCNA5 expression plays a role in the cell cycle for the amnion epithelial layer.

Both the extracellular matrix and amnion epithelial cells contribute to the tensile strength of the amnion (Tanaka *et al.*, 2010). Additionally, amnion epithelial cells are primarily responsible for healing wounds and microfractures within the amnion. Amnion epithelial cells proliferate and undergo epithelial-mesenchyme transition to repopulate both the epithelial layer and the collagen producing mesenchyme layer beneath it (Richardson and Menon, 2018). Microfractures in the amnion that remain unhealed are more prevalent in laboring membranes than non-laboring membranes when matched for gestational age (Richardson *et al.*, 2017). We have found evidence that KCNA5 changes expression in response to glucocorticoid signaling in amnion epithelial cells. These changes in KCNA5 expression alter cellular proliferation and may lead to cell cycle arrest. Physiologically, these changes could reduce the tensile strength of fetal membranes and their ability to heal microfractures and wounds, potentially leading to PPROM. Even in the absence of microfractures, premature arrest in amnion epithelial cell proliferation will likely have an impact on the ability of fetal membrane to remodel in the face of a growing fetus affecting its tensile strength and lead to fetal membrane weakening.

3.4 Methods

3.4.1 Primary Amnion Epithelial Cell Culture

Primary amniotic epithelial cells were isolated from 12 healthy term cesarean section patients for knockdown studies and 10 patients for RNA-seq studies according

to Casey and MacDonald 1996 (Casey and MacDonald, 1996). The collection and use of these samples were approved by the Duke University Institutional Review Board as an exempt protocol for using discarded placentas after schedules normal term caesarean sections. Briefly, the amnion layer was removed from the rest of the membrane with sterile forceps. We rinsed the layer three times in fresh Dulbecco's Modified Eagle Medium/Nutrient Mixture 12 (DMEM/F12) supplemented with 100x antibiotic-antimycotic supplement containing 10,000 units/mL of penicillin, 10,000 μg/mL of streptomycin, and 25 μg/mL of Gibco Amphotericin B (Thermo Fisher, Waltham, Massachusetts) to remove other cell types. The rinsed amniotic membrane was cut into pieces and incubated in DMEM/F12 media with the same antibiotic-antimycotics as described above and 1 g of Gibco trypsin 1:250 powder (MilliporeSigma, St Louis, Missouri) for 30 minutes at 37 °C in a shaking water bath. After 30 minutes, we ran the mixture through a metal strainer to separate disassociated cells in the first digest from the remaining intact membrane. The remaining membrane was placed back in fresh DMEM/F12 trypsin mixture for a second digest. We added DMEM/F12 with 100x Antibiotic-Antimycotic and 10% fetal bovine serum (FBS) (Gibco, Gaithersburg, MD) to the filtered portion and then spun cells at 2000 RCF for 5 minutes. We removed the supernatant and the resuspended pelleted cells in DMEM/F12 with Antibiotic-Antimycotic and 10% FBS. Incubation and shaking with the trypsin solution was repeated with the second digest of the membranes. We combined the cells from the first

and second digest and plated on 10 cm tissue culture treated petri dishes. The cells were incubated in humidified air with 5% CO_2 and media was changed every two days. At 95% confluence, approximately a week after initial plating, we passaged the cells using 0.25% trypsin with EDTA (Gibco, Gaithersburg, MD) and plated at approximately 0.5 x 10^6 cells/mL in 6-well and 96-well tissue culture treated plates for subsequent experiments.

3.4.2 RNA-seq

To measure changes in gene expression, we used primary amnion epithelial cells collected and treated previously (Allen *et al.*, 2019). For samples from each of 12 individuals, we treated primary amnion epithelial cells with a control siRNA (siRNA, ID: AM4611; Thermo- Fisher, Waltham, Massachusetts) or glucocorticoid receptor siRNA (ID: AM51331; Thermo Fisher, Waltham, Massachusetts) using Lipofectamine RNAimax (Thermo Fisher, Waltham, Massachusetts). Stock solution of Medroxyprogesterone Acetate (MPA) was made by dissolving solid MPA (MilliporeSigma, St Louis, Missouri) in 200 proof ethanol at a concentration of 10^{-2} M. Then 72 hours after siRNA transfection, we treated the cells for 6 h with 1 μL of stock MPA solution for a final concentration of 10^{-6} M MPA for 6 hours. We added 10 ng/mL Tumor Necrosis Factor (TNFα) challenge (R&D Systems, Minneapolis, Minnesota) to a half of the cells for an additional 24 hours. Cells were lysed with TRIzol reagent

(Thermo Fisher, Waltham, Massachusetts). RNA was isolated using the RNeasy mini kit (Qiagen, Hilden, Germany). RNA was quantified with a Qubit fluorometer (Thermo Fisher, Waltham, Massachusetts) and analyzed with an RNA tape station screen tape (Agilent, Santa Clara, California). For each sample, we constructed RNA-seq libraries from 0.5 μg of RNA using the TruSeq stranded mRNA kit following the standard protocol (Illumina, San Diego, California). We sequenced resulting libraries on an Illumina Next seq using 25 bp paired end sequencing.

3.4.3 Read Alignment and Signal Estimation

Samples were sequenced to a depth of 7.5 and 215 M. Illumina adapters found in the FASTQ reads were removed using Trimmomatic v0.32 (Bolger, Lohse and Usadel, 2014). Reads less than 20 nt after trimming were filtered out from further analysis. Sequences were aligned to GRCh38 human reference genome using the alignment tool STAR v2.4.1a (Dobin *et al.*, 2013) following the a 2-pass strategy to first identify a splice junctions to improve the overall mapping quality. STAR was run with default parameters except for '--outFilterMultimapNmax 1' to remove multi-mapping reads. TPM (transcripts per million) and RPKM (reads per kilobase of transcript per million reads mapped) were computed for each mapped gene using RSEM v1.2.25 (Li and Dewey, 2011).

We removed genes with less than 10 reads in at least two libraries. Library size was normalized using trimmed mean of M values (TMM) normalization in the

Bioconductor edgeR package (Robinson, McCarthy and Smyth, 2009) within the R statistical programming environment. We fit a linear negative binomial mixed model to the resultant gene matrix with patient identifier set as a random intercept and siRNA and TNFα as factors. We calculated the false discovery rate (FDR) using the Benjamini-Hochberg method. Genes with FDR below 0.05 were considered for follow up analysis.

3.4.4 KCNA5 Knockdown

We cultured primary amnion epithelial cells as described above and split into 6-well or 96-well tissue culture treated plates at 0.5-1.0x10^6 cell/mL density for 24 hours. We washed cells with serum and antibiotic-antimycotic free DMEM/F12 and then incubated in serum and antibiotic-antimycotic free DMEM/F12. The cells were transfected with control (ID# s7689, Thermo Fisher, Waltham, Massachusetts) or KCNA5 (ID #s7689, Thermo Fisher, Waltham Massachusetts) siRNA using Lipofectamine RNAiMAX (Invitrogen. Carlsbad, CA) and opti-MEM (Gibco, Gaithersburg, Maryland) and the standard RNAiMAX protocol. The final concentration of siRNA was 10 nM in all conditions. Twenty-four hours after lipofection, we added DMEM/F12 media supplemented with 20% FBS to the wells for a final FBS concentration of approximately 8%. We treated the first nine wells per row of the 96 well plate with bromodeoxyuridine. Seventy-two hours post transfection, all cells were harvested for ELISA (described below) or RNA isolation. For RNA isolation, we collected cell lysate with buffer RLT and isolated RNA using the RNeasy mini kit with the optional DNase digestion (Qiagen,

Hilden, Germany). We measured the success of the siRNA using real time quantitative polymerase chain reaction (RT-qPCR). We quantified RNA with Qubit fluorometer (Thermo Fisher, Waltham, Massachusetts) and analyzed with RNA tape station screen tape (Agilent, Santa Clara, California). For each sample, we reverse transcribed 100 ng of RNA to cDNA using the Superscript III first strand synthesis system (Invitrogen, Carlsbad, CA) with oligo dT 12-18 (Invitrogen, Carlsbad, CA) as the primer. We used fifty ng of cDNA as a template for real time quantitative polymerase chain reaction (RT-qPCR) using validated TaqMan gene expression probes targeting KCNA5 (Thermo Fisher, Waltham, Massachusetts, assay ID: Hs04991697_s1) and GAPDH (Thermo Fisher, Waltham, Massachusetts, assay ID: Hs02786624_g1) with the Taqman universal PCR master mix (Applied Biosystems, Foster City, California). We performed RT-qPCR using the Applied Biosystems Step One Real Time PCR system (Applied Biosystems, Foster City, California) using the following protocol: initial denaturation and activation of polymerase at 95 °C for 10 minutes, then 40 cycles of a two-step amplification process of 95 °C for 15 seconds and 60 °C for one minute. Selected patient samples were tested, and we evaluated knockdown using the $2^{-\Delta\Delta CT}$ method normalizing relative KCNA5 expression to GAPDH.

3.4.5 BrdU ELISA

We cultured primary amnion epithelial cells from 12 patients in a 96 well tissue culture treated plate with 50,000 cells per well. One day after plating, we added KCNA5

siRNA to half the wells and control siRNA to the other half using Lipofectamine RNAiMax to transfect cells. We diluted BrdU stock reagent from Abcam BrdU Cell Proliferation Colorimetric Assay (Abcam, Cambridge, United Kingdom) 1:500 in completed DMEM/F12 media. We added BrdU to the first nine rows of cells fifty-four hours after knockdown to begin to measure cell proliferation. Eighteen hours after the addition of BrdU, we aspirated media from the wells and added 200 μL of fixing solution from the same Abcam BrdU kit to each well. We incubated plates at room temperature for 30 minutes. After 30 minutes, we removed the fixing solution. The plates were stored in a Ziplock bag at 4 °C for no more than one month. After 3-4 membranes were collected, we followed the standard Abcam BrdU assay protocol. We measured absorbance at 450 nm using GloMax Discover system (Promega, Madison, Wisconsin). Nine well technical replicates and three well blank measurements from each row were averaged separately. We subtracted the average of the blank measurements from the average of the assay measurements.

3.4.6 Active Caspase 3 ELISA

We measured human active Caspase 3 Ser29 levels using the SimpleStep Elisa Human Caspase 3 ser29 kit from Abcam (Abcam, Cambridge, United Kingdom). We lysed cells in media with provided cell extraction buffer supplemented with Halt 100x proteinase inhibitor cocktail (Thermo Fisher, Waltham, Massachusetts). Lysed cells were stored at -80 °C. After 3-4 membranes had been collected, we thawed samples on ice and

then we followed the SimpleStep kit protocol with each sample run in duplicate. We measured absorbance at 450 nm using GloMax Discover system (Promega, Madison, Wisconsin). Technical replicates were averaged for downstream analysis.

3.4.7 KCNA5 Overexpression

We designed eight guides using GuideScan (Perez *et al.*, 2017) for the coordinates annotated as promoters immediately upstream of KCNA5 in the ENCODE candidate cis regulatory element data set (Abascal *et al.*, 2020). Those guides are listed in Additional File 2. We added selected target sequence and a nontargeting control into the guide RNA template DNA fragment outlined by Mali et al. 2013 (Mali *et al.*, 2013). We ordered DNA fragments from Eurofins and cloned them into the Zero Blunt TOPO PCR Cloning Kit (Thermo fisher, Waltham, Massachusetts). We plated bacteria onto LB-agar plates containing 50 μg/mL of kanamycin. We selected single colonies of bacteria and grew them in 100 mL LB with 50 μg/mL kanamycin overnight. We then isolated plasmids using the Machery-Nagel endotoxin free Nucleobond Xtra Midi Kit (Machery Nagel, Düren, Germany). HEK293T cells stably expressing dCas9-P300 (Addgene ID #83889) were gifted from Charles Gersbach (Klann *et al.*, 2017). We transfected cells with each guide plasmid using the Lonza SF Cell Line 4D-NucleofectorTM X Kit S (Lonza, Basel, Switzerland). We transfected guides three times in three independent transfections of 400,000 cells each. Each transfection was split into three wells of a 12 well plate. We harvested cells from each individual transfection at 24, 48, and 72 hours post

transfection. We isolated RNA from cells using the Qiagen RNeasy 96 Kit (Qiagen Hilden, Germany). One replicate of the 24-hour timepoint for all guides was lost during RNA isolation. We reverse transcribed the RNA into cDNA using Superscript 3 first strand synthesis system (Thermo Fisher, Waltham, Massachusetts). We used TaqMan probes for KCNA5 (Thermo Fisher, Waltham, Massachusetts, assay ID: Hs04991697_s1) and Beta Actin (Thermo Fisher, Waltham, Massachusetts, assay ID: Hs03023943_g1) in qPCR to measure induction. Guide 8 performed the best by qPCR 48 hours post transfection with increases in expression largely maintained through 72 hours post transfection. We then transfected HEK293T cells used above with a nontargeting guide (Additional File 2) or guide 8 using five cuvettes each of Lonza SF Cell Line 4D NucleofectorTM X Kit L (Lonza Basel, Switzerland). We pooled each transfection on the same guide. We plated approximately 20,000 cells per well in a separate 96 well plate filled for each guide. Additionally, we plated 3 wells of a 6 well plate for each guide transfection with approximately 100,000 cells per well. At 48 hours, we added BrdU to the first 9 rows of each 96 well plate. We harvested the cells in the 6 well plate, isolated RNA and made cDNA as described above. We used the same TaqMan probes as described above for qPCR and found an approximately 3.6 cycle difference in Δ CT values as shown in Fig. 5A. Eighteen hours after the addition of BrdU, we fixed the cells and measured cell proliferation as described in the BrdU ELISA above.

3.4.7 ChIP-seq

Primary amnion epithelial cells were cultured as described above. Once cells reached confluence (about seven days after harvest) the cells were split into eight 10cm culture plates. The next day, 4 plates were treated with medroxyprogesterone acetate (MPA) at 1uM final concentration (MilliporeSigma, St Louis, Missouri) or an equivalent volume of ethanol as a control. Four hours after treatment, cells were harvested for ChIP-seq. They were cross linked by adding formaldehyde to a final concentration of 1% at room temperature. After 10 minutes, the reaction was quenched by adding glycine to a final concentration of 0.125M for 5 minutes at room temperature. Cells were rinsed with phosphate buffered saline and then lysed with 1.5 mL of 15 mL of Farnham lysis buffer (5 mM PIPES pH 8, 85 mM KCl, 0.5% NP-40) with added protease inhibitor (sigma product #04693124001). Cells were manually scrapped and pipetted into 1.5mL tubes. The cells were spun down at 2000 RCF at 4 degrees Celsius. The supernatant was removed, and the pellets were snap frozen with dry ice and then stored at -80 Celsius for further processing. This process was repeated two additional time for a total of three patient biological replicates.

Cells were resuspended in 30 uL of 4 degree C RIPA buffer (1X PBS, 1% NP-40, 0.5% sodium deoxycholate, 0.1% SDS) with protease inhibitor added and then technical replicates for each condition were combined for shearing. Cells were sheared on the Biorupter Twin with 10 cycles of 30 seconds on, 30 seconds off. The cells were

centrifuged after shearing at 14,000 rpm for 15 min at 4°C. Supernatant was collected and 15 uL was reserved for size check and input control. The sheared chromatin was snap frozen and stored at -80 Celsius. The reserved chromatin was combined with 45 uL of RIPA buffer and split into two 30 uL aliquots. One was soap frozen and stored at -80C for input control. To check the size of the sheared chromatin, 200 uL of IP elution buffer (1% SDS, 0.1M NaHCO3) was added to the other aliquot and it was reverse cross linked overnight at 65C. Reverse cross linked chromatin was purified with the Qiagen PCR Purification kit and size was checked using an Agilent Tapestation Genomic Tape.

ChIP was performed as described in (Reddy, Pauli and Sprouse, 2009). After reverse cross linking, DNA was cleaning using the Qiagen PCR Purification kit. Post-IP qualification was assessed using the Qubit dsDNA High Sensitivity and Broad Range assay kit. Sequencing libraries were prepared using 7ng of input DNA into the Kapa Biosystems Hyper Prep kit for Illumina sequencing. Illumina Truseq indexes were added as barcodes to each library. Libraries were normalized to 10 uM and pooled to run on a NextSeq 500 for 25 base pair paired end sequencing

4. Conclusion and Future Direction

4.1 Summary

In this work we have advanced understanding of the maternal genetic and fetal responses that contribute to preterm birth. Previous studies (Zhang *et al.*, 2017) identified genetic loci associated with gestation length and preterm birth. Our work has shown that the GWAS regions have peaks of regulatory activity in endometrial stromal fibroblasts. Additionally, the loci have regulatory activity specific to decidualization, suggesting that they may be involved with key endometrial responses to decidualization.

A key outcome of this work is additional evidence for the role of decidualization in preterm birth loci through the identification of decidualization specific transcription factor motifs where genetic associations with preterm birth have been identified. Key transcription factors involved in decidualization, such as FOXO1 and ATF3, have binding sites enriched in active peaks sets. The overlap of transcription factor motifs within proteins of the same family (i.e., AP-1 motifs) limit the specificity of transcription factor identification with motifs. FOXO1 binding has been identified by ChIP-seq in active STARR-seq peaks, strengthening evidence for its role specifically but other transcription factors have not been analyzed with ChIP-seq.

While maternal genetics account for about a quarter of preterm birth risk (Zhang *et al.*, 2017), many other factors are involved. Maternal psychological stress is a major

risk factor for preterm birth (Olsen, 2018; Sulaiman *et al.*, 2021; Hardcastle, Ford and Bellis, 2022) and increased long term exposure to cortisol is a significant contributor to this risk (Mercer *et al.*, 2006; Diego *et al.*, 2009). The increased risk of preterm is particularly prominent in PPROM (Lilliecreutz *et al.*, 2016), suggesting altered cortisol in fetal membranes alter their ability to maintain the pregnancy.

To investigate glucocorticoid signaling in amnion epithelial cells, we performed RNA-seq on primary amnion epithelial cells from 10 patients that were treated with medroxyprogesterone acetate with and without the glucocorticoid receptor knocked down and identified that KCNA5, the voltage gated potassium channel, was significantly upregulated by glucocorticoid receptor knockdown. There is evidence that alterations of KCNA5 expression play a role in proliferation (Ryland *et al.*, 2015, 2016; Gao *et al.*, 2020) and apoptosis (Brevnova *et al.*, 2004). To investigate the role of KCNA5 expression in amnion epithelial cells, we directly modified the expression of KCNA5. We found evidence that KNCA5 expression is inversely related to proliferation but does not affect apoptosis. This research suggested that KCNA5 expression is finely tuned and deviations from baseline expression alter proliferation.

4.2 Place in current research

In our work, we used STARR-seq to identify peaks of active regulation in preterm birth GWAS regions to follow up on a previously published GWAS and better understand the impact of genetic risk on regulation of gestation duration. Identification

of STARR-seq peaks of activity is even more valuable when combined with ChIP-seq and Hi-C data sets collected in endometrial cells by Sakabe et al. 2020 and DeMayo (unpublished). These datasets together show gene regulation in endometrial stromal fibroblasts and the change in gene regulation that occurs when cells are decidualized. STARR-seq signals point to specific putative enhancers within GWA regions. Variants in these regions can alter transcription factor motifs. Promoter capture Hi-C can then predict which genes would have expression altered by this genetic variation.

While motif enrichment can suggest transcription factors involved in regulation, binding identified with ChIP-seq is needed to definitely prove the transcription factor is involved with regulation at that site. Unfortunately, ChIP-seq of decidualization in endometrial stromal cells is still limited. While several transcription factors have ChIP-seq data available, many other identified transcription factors do not. Generating ChIP-seq data for transcription factors identified by motif analysis would allow us to understand the pathways involved in decidualization better.

We have also identified glucocorticoid regulated KCNA5 impacts cell proliferation. Potassium channels have long been known to play a role in cell cycle progression and proliferation by regulating potassium levels in the cells and impacting the cells ability to move through the G1 checkpoint (Chiu and Wilson, 1989; Day *et al.*, 1993; Wonderlin and Strobl, 1996). While we have evidence that KCNA5 expression levels alter proliferation in amnion epithelial cells, the effect on Kv1.5 activity and

membrane potential have not been tested in the amnion. The proliferative effect of blocking Kv1.5 activity would provide further evidence of the effect of KCNA5 in amnion cells. Additionally, the effect of KCNA5 knockdown in amnion epithelial cells on membrane potential would allow for a mechanistic link to be formed between the alteration of KCNA5 expression in amnion cells and the effect on proliferation.

Alteration of proliferation of amnion epithelial cells has consequences for fetal membrane integrity. Fetal membranes from in labor patients and particularly fetal membrane samples from PPROM patients have significantly greater and deeper microfractures (Richardson *et al.*, 2017). Amnion epithelial cells are responsible for healing these microfractures. Amnion epithelial cells proliferation and then undergo epithelial mesenchymal transition to replace the collagen producing amnion fibroblast cells (Richardson and Menon, 2018). Reduced proliferation of amnion epithelial cells could impair the ability of the membrane to repair microfractures, potentially leading to PPROM.

4.3 Future directions

While our study moved forward out understanding of gene regulation in response to decidualization, a parallel approach to greater understand specific genes involved in regulating decidualization more broadly would be to assess decidualization in a CRISPR screen. Progesterone and cAMP are sufficient to induce decidualization on their own. A CRISPR knockout screen (Koike-Yusa *et al.*, 2014; Wang *et al.*, 2014; Zhou *et*

al., 2014) can be used to detect all genes necessary for decidualization to occur. To do this, endometrial cells can be transfected with a guide library aimed at knocking out every gene in the genome. These cells will be exposed to progesterone and cAMP to induce decidualization. After decidualization in vitro, the cells can be sorted on IGFBP1 and Prolactin expression. The guides identified in cells with low expression of both gene will likely be essential for decidualization of endometrial cells. This unbiased screen can identify more genes in the key pathways regulating decidualization than originally known.

In our study, we provided evidence that KCNA5 expression impacts amnion epithelial cell proliferation. We hypothesized this would impact the amnion's ability to repair wounds and microfractures, but directly assessing the impact of KCNA5 expression on the fetal membrane's ability to repair microfractures would provide further evidence of the role of KCNA5 on fetal membrane integrity. This can be achieved through a scratch test in which a pipette tip makes scratch through the center of amnion epithelial cells grown in culture and cells are marked with dye that is removed from newly proliferating cells (Richardson and Menon, 2018). The dye differentiates proliferating from migrating cells in the healed scratch. Comparison of scratch healing from cells with KCNA5 overexpression or knocked down could provide direct evidence for consequences of KCNA5 expression changes on membrane integrity.

While the focus of this work has been on amnion epithelial cells, several cell types interact within the amnion to promote membrane integrity. Recently, an amnion membrane organ-on-chip model has been developed (Richardson *et al.*, 2019) to study the interaction of amnion epithelial and mesenchymal cells. In this model, the amnion mesenchymal cells and amnion epithelial cells are seeded in opposite chambers of a microfluidics devise with a microchannel containing collagen matrix between the two. This device would show amnion epithelial cells migrating and transitioning to mesenchymal cells. If this process is disrupted by reduced proliferation, the organ on a chip model would be able to detect it.

Our work provides evidence for one glucocorticoid regulated gene in amnion epithelial cellular responses but the glucocorticoid receptor has broad impacts on gene regulation (McDowell *et al.*, 2018). Additional effects of cortisol signaling on amnion epithelial cells can be assessed by performing RNA-seq on primary amnion epithelial cells directly treated with cortisol. Additionally, glucocorticoid receptor ChIP-seq can identify direct glucocorticoid receptor binding in response to cortisol. Although we were not able to perform glucocorticoid receptor ChIP-seq on primary amnion epithelial cells due limits of cell expansion, a newly created immortalized amnion epithelial cell line (Ram Menon, unpublished) would allow amnion cells to be expanded with less limitation to cell number.

The availability of an immortalized amnion cell line would vastly expand possible experiments available. With an immortalized amnion epithelial cell, the effects of chronic stress can be modeled and compared to acute glucocorticoid exposure. Chronic stress is model in vitro by seven days of continuous cortisol exposure (Heard *et al.*, 2021) or seven days of continuous cortisol and norepinephrine exposure (Z. Q. Zhang *et al.*, 2021). Chronic stress exposure would stimulate the fetal membrane response of maternal psychological stress better than acute exposure would.

Additionally, more functional tests can be done on acute and chronic stress models. The scratch test described above can be repeated on immortalized amnion epithelial cells after acute, chronic or mock glucocorticoid exposure. The tensile strength and puncture force of the membrane can also be tested (Oyen, Calvin and Landers, 2006; Tanaka *et al.*, 2010). Comparing functionally relevant tests of immortalized amnion epithelial cells after acute, chronic or mock glucocorticoid exposure would provide valuable information about the impact of stress on the membranes. Significant differences in scratch healing and/or puncture force would point to effects of stress that have functional consequences for the maintenance of pregnancy.

4.4 Final remarks

In summary, our work identified peaks of regulatory activity in preterm birth genome wide associated regions. We also discovered a glucocorticoid regulated gene, KCNA5, that impacts proliferation in fetal amnion epithelial cells. In both cases, we were

able to study not just the cellular function itself but the cells response to endocrine signaling, decidualization with progesterone and cAMP in the case of endometrial cells and glucocorticoid signaling in the case of fetal amnion cells. Because preterm birth is a complex multifactorial problem, understanding cellular responses to physiologically relevant stimuli is key to gaining a better understanding of pregnancy and the mechanisms that lead to preterm birth. The increased availability of immortalized cell lines significantly impacted our ability to study endometrial cells and would vastly increase our capability to study amnion epithelial cells. Although some context is lost with cell lines, the ability to test stimuli on genetically identical cells more easily allows us to understand endocrine signaling responses in pregnancy relevant cell types.

Appendix A

Table 3: RNA-seq quality. Reads sequenced and alignment rate for each library are listed as an estimate of library quality.

sample	reads sequenced	reads mapped 2-pass	% Reads mapped 2-pass	reads quant. in transcripts	% Reads quant. in transcripts
FM_AEN_Control_siRNA.MPA	35174544	27184026	87.289298	11651018.3	74.8240317
FM_AEN_Control_siRNA.MPA_TNF	80572364	67984574	92.7748612	29567333	80.6978716
FM_AEN_GR_siRNA.MPA	88546028	73573316	94.1060207	32576537.6	83.3358748
FM_AEN_GR_siRNA.MPA_TNF	51246532	42000940	93.9625281	18543665.2	82.9700319
FM_AEU_Control_siRNA.MPA	18311700	14034766	86.2600109	6120042.64	75.2296041
FM_AEU_Control_siRNA.MPA_TNF	35466334	29452552	91.6615679	12760202.7	79.4240298
FM_AEU_GR_siRNA.MPA_TNF	52631076	43524880	92.418	19697768.6	83.6500124
FM_AEW_Control_siRNA.MPA	55531264	42709436	92.5873755	19400892.4	84.116199
FM_AEW_Control_siRNA.MPA_TNF	104077054	88539468	94.3064709	39032701.4	83.1501793

FM_AEW_GR_siRNA.MPA	93718324	75351030	91.6337655	33665901.9	81.8816508
FM_AEW_GR_siRNA.MPA_TNF	73112680	61034702	93.4664582	27130173	83.0924409
FM_AED_Control_siRNA.MPA	54783182	40717298	86.7679069	19253364.1	82.0572184
FM_AED_Control_siRNA.MPA_TNF	48435916	34624962	87.0607669	15924438.8	80.0805992
FM_AED_GR_siRNA.MPA	60680636	48322684	88.5556922	22910859.8	83.9724484
FM_AED_GR_siRNA.MPA_TNF	96805738	76798156	88.763589	36516755.2	84.4123979
FM_AEF_Control_siRNA.MPA	141637596	102313274	86.8906613	47512454.5	80.700938
FM_AEF_Control_siRNA.MPA_TNF	121828446	91705044	87.5528852	42257163.4	80.6877443
FM_AEF_GR_siRNA.MPA	65703916	49758856	88.4063399	23335839.6	82.9213664
FM_AEF_GR_siRNA.MPA_TNF	43051946	32244676	88.9692869	15013472.9	82.8501411
FM_AEG_Control_siRNA.MPA	168375598	125044994	86.591285	58015295.8	80.3489824
FM_AEG_Control_siRNA.MPA_TNF	121490226	92940106	86.8501995	43703370	81.6794077
FM_AEG_GR_siRNA.MPA	9585994	6682048	76.1642839	2767948.75	63.1000658

FM_AEG_GR_siRNA.MPA_TNF	99831082	79637474	86.1420461	37217328.2	80.5142765
FM_AEJ_Control_siRNA.MPA	91918818	66518460	85.3914383	31505468.8	80.8887427
FM_AEJ_Control_siRNA.MPA_TNF	102327120	74202596	84.9036636	36224465	82.8970941
FM_AEJ_GR_siRNA.MPA	109110666	80568060	84.2406578	39317475	82.2194294
FM_AEJ_GR_siRNA.MPA_TNF	40453800	28863984	85.523767	13907923.5	82.4181448
FM_AEO_Control_siRNA.MPA	117938292	87585980	81.9427852	42803104.7	80.0905718
FM_AEO_Control_siRNA.MPA_TNF	147974140	104535088	84.4389123	49935674.6	80.6717462
FM_AEO_GR_siRNA.MPA	122059252	86762994	80.1796306	42458009.2	78.472799
FM_AEO_GR_siRNA.MPA_TNF	131702424	105191360	86.3639442	52280153.1	85.845838
FM_AES_Control_siRNA.MPA	17589638	7036210	44.5835742	724912.94	9.18653931
FM_AES_Control_siRNA.MPA_TNF	9944522	2908742	52.1418413	390007.63	13.9824817
FM_AES_GR_siRNA.MPA	7404662	2440610	36.6697357	278938.96	8.38201757
FM_AES_GR_siRNA.MPA_TNF	64016268	51083592	84.1242294	25111408.7	82.7067096

FM_AEV_Control_siRNA.MPA	40396102	30605170	86.7361508	14680883	83.212299
FM_AEV_Control_siRNA.MPA_TNF	57317232	45806290	86.6259437	22364218	84.5875747
FM_AEV_GR_siRNA.MPA	61550534	38896736	69.7584008	20185415.2	72.4020793
FM_AEV_GR_siRNA.MPA_TNF	215068060	163241230	83.7614496	79788690.1	81.881475

Table 4: Guide RNAs tested. Sequence data for each guide RNA tested in dCas9-P300 CRISPR experiment.

Name	Sequence
Non-targeting	GTATTACTGATATTGGTGGGG
1	ACACCCGCTGCCACGAGACCG
2	AACCTTCAGCCGCCCCTCTCG
3	TTGACGTCAGGGCCAAGCGAG
4	GGCAGCGGGTGTCTCCCCGGG
5	CGCCCCCTACTCACGCTCCGG
6	CGCCCGCGGAGCGTGAGTAGG
7	GCCCGCGGAGCGTGAGTAGGG

8	GCGCCCGCGGAGCGTGAGTAG

References

Abascal, F. *et al.* (2020) 'Expanded encyclopaedias of DNA elements in the human and mouse genomes', *Nature*, 583(7818), pp. 699–710. doi: 10.1038/s41586-020-2493-4.

Adiguzel, D. and Celik-Ozenci, C. (2021) 'FoxO1 is a cell-specific core transcription factor for endometrial remodeling and homeostasis during menstrual cycle and early pregnancy', *Human reproduction update*, 27(3), pp. 570–583. doi: 10.1093/humupd/dmaa060.

Alexander, G. R. (2007) *Prematurity at Birth: Determinants, Consequences, and Geographic Variation*, *Preterm birth: causes, consequences and prevention*. doi: 10.1080/01443610802243047.

Allen, T. K. *et al.* (2019) 'Progestins Inhibit Tumor Necrosis Factor α–Induced Matrix Metalloproteinase 9 Activity via the Glucocorticoid Receptor in Primary Amnion Epithelial Cells', *Reproductive Sciences*, 26(9), pp. 1193–1202. doi: 10.1177/1933719118811646.

Amemiya, H. M., Kundaje, A. and Boyle, A. P. (2019) 'The ENCODE Blacklist: Identification of Problematic Regions of the Genome', *Scientific Reports*, 9(1), pp. 1–5. doi: 10.1038/s41598-019-45839-z.

van Arensbergen, J. *et al.* (2019) 'High-throughput identification of human SNPs affecting regulatory element activity', *Nature Genetics*. Springer US, 51(7), pp. 1160–1169. doi: 10.1038/s41588-019-0455-2.

Arnold, C. D. *et al.* (2013) 'Genome-Wide Quantitative Enhancer Activity Maps Identified by STARR-seq', *Science*, 339(6123), pp. 1074–1077. doi: 10.1126/science.1232542.

Athayde, N. *et al.* (1998) 'A role for matrix metalloproteinase-9 in spontaneous rupture of the fetal membranes', *American Journal of Obstetrics and Gynecology*, 179(5), pp. 1248–1253. doi: 10.1016/S0002-9378(98)70141-3.

Balsalobre, A. *et al.* (2000) 'Resetting of Circadian Time in Peripheral Tissues by Glucocorticoid Signalling', pp. 2344–2347.

Bamshad, M. J. *et al.* (2011) 'Exome sequencing as a tool for Mendelian disease gene discovery', *Nature Reviews Genetics*. Nature Publishing Group, 12(11), pp. 745–755.

doi: 10.1038/nrg3031.

Behnia, F. *et al.* (2015) 'Chorioamniotic membrane senescence: A signal for parturition?', *American Journal of Obstetrics and Gynecology*. Elsevier Inc., 213(3), pp. 359.e1-359.e16. doi: 10.1016/j.ajog.2015.05.041.

Björntorp, P. (1997) 'Body fat distribution, Insulin Resistance, and Metabolic Deseaese', *Nutrition*, 13(9). doi: 10.3390/nu5062019.

Blackwood, E. M. and Kadonaga, J. T. (1998) 'Going the distance: A current view of enhancer action', *Science*, 281(5373), pp. 60–63. doi: 10.1126/science.281.5373.60.

Bolger, A. M., Lohse, M. and Usadel, B. (2014) 'Trimmomatic: A flexible trimmer for Illumina sequence data', *Bioinformatics*, 30(15), pp. 2114–2120. doi: 10.1093/bioinformatics/btu170.

Bowers, K. *et al.* (2018) 'Maternal distress and hair cortisol in pregnancy among women with elevated adverse childhood experiences', *Psychoneuroendocrinology*. Elsevier, 95(May), pp. 145–148. doi: 10.1016/j.psyneuen.2018.05.024.

Brevnova, E. E. *et al.* (2004) 'Overexpression of human KCNA5 increases IK(V) and enhances apoptosis', *American Journal of Physiology - Cell Physiology*, 287(3 56-3), pp. 715–722. doi: 10.1152/ajpcell.00050.2004.

Brocklehurst, P. *et al.* (2013) 'Antibiotics for treating bacterial vaginosis in pregnancy', *Cochrane Database of Systematic Reviews*, 2013(1). doi: 10.1002/14651858.CD000262.pub4.

Brosens, J. J., Pijnenborg, R. and Brosens, I. A. (2002) 'The myometrial junctional zone spiral arteries in normal and abnormal pregnancies', *American Journal of Obstetrics and Gynecology*, 187(5), pp. 1416–1423. doi: 10.1067/mob.2002.127305.

Buniello, A. *et al.* (2019) 'The NHGRI-EBI GWAS Catalog of published genome-wide association studies, targeted arrays and summary statistics 2019', *Nucleic Acids Research*. Oxford University Press, 47(D1), pp. D1005–D1012. doi: 10.1093/nar/gky1120.

Burd, C. J. and Archer, T. K. (2013) 'Chromatin architecture defines the glucocorticoid response', *Molecular and Cellular Endocrinology*. Elsevier Ireland Ltd, 380(1–2), pp. 25–31. doi: 10.1016/j.mce.2013.03.020.

Burton, G. J. *et al.* (2009) 'Rheological and Physiological Consequences of Conversion of the Maternal Spiral Arteries for Uteroplacental Blood Flow during

Human Pregnancy', *Placenta*. Elsevier Ltd, 30(6), pp. 473–482. doi: 10.1016/j.placenta.2009.02.009.

Bush, W. S. and Moore, J. H. (2012) 'Chapter 11: Genome-Wide Association Studies', *PLoS Computational Biology*, 8(12). doi: 10.1371/journal.pcbi.1002822.

Casey, M. L. and MacDonald, P. C. (1996) 'Interstitial collagen synthesis and processing in human amnion: A property of the mesenchymal cells', *Biology of Reproduction*, 55(6), pp. 1253–1260. doi: 10.1095/biolreprod55.6.1253.

Chen, C. H. *et al.* (2020) 'Determinants of transcription factor regulatory range', *Nature Communications*. Springer US, 11(1), pp. 1–15. doi: 10.1038/s41467-020-16106-x.

Chen, X. *et al.* (2015) 'Dominant genetic variation and missing heritability for human complex traits: Insights from twin versus genome-wide common SNP models', *American Journal of Human Genetics*, 97(5), pp. 708–714. doi: 10.1016/j.ajhg.2015.10.004.

Chinenov, Y. *et al.* (2014) 'Glucocorticoid receptor coordinates transcription factor-dominated regulatory network in macrophages', *BMC Genomics*, 15(1). doi: 10.1186/1471-2164-15-656.

Chiu, S. Y. and Wilson, G. F. (1989) 'The role of potassium channels in Schwann cell proliferation in Wallerian degeneration of explant rabbit sciatic nerves.', *The Journal of Physiology*, 408(1), pp. 199–222. doi: 10.1113/jphysiol.1989.sp017455.

Cohen, G. M. (1997) 'Caspases: the executioners of apoptosis', *Biochemical Journal*, 326(1), pp. 1–16. doi: 10.1042/bj3260001.

Cohen, S. *et al.* (2012) 'Chronic stress, glucocorticoid receptor resistance, inflammation, and disease risk', *Proceedings of the National Academy of Sciences of the United States of America*, 109(16), pp. 5995–5999. doi: 10.1073/pnas.1118355109.

Cole, S. W. *et al.* (2007) 'Social regulation of gene expression in human leukocytes', *Genome Biology*, 8(9). doi: 10.1186/gb-2007-8-9-r189.

Crider, K. S., Whitehead, N. and Buus, R. M. (2005) 'Genetic variation associated with preterm birth: A HuGE review', *Genetics in Medicine*. Elsevier Masson SAS, 7(9), pp. 593–604. doi: 10.1097/01.gim.0000187223.69947.db.

Crispatzu, G. *et al.* (2021) 'The chromatin, topological and regulatory properties of pluripotency-associated poised enhancers are conserved in vivo', *Nature Communications*. Springer US, 12(1), pp. 1–17. doi: 10.1038/s41467-021-24641-4.

Dachet, C. *et al.* (2000) 'New functional promoter polymorphism, CETP/-629, in cholesteryl ester transfer protein (CETP) gene related to CETP mass and high density lipoprotein cholesterol levels: Role of Sp1/Sp3 in transcriptional regulation', *Arteriosclerosis, Thrombosis, and Vascular Biology*, 20(2), pp. 507–515. doi: 10.1161/01.ATV.20.2.507.

Dai, H. and Wang, Z. (2014) 'Histone Modification Patterns and Their Responses to Environment', *Current environmental health reports*, 1(1), pp. 11–21. doi: 10.1007/s40572-013-0008-2.

Danial, N. N. and Korsmeyer, S. J. (2004) 'Cell Death: Critical Control Points', *Cell*, 116(2), pp. 205–219. doi: 10.1016/S0092-8674(04)00046-7.

Davis, C. A. *et al.* (2006) 'PRISM/PRDM6, a Transcriptional Repressor That Promotes the Proliferative Gene Program in Smooth Muscle Cells', *Molecular and Cellular Biology*, 26(7), pp. 2626–2636. doi: 10.1128/mcb.26.7.2626-2636.2006.

Day, M. L. *et al.* (1993) 'Cell-cycle control of a large-conductance K+ channel in mouse early embryos', *Nature*, 365(6446), pp. 560–562. doi: 10.1038/365560a0.

Dean, A. (2011) 'In the loop: Long range chromatin interactions and gene regulation', *Briefings in Functional Genomics*, 10(1), pp. 3–10. doi: 10.1093/bfgp/elq033.

Diego, M. A. *et al.* (2009) 'Prenatal depression restricts fetal growth', *Early Human Development*. Elsevier Ireland Ltd, 85(1), pp. 65–70. doi: 10.1016/j.earlhumdev.2008.07.002.

Dobin, A. *et al.* (2013) 'STAR: Ultrafast universal RNA-seq aligner', *Bioinformatics*, 29(1), pp. 15–21. doi: 10.1093/bioinformatics/bts635.

Dutta, E. H. *et al.* (2015) 'Oxidative stress damage-associated molecular signaling pathways differentiate spontaneous preterm birth and preterm premature rupture of the membranes', *Molecular Human Reproduction*, 22(2), pp. 143–157. doi: 10.1093/molehr/gav074.

Engel, S. A. M. *et al.* (2005) 'Risk of small-for-gestational age is associated with common anti-inflammatory cytokine polymorphisms', *Epidemiology*, 16(4), pp. 478–486. doi: 10.1097/01.ede.0000164535.36412.6b.

Fan, W. *et al.* (2012) 'FOXO1 expression and regulation in endometrial tissue during the menstrual cycle and in early pregnancy decidua', *Gynecologic and Obstetric Investigation*, 74(1), pp. 56–63. doi: 10.1159/000336633.

Faresjö, T. *et al.* (2020) 'Elevated levels of cortisol in hair precede acute myocardial infarction', *Scientific Reports*. Nature Publishing Group UK, 10(1), pp. 1–8. doi: 10.1038/s41598-020-80559-9.

Farine, T. *et al.* (2018) 'Isolation of primary human decidual cells from the fetal membranes of term placentae', *Journal of Visualized Experiments*, 2018(134), pp. 1–8. doi: 10.3791/57443.

Felipe, A., Soler, C. and Comes, N. (2010) 'Kv1.5 in the immune system: The good, the bad, or the ugly?', *Frontiers in Physiology*, 1 NOV(November), pp. 1–8. doi: 10.3389/fphys.2010.00152.

da Fonseca, E. B., Damião, R. and Moreira, D. A. (2020) 'Preterm birth prevention', *Best Practice and Research: Clinical Obstetrics and Gynaecology*, 69(2020), pp. 40–49. doi: 10.1016/j.bpobgyn.2020.09.003.

French, J. D. and Edwards, S. L. (2020) 'The Role of Noncoding Variants in Heritable Disease', *Trends in Genetics*. Elsevier Ltd, 36(11), pp. 880–891. doi: 10.1016/j.tig.2020.07.004.

Freshney, R. I. *et al.* (1980) 'Control of cell proliferation in human glioma by glucocorticoids', *British Journal of Cancer*, 41(6), pp. 857–866. doi: 10.1038/bjc.1980.161.

Gadd, R. L. (1966) ' The Volume and Circulation of the Liquor Amnii [Abridged] ', *Proceedings of the Royal Society of Medicine*, 59(11P1), pp. 1131–1133. doi: 10.1177/003591576605911p130.

Gao, L. *et al.* (2020) 'MiR-3940-5p promotes granulosa cell proliferation through targeting KCNA5 in polycystic ovarian syndrome', *Biochemical and Biophysical Research Communications*. Elsevier Ltd, 524(4), pp. 791–797. doi: 10.1016/j.bbrc.2020.01.046.

Gellersen, B., Brosens, I. A. and Brosens, J. J. (2007) 'Decidualization of the human endometrium: Mechanisms, functions, and clinical perspectives', *Seminars in Reproductive Medicine*, 25(6), pp. 445–453. doi: 10.1055/s-2007-991042.

Gellersen, B. and Brosens, J. (2003) 'Cyclic AMP and progesterone receptor cross-talk in human endometrium: A decidualizing affair', *Journal of Endocrinology*, 178(3), pp. 357–372. doi: 10.1677/joe.0.1780357.

George, A. A., Schiltz, R. L. and Hager, G. L. (2009) 'Dynamic Access of the Glucocorticoid Receptor to Response Elements in Chromatin', *Int J Biochem Cell Biol*, 41(1), pp. 214–224. doi: 10.1016/j.biocel.2008.09.019.Dynamic.

Goldenberg, R. L. *et al.* (2008) 'Epidemiology and causes of preterm birth', *Lancet*, 371, pp. 75–84.

Goldkrand, J. W., Schulte, R. L. and Messer, R. H. (1976) 'Maternal and fetal plasma cortisol levels at parturition', *Obstetrics and Gynecology*, pp. 41–45.

González-Cabrera, J. *et al.* (2014) 'Acute and chronic stress increase salivary cortisol: A study in the real-life setting of a national examination undertaken by medical graduates', *Stress*, 17(2), pp. 149–156. doi: 10.3109/10253890.2013.876405.

Gratacós, E. *et al.* (2006) 'A histological study of fetoscopic membrane defects to document membrane healing', *Placenta*, 27(4–5), pp. 452–456. doi: 10.1016/j.placenta.2005.03.008.

Grisé, K. N. *et al.* (2021) 'Glucocorticoid agonists enhance retinal stem cell self-renewal and proliferation', *Stem Cell Research and Therapy*. Stem Cell Research & Therapy, 12(1), pp. 1–19. doi: 10.1186/s13287-021-02136-9.

Guo, C. *et al.* (2014) 'Induction of PGF2α synthesis by cortisol through GR dependent induction of CBR1 in human amnion fibroblasts', *Endocrinology*, 155(8), pp. 3017–3024. doi: 10.1210/en.2013-1848.

Guo, C. *et al.* (2015) 'Coordinated regulatory variation associated with gestational hyperglycaemia regulates expression of the novel hexokinase HKDC1', *Nature Communications*. Nature Publishing Group, 6, pp. 4–11. doi: 10.1038/ncomms7069.

Gusella, J. F. *et al.* (1983) 'A polymorphic DNA marker genetically linked to Huntington's disease', *Nature*, 306(5940), pp. 234–238. doi: 10.1038/306234a0.

Guzeloglu-Kayisli, O. *et al.* (2021) 'Decidual cell FKBP51-progesterone receptor binding mediates maternal stress-induced preterm birth', *Proceedings of the National Academy of Sciences of the United States of America*, 118(11), pp. 1–12. doi: 10.1073/pnas.2010282118.

Hardcastle, K., Ford, K. and Bellis, M. A. (2022) 'Maternal adverse childhood experiences and their association with preterm birth: secondary analysis of data from universal health visiting', *BMC Pregnancy and Childbirth*. BioMed Central, 22(1), pp. 1–11. doi: 10.1186/s12884-022-04454-z.

Harding, J. E. *et al.* (2001) 'Do antenatal corticosteroids help in the setting of preterm rupture of membranes?', *American Journal of Obstetrics and Gynecology*, 184(2), pp. 131–139. doi: 10.1067/mob.2001.108331.

Hatano, A. *et al.* (2011) 'CELLPEDIA: A repository for human cell information for cell studies and differentiation analyses', *Database*, 2011, pp. 1–10. doi: 10.1093/database/bar046.

Heard, K. J. *et al.* (2021) 'Chronic cortisol differentially impacts stem cell-derived astrocytes from major depressive disorder patients', *Translational Psychiatry*. Springer US, 11(1), pp. 1–9. doi: 10.1038/s41398-021-01733-9.

Heintzman, N. D. *et al.* (2007) 'Distinct and predictive chromatin signatures of transcriptional promoters and enhancers in the human genome', *Nature Genetics*, 39(3), pp. 311–318. doi: 10.1038/ng1966.

Hellal-Levy, C. *et al.* (2000) 'Mechanistic aspects of mineralocorticoid receptor activation', *Kidney International*, 57(4), pp. 1250–1255. doi: 10.1046/j.1523-1755.2000.00958.x.

Hilton, I. B. *et al.* (2015) 'Epigenome editing by a CRISPR/Cas9-based acetyltransferase activates genes from promoters and enhancers', *Nature Biotechnology*, 33(5), pp. 510–517. doi: 10.1038/nbt.3199.Epigenome.

Hong, E. P. and Park, J. W. (2012) 'Sample Size and Statistical Power Calculation in Genetic Association Studies', *Genomics & Informatics*, 10(2), p. 117. doi: 10.5808/gi.2012.10.2.117.

Huang, P. *et al.* (2022) 'SOX4 facilitates PGR protein stability and FOXO1 expression conducive for human endometrial decidualization', *eLife*, 11, pp. 1–24. doi: 10.7554/eLife.72073.

Hunt, S. M. N. and Clarke, C. L. (1999) 'Expression and hormonal regulation of the Sox4 gene in mouse female reproductive tissues', *Biology of Reproduction*, 61(2), pp. 476–481. doi: 10.1095/biolreprod61.2.476.

Ikegawa, S. (2012) 'A Short History of the Genome-Wide Association Study: Where We Were and Where We Are Going', *Genomics & Informatics*, 10(4), p. 220. doi: 10.5808/GI.2012.10.4.220.

Ingram, V. M. (1958) 'Abnormal human haemoglobins', *Biochimica et Biophysica Acta*, 28, pp. 539–545. doi: 10.1016/0006-3002(58)90516-X.

Jenuwein, T. and Allis, C. D. (2001) 'Translating the histone code', *Science*, 293(5532), pp. 1074–1080. doi: 10.1126/science.1063127.

John, S. *et al.* (2011) 'Chromatin accessibility pre-determines glucocorticoid receptor binding patterns', *Nature Genetics*. Nature Publishing Group, 43(3), pp. 264–268. doi: 10.1038/ng.759.

Johnson, G. D. *et al.* (2018) 'Human genome-wide measurement of drug-responsive regulatory activity', *Nature Communications*, 9(1), p. 5317. doi: 10.1038/s41467-018-07607-x.

Kajihara, T., Brosens, J. J. and Ishihara, O. (2013) 'The role of FOXO1 in the decidual transformation of the endometrium and early pregnancy', *Medical Molecular Morphology*, 46(2), pp. 61–68. doi: 10.1007/s00795-013-0018-z.

Kaup, B. *et al.* (2001) 'Time-dependent inhibition of glioblastoma cell proliferation by dexamethasone', *Journal of Neuro-Oncology*, 51(2), pp. 105–110. doi: 10.1023/A:1010684921099.

Kawamura, A., Tamaki, N. and Kokunai, T. (1998) 'Effect of dexamethasone on cell proliferation of neuroepithelial tumor cell lines', *Neurologia Medico-Chirurgica*, 38(10), pp. 633–638. doi: 10.2176/nmc.38.633.

Kim, Y. S. *et al.* (2021) 'Correcting signal biases and detecting regulatory elements in STARR-seq data', *Genome Research*, 31(5), pp. 877–889. doi: 10.1101/GR.269209.120.

Klann, T. S. *et al.* (2017) 'CRISPR–Cas9 epigenome editing enables high-throughput screening for functional regulatory elements in the human genome', *Nature Biotechnology*, 35(6), pp. 561–568. doi: 10.1038/nbt.3853.

Koike-Yusa, H. *et al.* (2014) 'Genome-wide recessive genetic screening in mammalian cells with a lentiviral CRISPR-guide RNA library', *Nature Biotechnology*, 32(3), pp. 267–273. doi: 10.1038/nbt.2800.

Krikun, G. *et al.* (2004) 'A novel immortalized human endometrial stromal cell line with normal progestational response', *Endocrinology*, 145(5), pp. 2291–2296. doi: 10.1210/en.2003-1606.

Kulakovskiy, I. V. *et al.* (2018) 'HOCOMOCO: Towards a complete collection of transcription factor binding models for human and mouse via large-scale ChIP-Seq analysis', *Nucleic Acids Research*. Oxford University Press, 46(D1), pp. D252–D259. doi: 10.1093/nar/gkx1106.

Kuroda, K. *et al.* (2013) 'Induction of 11β-HSD 1 and activation of distinct mineralocorticoid receptor- and glucocorticoid receptor-dependent gene networks in

decidualizing human endometrial stromal cells', *Molecular Endocrinology*, 27(2), pp. 192–202. doi: 10.1210/me.2012-1247.

Lachance, J. and Tishkoff, S. A. (2013) 'SNP ascertainment bias in population genetic analyses: Why it is important, and how to correct it', *BioEssays*, 35(9), pp. 780–786. doi: 10.1002/bies.201300014.

Lander, E. S. *et al.* (2001) 'Initial sequencing and analysis of the human genome', *Nature*, 409(6822), pp. 860–921. doi: 10.1038/35057062.

Langmead, B. and Salzberg, S. L. (2012) 'Fast gapped-read alignment with Bowtie 2', *Nature Methods*, 9(4), pp. 357–359. doi: 10.1038/nmeth.1923.

Lee, D. *et al.* (2020) 'STARRPeaker: uniform processing and accurate identification of STARR-seq active regions', *Genome Biology*. Genome Biology, 21(1), pp. 1–24. doi: 10.1186/s13059-020-02194-x.

Li, B. and Dewey, C. N. (2011) 'RSEM: accurate transcript quantification from RNA-Seq data with or without a reference genome', *BMC Bioinformatics*, 12(323). doi: 10.1201/b16589.

Li, Q. *et al.* (2013) 'WNT4 Acts Downstream of BMP2 and Functions via β-Catenin Signaling Pathway to Regulate Human Endometrial Stromal Cell Differentiation', *Endocrinology*, 154(1), pp. 446–457. doi: 10.1210/en.2012-1585.

Lilliecreutz, C. *et al.* (2016) 'Effect of maternal stress during pregnancy on the risk for preterm birth', *BMC Pregnancy and Childbirth*. BMC Pregnancy and Childbirth, pp. 1–8. doi: 10.1186/s12884-015-0775-x.

Liu, Y. *et al.* (2017) 'Functional assessment of human enhancer activities using whole-genome STARR-sequencing', *Genome Biology*. Genome Biology, 18(1), pp. 1–13. doi: 10.1186/s13059-017-1345-5.

Locksmith, G. and Duff, P. (2001) 'Infection, antibiotics, and preterm delivery', *Seminars in Perinatology*, 25(5), pp. 295–309. doi: 10.1053/sper.2001.27163.

Longini, M. *et al.* (2007) 'Association between oxidative stress in pregnancy and preterm premature rupture of membranes', *Clinical Biochemistry*, 40(11), pp. 793–797. doi: 10.1016/j.clinbiochem.2007.03.004.

López-Cortegano, E. and Caballero, A. (2019) 'Inferring the nature of missing heritability in human traits using data from the GWAS catalog', *Genetics*, 212(3), pp. 891–

904. doi: 10.1534/genetics.119.302077.

Lu, G. *et al.* (2019) 'Spironolactone suppresses aldosterone-induced Kv1.5 expression by attenuating mineralocorticoid receptor-Nox1/2/4-mediated ROS generation in neonatal rat atrial myocytes', *Biochemical and Biophysical Research Communications*. Elsevier Ltd, 520(2), pp. 379–384. doi: 10.1016/j.bbrc.2019.10.039.

Luu, T. M., Rehman Mian, M. O. and Nuyt, A. M. (2017) 'Long-Term Impact of Preterm Birth: Neurodevelopmental and Physical Health Outcomes', *Clinics in Perinatology*, 44(2), pp. 305–314. doi: https://doi.org/10.1016/j.clp.2017.01.003.

Lv, S. *et al.* (2019) 'Impaired decidualization caused by downregulation of circadian clock gene BMAL1 contributes to human recurrent miscarriage', *Biology of Reproduction*, 101(1), pp. 138–147. doi: 10.1093/biolre/ioz063.

Macones, G. A. *et al.* (2004) 'A polymorphism in the promoter region of TNF and bacterial vaginosis: Preliminary evidence of gene-environment interaction in the etiology of spontaneous preterm birth', *American Journal of Obstetrics and Gynecology*, 190(6), pp. 1504–1508. doi: 10.1016/j.ajog.2004.01.001.

Malak, T. M. *et al.* (1993) 'Confocal immunofluorescence localization of collagen types I, III, IV, V and VI and their ultrastructural organization in term human fetal membranes', *Placenta*, 14(4), pp. 385–406. doi: 10.1016/S0143-4004(05)80460-6.

Mali, P. *et al.* (2013) 'RNA-Guided Human Genome Engineering via Cas9', 339(6121), pp. 823–826.

Manabe, Y., Himeno, N. and Fukumoto, M. (1991) 'Tensile strength and collagen content of amniotic membrane do not change after the second trimester or during delivery', *Obstetrics and Gynecology*, pp. 24–27.

Marinello, W., Feng, L. and Allen, T. K. (2020) 'Progestins Inhibit Interleukin-1β-Induced Matrix Metalloproteinase 1 and Interleukin 8 Expression via the Glucocorticoid Receptor in Primary Human Amnion Mesenchymal Cells', *Frontiers in Physiology*, 11(July), pp. 1–12. doi: 10.3389/fphys.2020.00900.

Martin, L. F. *et al.* (2017) 'Histologic chorioamnionitis does not modulate the oxidative stress and antioxidant status in pregnancies complicated by spontaneous preterm delivery', *BMC Pregnancy and Childbirth*. BMC Pregnancy and Childbirth, 17(1), pp. 1–8. doi: 10.1186/s12884-017-1549-4.

Martin, L., Richardson, L. and Menon, R. (2018) 'Characteristics, Properties, and

Functionality of Fetal Membranes: An Overlooked Area in the Field of Parturition', *Encyclopedia of Reproduction (2nd Edition) Volume 3*.

Mattern, J., Büchler, M. W. and Herr, I. (2007) 'Cell cycle arrest by glucocorticoids may protect normal tissue and solid tumors from cancer therapy', *Cancer Biology and Therapy*, 6(9), pp. 1341–1350. doi: 10.4161/cbt.6.9.4765.

McCabe, E. R. B. *et al.* (2014) 'Fighting for the Next Generation: US Prematurity in 2030', *Pediatrics*, 134(6), pp. 1193–1199. doi: 10.1542/peds.2014-2541.

McCormick, M. C. (1985) 'The Contribution of Low Birth Weight to Infant Mortality and Childhood Morbidity', *New England Journal of Medicine*, 312(2), pp. 82–90. doi: 10.1056/NEJM198501103120204.

McDowell, I. C. *et al.* (2018) 'Glucocorticoid receptor recruits to enhancers and drives activation by motif-directed binding', *Genome Research*, 28(9), pp. 1272–1284. doi: 10.1101/gr.233346.117.

McGregor, J. A. *et al.* (1987) 'Bacterial protease-induced reduction of chorioamniotic membrane strength and elasticity.', *Obstetrics and gynecology*, 69(2), pp. 167–74.

McLeay, R. C. and Bailey, T. L. (2010) 'Motif Enrichment Analysis: A unified framework and an evaluation on ChIP data', *BMC Bioinformatics*, 11. doi: 10.1186/1471-2105-11-165.

Medina, T. M. and Hill, D. A. (2006) 'Preterm premature rupture of membranes: Diagnosis and management', *American Family Physician*, 73(4), pp. 659–664. doi: 10.5005/jp/books/10466_13.

Meijsing, S. H. *et al.* (2009) 'DNA binding site sequence directs glucocorticoid receptor structure and activity', *Science*, 324(5925), pp. 407–410. doi: 10.1126/science.1164265.

Melnikov, A. *et al.* (2012) 'Systematic dissection and optimization of inducible enhancers in human cells using a massively parallel reporter assay', *Nature Biotechnology*. Nature Publishing Group, 30(3), pp. 271–277. doi: 10.1038/nbt.2137.

Menon, R. (2004) 'Fetal membrane inflammatory cytokines: a switching mechanism between the preterm premature rupture of the membranes and preterm labor pathways', *Journal of Perinatal Medicine*, 32(5), p. 391.

Menon, R. *et al.* (2006) 'Multilocus interactions at maternal tumor necrosis factor-α, tumor necrosis factor receptors, interleukin-6 and interleukin-6 receptor genes predict spontaneous preterm labor in European-American women', *American Journal of Obstetrics and Gynecology*, 194(6), pp. 1616–1624. doi: 10.1016/j.ajog.2006.03.059.

Menon, R. (2014) 'Oxidative stress damage as a detrimental factor in preterm birth pathology', *Frontiers in Immunology*, 5(NOV), pp. 1–14. doi: 10.3389/fimmu.2014.00567.

Mercer, B. M. *et al.* (2006) 'Are women with recurrent spontaneous preterm births different from those without such history?', *American Journal of Obstetrics and Gynecology*, 194(4), pp. 1176–1184. doi: 10.1016/j.ajog.2006.01.069.

Mercer, B. M. (2010) 'Preterm Premature Rupture of the Membranes', *Preterm Birth: Prevention and Management*, 101(1), pp. 217–231. doi: 10.1002/9781444317619.ch19.

Merlino, A. *et al.* (2009) 'Nuclear progesterone receptor expression in the human fetal membranes and decidua at term before and after labor', *Reproductive Sciences*, 16(4), pp. 357–363. doi: 10.1177/1933719108328616.

Miller, G. E. *et al.* (2008) 'A Functional Genomic Fingerprint of Chronic Stress in Humans: Blunted', *Biol Psychiatry*, 64(4), pp. 266–272. doi: 10.1016/j.biopsych.2008.03.017.A.

Miller, G. E. *et al.* (2009) 'Low early-life social class leaves a biological residue manifested by decreased glucocorticoid and increased proinflammatory signaling', *Proceedings of the National Academy of Sciences of the United States of America*, 106(34), pp. 14716–14721. doi: 10.1073/pnas.0902971106.

Miller, G. E., Cohen, S. and Ritchey, A. K. (2002) 'Chronic psychological stress and the regulation of pro-inflammatory cytokines: A glucocorticoid-resistance model', *Health Psychology*, 21(6), pp. 531–541. doi: 10.1037/0278-6133.21.6.531.

Miller, W. L. and Auchus, R. J. (2011) 'The molecular biology, biochemistry, and physiology of human steroidogenesis and its disorders', *Endocrine Reviews*, 32(1), pp. 81–151. doi: 10.1210/er.2010-0013.

Mori, M. *et al.* (2016) 'The decidua—the maternal bed embracing the embryo—maintains the pregnancy', *Seminars in Immunopathology*. Seminars in Immunopathology, 38(6), pp. 635–649. doi: 10.1007/s00281-016-0574-0.

Muerdter, F. *et al.* (2018) 'Resolving systematic errors in widely used enhancer

activity assays in human cells', *Nature Methods*, 15(2), pp. 141–149. doi: 10.1038/nmeth.4534.

Murtha, A. P. and Menon, R. (2015) 'Regulation of fetal membrane inflammation: A critical step in reducing adverse pregnancy outcome', *American Journal of Obstetrics and Gynecology*. Elsevier Inc., 213(4), pp. 447–448. doi: 10.1016/j.ajog.2015.07.008.

Myking, S. *et al.* (2013) 'X-Chromosomal Maternal and Fetal SNPs and the Risk of Spontaneous Preterm Delivery in a Danish/Norwegian Genome-Wide Association Study', *PLoS ONE*, 8(4). doi: 10.1371/journal.pone.0061781.

Nader, N., Chrousos, G. P. and Kino, T. (2010) 'Interactions of the circadian CLOCK system and the HPA axis', *Trends in Endocrinology and Metabolism*. Elsevier Ltd, 21(5), pp. 277–286. doi: 10.1016/j.tem.2009.12.011.

Nelson, D. B. *et al.* (2017) '17-alpha Hydroxyprogesterone caproate did not reduce the rate of recurrent preterm birth in a prospective cohort study', *American Journal of Obstetrics and Gynecology*. Elsevier Inc., 216(6), pp. 600.e1-600.e9. doi: 10.1016/j.ajog.2017.02.025.

Ng, S. W. *et al.* (2020) 'Endometrial decidualization: The primary driver of pregnancy health', *International Journal of Molecular Sciences*, 21(11), pp. 1–20. doi: 10.3390/ijms21114092.

Ni, G. *et al.* (2019) 'Genotype–covariate correlation and interaction disentangled by a whole-genome multivariate reaction norm model', *Nature Communications*, 10(1). doi: 10.1038/s41467-019-10128-w.

Olsen, J. M. (2018) 'Integrative Review of Pregnancy Health Risks and Outcomes Associated With Adverse Childhood Experiences', *JOGNN - Journal of Obstetric, Gynecologic, and Neonatal Nursing*. Elsevier Inc, 47(6), pp. 783–794. doi: 10.1016/j.jogn.2018.09.005.

Organization, W. H. (2016) *Preterm Birth Fact Sheet*.

Oyen, M. L., Calvin, S. E. and Landers, D. V. (2006) 'Premature rupture of the fetal membranes: Is the amnion the major determinant?', *American Journal of Obstetrics and Gynecology*, 195(2), pp. 510–515. doi: 10.1016/j.ajog.2006.02.010.

Papadopulos, N. A. *et al.* (2006) 'Amnion cells engineering: A new perspective in fetal membrane healing after intrauterine surgery?', *Fetal Diagnosis and Therapy*, 21(6), pp. 494–500. doi: 10.1159/000095660.

Patwardhan, R. P. *et al.* (2012) 'Massively parallel functional dissection of mammalian enhancers in vivo', *Nature Biotechnology*. Nature Publishing Group, 30(3), pp. 265–270. doi: 10.1038/nbt.2136.

Perez, A. R. *et al.* (2017) 'GuideScan software for improved single and paired CRISPR guide RNA design', *Nature Biotechnology*. Nature Publishing Group, 35(4), pp. 347–349. doi: 10.1038/nbt.3804.

Picard toolkit (2019) *Broad Institure, Github Repository*.

Pijnenborg, R., Vercruysse, L. and Hanssens, M. (2006) 'The Uterine Spiral Arteries In Human Pregnancy: Facts and Controversies', *Placenta*, 27(9–10), pp. 939–958. doi: 10.1016/j.placenta.2005.12.006.

Poot, M. (2011) 'Use of genome-wide oligonucleotide- or SNP-array platforms has widened the spectrum of detectable human genomic variation', *Cytogenetic and Genome Research*, 135(3–4), pp. 171–173. doi: 10.1159/000334062.

Portal, M. (1809) 'Considerations on the Nature and Treatment of Some Hereditary or Family Diseases.', *The Medical and physical journal*, 21(121), pp. 229–239.

Porter, T. F. *et al.* (1997) 'The risk of preterm birth across generations', *Obstetrics and Gynecology*, 90(1), pp. 63–67. doi: 10.1016/S0029-7844(97)00215-9.

Poulat, F. (2021) 'Non-Coding Genome, Transcription Factors, and Sex Determination', *Sexual Development*, 15(5–6), pp. 295–307. doi: 10.1159/000519725.

Pringle, K. G. *et al.* (2015) 'Effects of Fetal Sex on Expression of the (Pro)renin Receptor and Genes Influenced by its Interaction With Prorenin in Human Amnion', *Reproductive Sciences*, 22(6), pp. 750–757. doi: 10.1177/1933719114561555.

Purisch, S. E. and Gyamfi-Bannerman, C. (2017) 'Epidemiology of preterm birth', *Seminars in Perinatology*, 41(7), pp. 387–391. doi: 10.1053/j.semperi.2017.07.009.

Quatrini, L. *et al.* (2021) 'Glucocorticoids inhibit human hematopoietic stem cell differentiation toward a common ILC precursor', *Journal of Allergy and Clinical Immunology*. Elsevier Inc., pp. 1–14. doi: 10.1016/j.jaci.2021.10.012.

Querfurth, H. W. *et al.* (1999) 'Enhancer function and novel DNA binding protein activity in the near upstream βAPP gene promoter', *Gene*, 232(1), pp. 125–141. doi: 10.1016/S0378-1119(99)00091-8.

Quinlan, A. R. and Hall, I. M. (2010) 'BEDTools: A flexible suite of utilities for comparing genomic features', *Bioinformatics*, 26(6), pp. 841–842. doi: 10.1093/bioinformatics/btq033.

Rada-Iglesias, A. *et al.* (2011) 'A unique chromatin signature uncovers early developmental enhancers in humans', *Nature*. Nature Publishing Group, 470(7333), pp. 279–285. doi: 10.1038/nature09692.

Radosevich, P. M. *et al.* (1989) 'Effects of low- and high-intensity exercise on plasma and cerebrospinal fluid levels of ir-β-endorphin, ACTH, cortisol, norepinephrine and glucose in the conscious dog', *Brain Research*, 498(1), pp. 89–98. doi: 10.1016/0006-8993(89)90402-2.

Raff, H. *et al.* (1999) 'Elevated salivary cortisol in the evening in healthy elderly men and women: Correlation with bone mineral density', *Journals of Gerontology - Series A Biological Sciences and Medical Sciences*, 54(9), pp. 479–483. doi: 10.1093/gerona/54.9.M479.

Rajabi, M., Dean, D. D. and Woessner, J. F. (1987) 'High levels of serum collagenase in premature labor—a potential biochemical marker', *Obstetrics and Gynecology*, pp. 179–186.

Ramamoorthy, S. and Cidlowski, J. A. (2016) 'Corticosteroids. Mechanisms of Action in Health and Disease', *Rheumatic Disease Clinics of North America*, 42(1), pp. 15–31. doi: 10.1016/j.rdc.2015.08.002.

Ramezani, M. *et al.* (2020) 'Anxiety and Cortisol in Outcomes of Patients With Covid-19. Basic and Clinical Neuroscience, 11(2.Covid19)', *Basic and Clinical Neuroscience Journal*, Covid(April), pp. 179–184. doi: 10.32598/bcn.11.covid19.1168.2.

Ranabir, S. and Reetu, K. (2011) 'Stress and hormones', *Indian Journal of Endocrinology and Metabolism*, 15(1), p. 18. doi: 10.4103/2230-8210.77573.

Reddy, T. E. *et al.* (2009) 'Genomic determination of the glucocorticoid response reveals unexpected mechanisms of gene regulation', *Genome Research*, 19(12), pp. 2163–2171. doi: 10.1101/gr.097022.109.

Reddy, T. E., Pauli, F. and Sprouse, R. O. (2009) 'Genomic determination of the glucocorticoid response reveals unexpected mechanisms of gene regulation Genomic determination of the glucocorticoid response reveals unexpected mechanisms of gene regulation', *Genome Research*, pp. 2163–2171. doi: 10.1101/gr.097022.109.

Di Renzo, G. C., Tosto, V. and Giardina, I. (2018) 'The biological basis and prevention of preterm birth', *Best Practice and Research: Clinical Obstetrics and Gynaecology*. Elsevier Ltd, 52(2018), pp. 13–22. doi: 10.1016/j.bpobgyn.2018.01.022.

Richardson, L. *et al.* (2019) 'Amnion membrane organ-on-chip: an innovative approach to study cellular interactions', *FASEB Journal*, 33(8), pp. 8945–8960. doi: 10.1096/fj.201900020RR.

Richardson, L. and Menon, R. (2018) 'Proliferative, Migratory, and Transition Properties Reveal Metastate of Human Amnion Cells', *American Journal of Pathology*. American Society for Investigative Pathology, 188(9), pp. 2004–2015. doi: 10.1016/j.ajpath.2018.05.019.

Richardson, L. S. *et al.* (2017) 'Discovery and Characterization of Human Amniochorionic Membrane Microfractures', *American Journal of Pathology*. Elsevier, 187(12), pp. 2821–2830. doi: 10.1016/j.ajpath.2017.08.019.

Richardson, L. S., Taylor, R. N. and Menon, R. (2020) 'Reversible EMT and MET mediate amnion remodeling during pregnancy and labor', *Science Signaling*, 13(618), pp. 1–17. doi: 10.1126/scisignal.aay1486.

Robinson, M. D., McCarthy, D. J. and Smyth, G. K. (2009) 'edgeR: A Bioconductor package for differential expression analysis of digital gene expression data', *Bioinformatics*, 26(1), pp. 139–140. doi: 10.1093/bioinformatics/btp616.

Rohleder, N. *et al.* (2009) 'Biologic cost of caring for a cancer patient: Dysregulation of pro- and anti-inflammatory signaling pathways', *Journal of Clinical Oncology*, 27(18), pp. 2909–2915. doi: 10.1200/JCO.2008.18.7435.

Ryland, K. E. *et al.* (2015) 'Polycomb-dependent repression of the potassium channel-encoding gene KCNA5 promotes cancer cell survival under conditions of stress', *Oncogene*. Nature Publishing Group, 34(35), pp. 4591–4600. doi: 10.1038/onc.2014.384.

Ryland, K. E. *et al.* (2016) 'Promoter methylation analysis reveals that KCNA5 ion channel silencing supports Ewing sarcoma cell proliferation', *Molecular Cancer Research*, 14(1), pp. 26–34. doi: 10.1158/1541-7786.MCR-15-0343.

Sakabe, N. J. *et al.* (2020) 'Transcriptome and regulatory maps of decidua-derived stromal cells inform gene discovery in preterm birth', *Science Advances*, 6(49), pp. 1–16. doi: 10.1126/sciadv.abc8696.

Savory, J. G. A. *et al.* (2001) 'Glucocorticoid Receptor Homodimers and Glucocorticoid-Mineralocorticoid Receptor Heterodimers Form in the Cytoplasm through Alternative Dimerization Interfaces', *Molecular and Cellular Biology*, 21(3), pp. 781–793. doi: 10.1128/mcb.21.3.781-793.2001.

Schaid, D. J., Chen, W. and Larson, N. B. (2018) 'From genome-wide associations to candidate causal variants by statistical fine-mapping', *Nature Reviews Genetics*. Springer US, 19(8), pp. 491–504. doi: 10.1038/s41576-018-0016-z.

Scott, L. *et al.* (2021) 'NLRP3 inflammasome is a key driver of obesity-induced atrial arrhythmias', *Cardiovascular Research*, 117(7), pp. 1746–1759. doi: 10.1093/cvr/cvab024.

Shimba, A. and Ikuta, K. (2020) 'Control of immunity by glucocorticoids in health and disease', *Seminars in Immunopathology*. Seminars in Immunopathology, 42(6), pp. 669–680. doi: 10.1007/s00281-020-00827-8.

Smale, S. T. and Kadonaga, J. T. (2003) 'The RNA polymerase II core promoter', *Annual Review of Biochemistry*, 72, pp. 449–479. doi: 10.1146/annurev.biochem.72.121801.161520.

Smith, R. (2007) 'Parturition', *New England Journal of Medicine*, 356(3), pp. 271–283. doi: 10.1177/1461444810365020.

Sonderegger, S., Pollheimer, J. and Knöfler, M. (2010) 'Wnt signalling in implantation, decidualisation and placental differentiation - Review', *Placenta*, 31(10), pp. 839–847. doi: 10.1016/j.placenta.2010.07.011.

Sondike, S. B., Pisetsky, E. M. and Luzier, J. L. (2016) 'Recurrence of Preterm Birth and Early Term Birth', *Obstetrics & Gynecology*, 128(2), pp. 364–372. doi: 10.1007/s40519-015-0230-z.Development.

Spitz, F. and Furlong, E. E. M. (2012) 'Transcription factors: From enhancer binding to developmental control', *Nature Reviews Genetics*. Nature Publishing Group, 13(9), pp. 613–626. doi: 10.1038/nrg3207.

Steyn, P. S. *et al.* (2003) 'A randomised, double-blind placebo-controlled trial of ascorbic acid supplementation for the prevention of preterm labour', *Journal of Obstetrics and Gynaecology*, 23(2), pp. 150–155. doi: 10.1080/014436103000074673.

Strug, M. R. *et al.* (2018) 'RBPJ mediates uterine repair in the mouse and is reduced in women with recurrent pregnancy loss', *FASEB Journal*, pp. 2452–2466. doi:

10.1096/fj.201701032R.

Sulaiman, S. *et al.* (2021) 'Total Adverse Childhood Experiences and Preterm Birth: A Systematic Review', *Maternal and Child Health Journal*, 25(10), pp. 1581–1594. doi: 10.1007/s10995-021-03176-6.

Tam, V. *et al.* (2019) 'Benefits and limitations of genome-wide association studies', *Nature Reviews Genetics*. Springer US, 20(8), pp. 467–484. doi: 10.1038/s41576-019-0127-1.

Tanaka, K. *et al.* (2010) 'Tensile properties of amniotic membrane', *WIT Transactions on the Built Environment*, 112, pp. 197–206. doi: 10.2495/HPSM100191.

Thomas, J. C. *et al.* (2018) 'Adverse childhood experiences and HPA axis function in pregnant women', *Hormones and Behavior*. Elsevier, 102(May), pp. 10–22. doi: 10.1016/j.yhbeh.2018.04.004.

Thompson, J. F. (2018) 'SNP Selection and Concordance in Consumer Genetics Testing', *bioRxiv*. doi: https://doi.org/10.1101/352732.

Tian, D. *et al.* (2019) 'Increased glucocorticoid receptor activity and proliferation in metastatic colon cancer', *Scientific reports*. Springer US, 9(1), p. 11257. doi: 10.1038/s41598-019-47696-2.

Timmermans, S., Souffriau, J. and Libert, C. (2019) 'A general introduction to glucocorticoid biology', *Frontiers in Immunology*, 10(JULY). doi: 10.3389/fimmu.2019.01545.

To, M. S. *et al.* (2004) 'Cervical cerclage for prevention of preterm delivery in women with short cervix: Randomised controlled trial', *Lancet*, 363(9424), pp. 1849–1853. doi: 10.1016/S0140-6736(04)16351-4.

Uchide, K. *et al.* (2000) 'Matrix metalloproteinase-9 and tensile strength of fetal membranes in uncomplicated labor', *Obstetrics and Gynecology*, 95(6), pp. 851–855. doi: 10.1016/S0029-7844(00)00811-5.

Uffelmann, E. *et al.* (2021) 'Genome-wide association studies', *Nature Reviews Methods Primers*. Springer US, 1(1), p. 59. doi: 10.1038/s43586-021-00056-9.

Vasquez, Y. M. *et al.* (2018) 'FOXO1 regulates uterine epithelial integrity and progesterone receptor expression critical for embryo implantation', *PLoS Genetics*, 14(11), pp. 1–27. doi: 10.1371/journal.pgen.1007787.

Venkatesh, B. *et al.* (2015) 'Elevated plasma-free cortisol concentrations and ratios are associated with increased mortality even in the presence of statin therapy in patients with severe sepsis', *Critical Care Medicine*, 43(3), pp. 630–635. doi: 10.1097/CCM.0000000000000750.

Venter, J. C. *et al.* (2001) 'The Sequence of the Human Genome', *Science*, 291(5507), pp. 1304–1351. doi: 10.1126/science.1058040.

Vento-Tormo, R. *et al.* (2018) 'Single-cell reconstruction of the early maternal–fetal interface in humans', *Nature*, 563(7731), pp. 347–353. doi: 10.1038/s41586-018-0698-6.

Verbruggen, S. W. *et al.* (2017) 'Function and failure of the fetal membrane: Modelling the mechanics of the chorion and Amnion', *PLoS ONE*, 12(3), pp. 1–14. doi: 10.1371/journal.pone.0171588.

Verlouw, J. A. M. *et al.* (2021) 'A comparison of genotyping arrays', *European Journal of Human Genetics*. Springer US, 29(11), pp. 1611–1624. doi: 10.1038/s41431-021-00917-7.

Verschure, P. J. *et al.* (1999a) 'Spatial Relationship between Transcription Sites and Chromosome Territories', *Journal of Cell Biology*, 147(1), pp. 13–24. doi: 10.1083/jcb.147.1.13.

Verschure, P. J. *et al.* (1999b) 'Spatial Relationship between Transcription Sites and Chromosome Territories', *Journal of Cell Biology*, 147(1), pp. 13–24. doi: 10.1083/jcb.147.1.13.

Vockley, C. M. *et al.* (2015) 'Massively parallel quantification of the regulatory effects of noncoding genetic variation in a human cohort', *Genome Research*, 25(8), pp. 1206–1214. doi: 10.1101/gr.190090.115.

Walani, S. R. (2020) 'Global burden of preterm birth', *International Journal of Gynecology and Obstetrics*, 150(1), pp. 31–33. doi: 10.1002/ijgo.13195.

Walburn, J. *et al.* (2009) 'Psychological stress and wound healing in humans: A systematic review and meta-analysis', *Journal of Psychosomatic Research*. Elsevier Inc., 67(3), pp. 253–271. doi: 10.1016/j.jpsychores.2009.04.002.

Wang, T. *et al.* (2014) 'Genetic screens in human cells using the CRISPR-Cas9 system', *Science*, 343(6166), pp. 80–84. doi: 10.1126/science.1246981.

Wang, W., Liu, C. and Sun, K. (2016) 'Induction of amnion epithelial apoptosis

by cortisol via tPA/Plasmin system', *Endocrinology*, 157(11), pp. 4487–4498. doi: 10.1210/en.2016-1464.

Wang, Z. *et al.* (2021) 'ATF3 deficiency impairs the proliferative–secretory phase transition and decidualization in RIF patients', *Cell Death and Disease*. Springer US, 12(4). doi: 10.1038/s41419-021-03679-8.

Wetendorf, M. and DeMayo, F. J. (2012) 'The progesterone receptor regulates implantation, decidualization, and glandular development via a complex paracrine signaling network', *Molecular and Cellular Endocrinology*. Elsevier Ireland Ltd, 357(1–2), pp. 108–118. doi: 10.1016/j.mce.2011.10.028.

Winkvist, A., Mogren, I. and Högberg, U. (1998) 'Familial patterns in birth characteristics: Impact on individual and population risks', *International Journal of Epidemiology*, 27(2), pp. 248–254. doi: 10.1093/ije/27.2.248.

Wonderlin, W. F. and Strobl, J. S. (1996) 'Potassium Channels, Proliferation and G1 Progression', *Journal of Membrane Biology*, 154(2), pp. 91–107. doi: 10.1007/s002329900135.

Wray, N. R. *et al.* (2018) 'Common Disease Is More Complex Than Implied by the Core Gene Omnigenic Model', *Cell*. Elsevier Inc., 173(7), pp. 1573–1580. doi: 10.1016/j.cell.2018.05.051.

Yang, J. *et al.* (2010) 'Common SNPs explain a large proportion of the heritability for human height', *Nature Genetics*, 42(7), pp. 565–569. doi: 10.1038/ng.608.

Zannas, A. S. *et al.* (2019) 'Epigenetic upregulation of FKBP5 by aging and stress contributes to NF-κB-driven inflammation and cardiovascular risk', *Proceedings of the National Academy of Sciences of the United States of America*, 166(23), pp. 11370–11379. doi: 10.1073/pnas.1816847116.

Zhang, G. *et al.* (2017) 'Genetic Associations with Gestational Duration and Spontaneous Preterm Birth', *New England Journal of Medicine*, p. NEJMoa1612665. doi: 10.1056/NEJMoa1612665.

Zhang, H. *et al.* (2015) 'A Genome-Wide Association Study of Early Spontaneous Preterm Delivery', *Genetic Epidemiology*, 39(3), pp. 217–226. doi: 10.1002/gepi.21887.

Zhang, Y. *et al.* (2018) 'Estimation of complex effect-size distributions using summary-level statistics from genome-wide association studies across 32 complex traits', *Nature Genetics*. Springer US, 50(9), pp. 1318–1326. doi: 10.1038/s41588-018-0193-x.

Zhang, Z. *et al.* (2021) 'False positive findings during genome-wide association studies with imputation: influence of allele frequency and imputation accuracy', *Human Molecular Genetics*, 31(1), pp. 146–155. doi: 10.1093/hmg/ddab203.

Zhang, Z. Q. *et al.* (2021) 'Chronic stress promotes glioma cell proliferation via the PI3K/Akt signaling pathway', *Oncology Reports*, 46(3), pp. 1–12. doi: 10.3892/or.2021.8153.

Zhou, Y. *et al.* (2014) 'High-throughput screening of a CRISPR/Cas9 library for functional genomics in human cells', *Nature*. Nature Publishing Group, 509(7501), pp. 487–491. doi: 10.1038/nature13166.

Zuk, O. *et al.* (2012) 'The mystery of missing heritability: Genetic interactions create phantom heritability', *Proceedings of the National Academy of Sciences of the United States of America*, 109(4), pp. 1193–1198. doi: 10.1073/pnas.1119675109.

Zuk, O. *et al.* (2014) 'Searching for missing heritability: Designing rare variant association studies', *Proceedings of the National Academy of Sciences of the United States of America*, 111(4). doi: 10.1073/pnas.1322563111.

Biography

Sarah Jean Cunningham was born in New Brunswick, NJ. She attended the University of Georgia where she double majored in Genetics and Statistics in the honors program. As an undergraduate, Sarah performed research under the mentorship of Dr. Jonathan Arnold. This work led to her being awarded a Center for Undergraduate Research Opportunities Research Assistantship. She completed her thesis titled "The Genetic Network of Circadian Rhythms in *Neurospora crassa*" which was published in the *Journal of Undergraduate Research Opportunities*. In 2016, Sarah graduated with honors from the University of Georgia as an Undergraduate Research Scholar.

Sarah attended Duke University in the University Program in Genetics and Genomics. There she was mentored by Dr. Tim Reddy for her work on pregnancy complications. She co-authored several papers including a first author review article "Functional Consequences of Healthy and Pathological Fetal Membranes" and a first author manuscript "Glucocorticoid Receptor Regulated KCNA5 Mediates Cell Proliferation in Human Fetal Membranes." During her time at Duke, she served as treasurer and co-president of Women in Science and Engineering. She received a Bass Teaching Assistantship and a Bass Instructor of Record award.